

Simulation techniques for dense particulate matter

Corey S. O'Hern

Department of Mechanical Engineering & Materials Science

Department of Physics

Department of Applied Physics

Graduate Program in Computational Biology & Bioinformatics

Integrated Graduate Program in Physical & Engineering Biology

Outline

Lecture 1: What are granular materials? What is the jamming transition? Disk and sphere packings.

Lecture 2: Molecular dynamics (discrete element modeling) simulations

Lecture 3: Simulations of the glass transition

Lecture 4: Applications of simulation methods to granular and glassy materials

Jamming Transitions





Key features of granular materials:

- Macroscopic sizes, $> 50 \mu\text{m}$
- Not influenced by thermal fluctuations
- Highly frictional
- Highly dissipative, out of thermal equilibrium
- Polydisperse
- Nonspherical particles
- Jamming, avalanches, stick-slip, aging, shear banding, protocol dependence, nonlinear, non-elastic, ...

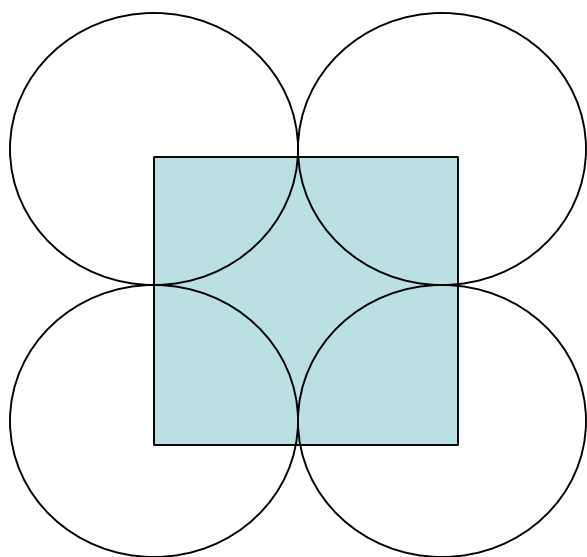
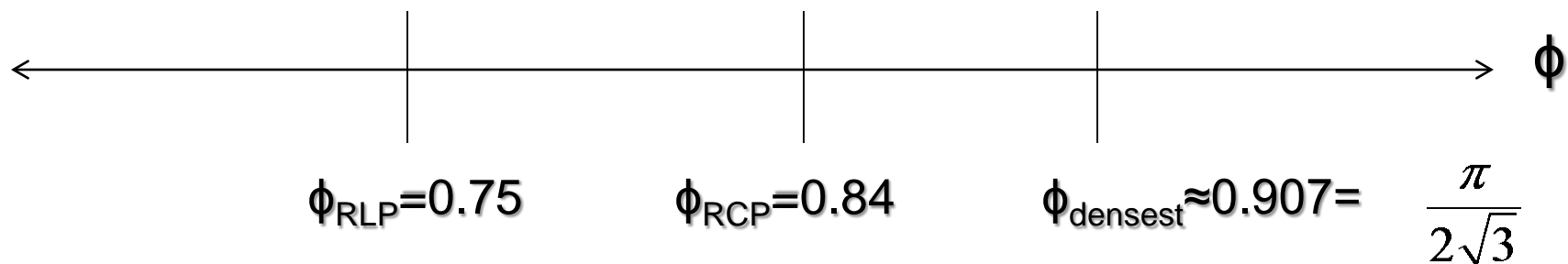
Forces involved in granular media

- Interparticle contact forces
- Gravity
- Electrostatic
- Hydrodynamic
- van der Waals

Three methods to generate jammed, frictionless packings

1. Monte Carlo Method
2. Lubachevsky-Stillinger Method
3. Soft-sphere Molecular Dynamics Method

Frictionless Disks: Weakly Polydisperse



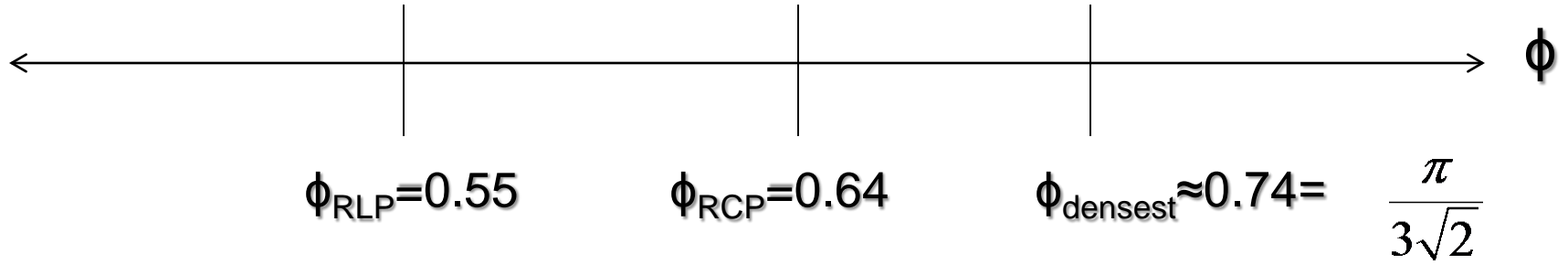
hexagonal

$$\phi_{\text{square}} = \frac{\pi R^2}{(2R)^2} = \frac{\pi}{4} \approx 0.785$$

2D Circle Packings

Structure	ϕ	z
Honeycomb	0.605	3
RLP	0.75	3
Square	0.78	4
RCP	0.84	4
Hexagonal	0.91	6

Frictionless Monodisperse Spheres



FCC, HCP

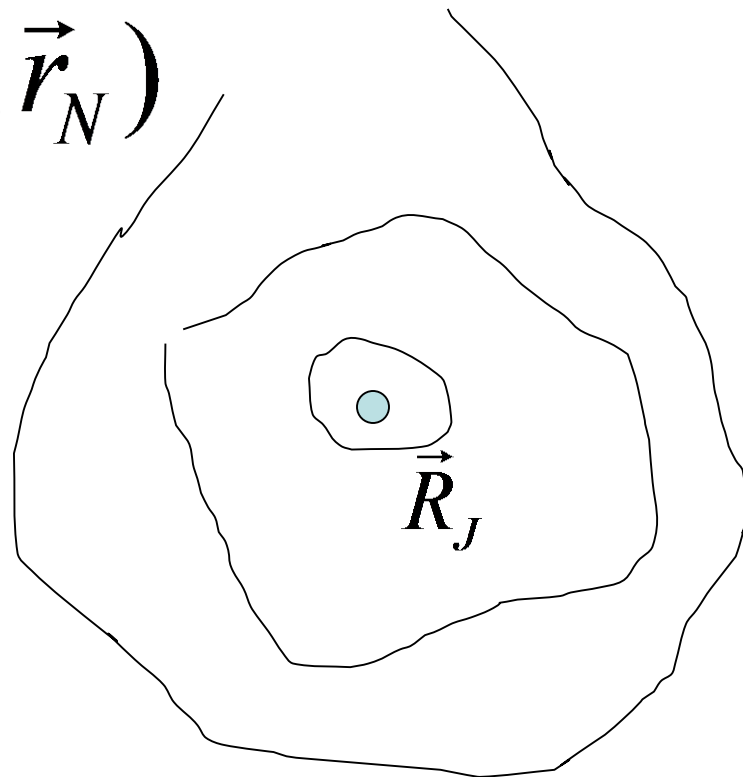
3D Sphere Packings

Structure	ϕ	z
Simple cubic	0.52	6
RLP	0.55	4
RCP	0.64	6
BCC	0.68	8
FCC, HCP	0.74	12

1. Monte Carlo Method

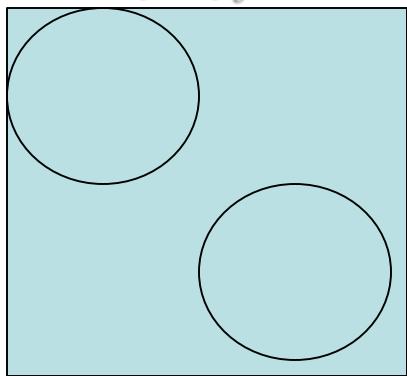
Configuration space

$$\vec{R} = (\vec{r}_1, \dots, \vec{r}_N)$$

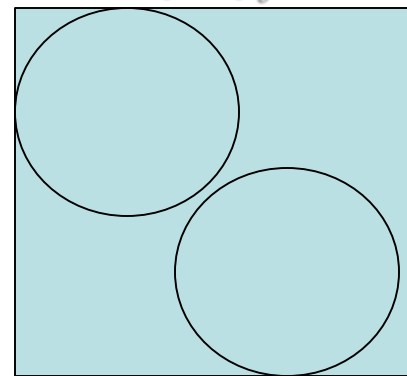


$$\Delta\phi = \phi_J - \phi$$

$$\phi < \phi_J \approx 0.539$$



$$\phi > \phi_J$$



Monte Carlo Packing Method

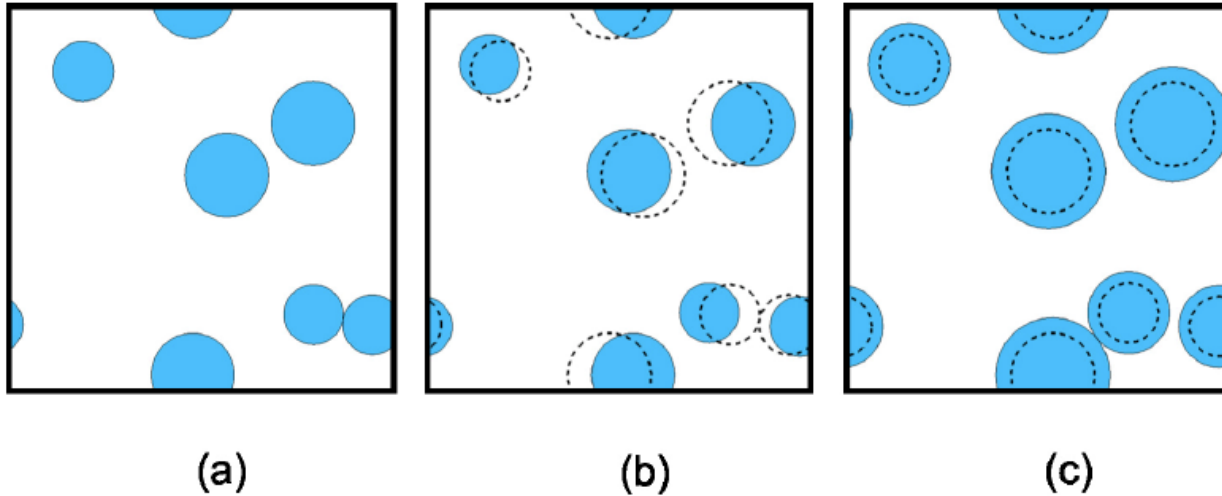
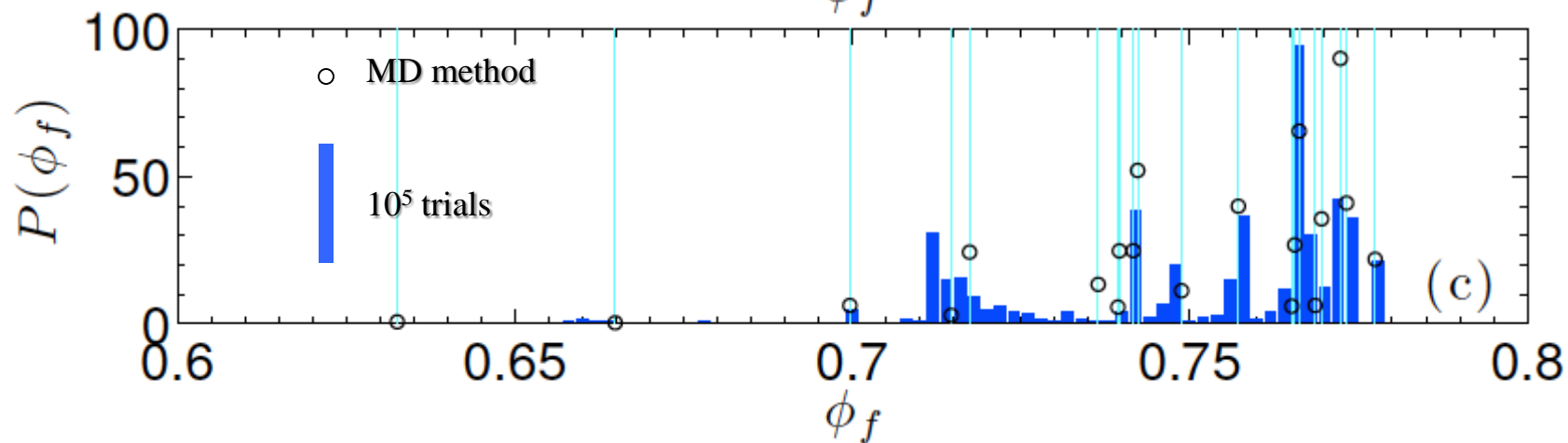
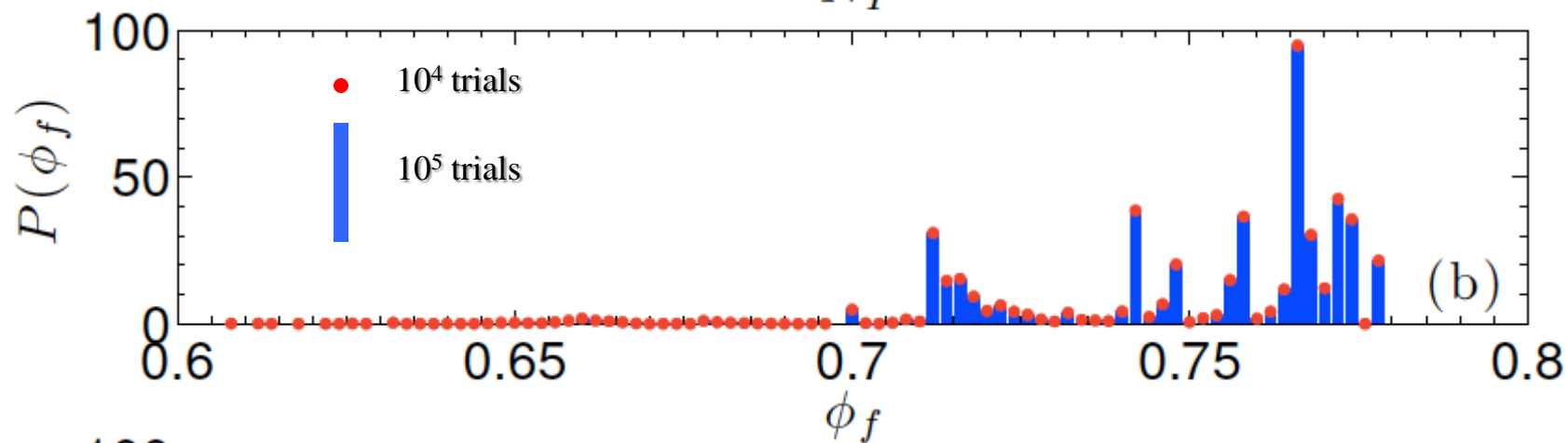
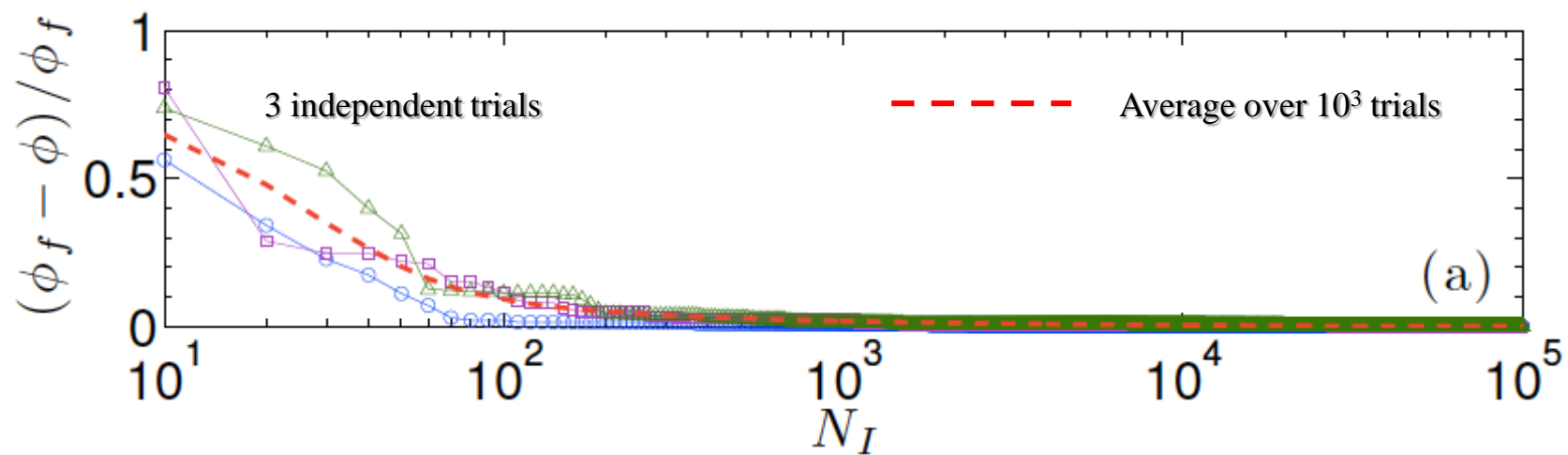
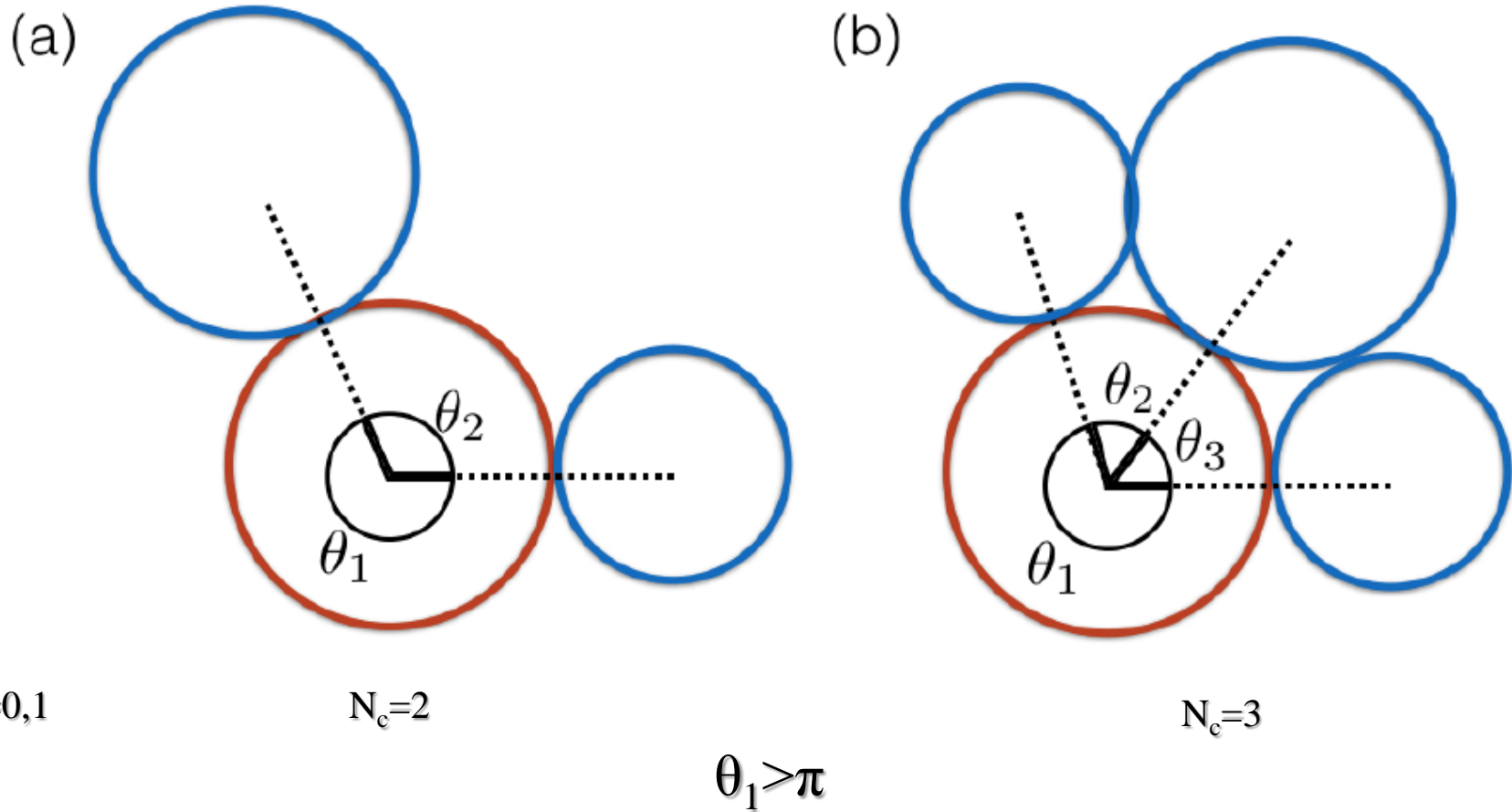
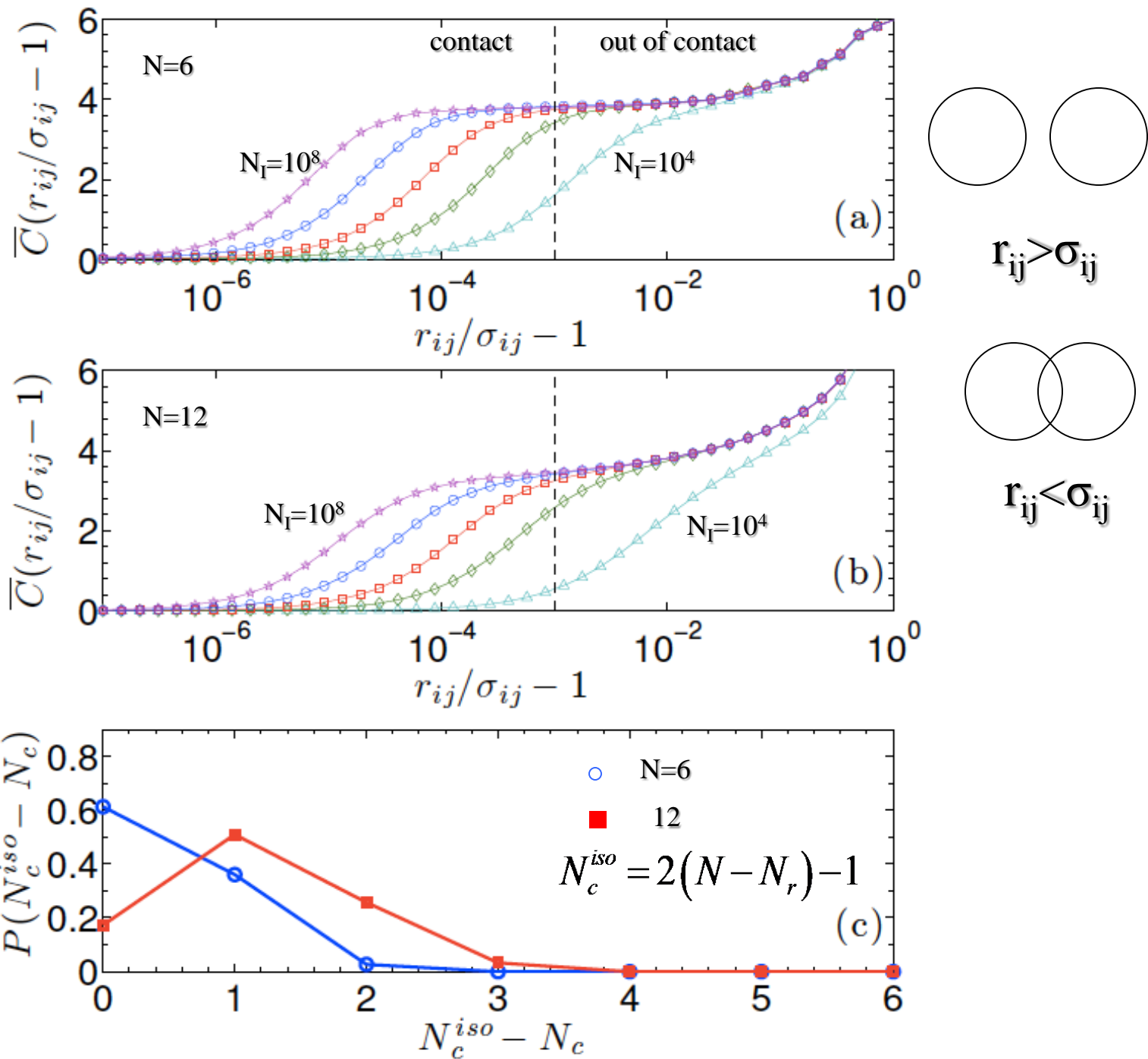


Figure 1.1: Illustration of the Monte Carlo packing-generation method for a system of $N = 6$ bidisperse frictionless disks (half small and half large with diameter ratio 1.4) in 2D. (a) The x - and y -coordinates for $N = 6$ random points are first generated in a square cell with periodic boundary conditions and the particles are grown uniformly until the closest pair of disks are in contact. (b) An attempt is made to move each particle randomly from the original (dashed outline) to the new position (shaded disk), and the move is accepted if it does not give rise to particle overlap. (c) The disks are expanded uniformly from the original (dashed outline) to the new size (shaded disk) until the two closest disks touch. This process is repeated for N_I iterations to obtain a single static packing.

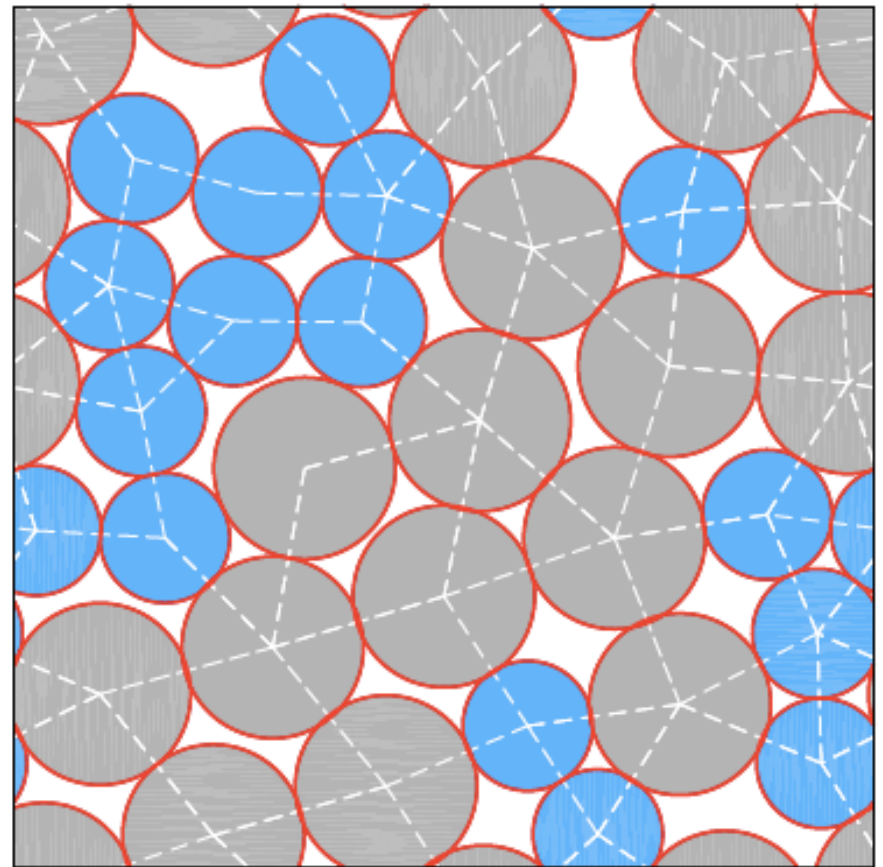
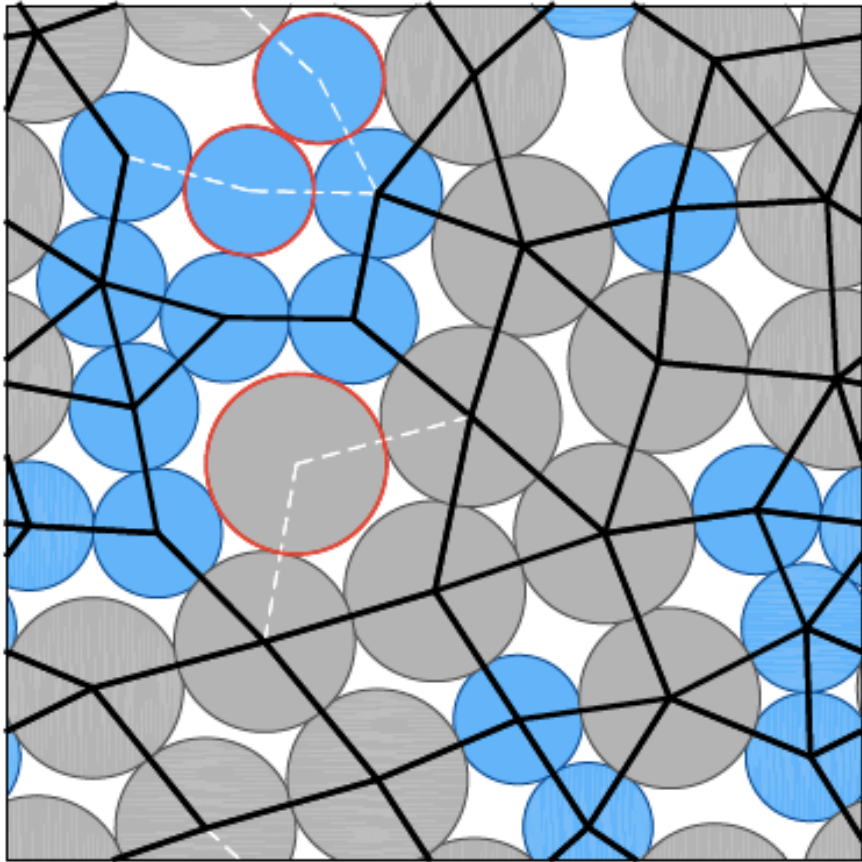


Rattler Particles





Pruning contacts from rattlers



$$N_c < N_c^{iso}$$

Automatic characterization and comparison of jammed packings

Packing fraction ϕ_J

NxN Adjacency Matrix $A_{ij} = 1$ if $r_{ij} \leq \sigma_{ij}$
 $= 0$ if $r_{ij} > \sigma_{ij}$

NxN Distance Matrix $D_{ij} = r_{ij}$

dNxNdN Dynamical Matrix $M_{ij} = \frac{\partial^2 V}{\partial r_i \partial r_j}$

Displacement matrix

$$D_{ij} = \left| \vec{r}_i - \vec{r}_j \right|$$

$$q_2 = \frac{1}{2} \left((TrD)^2 - TrD^2 \right)$$

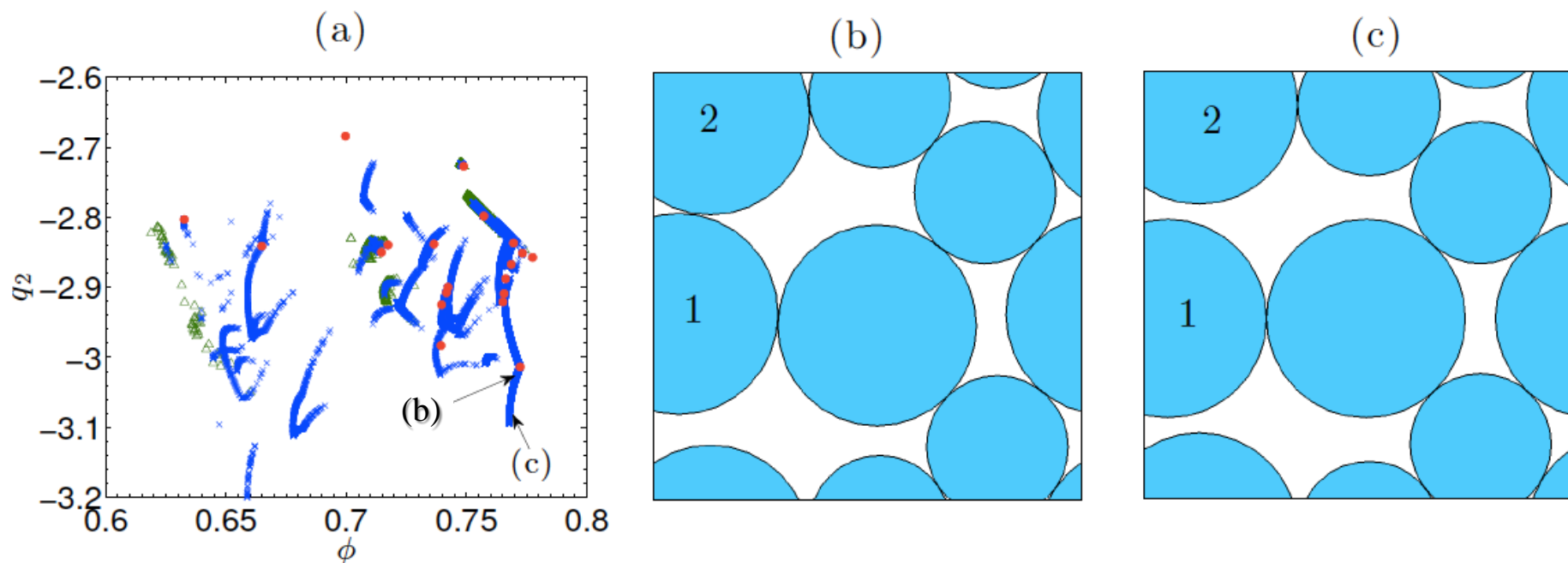
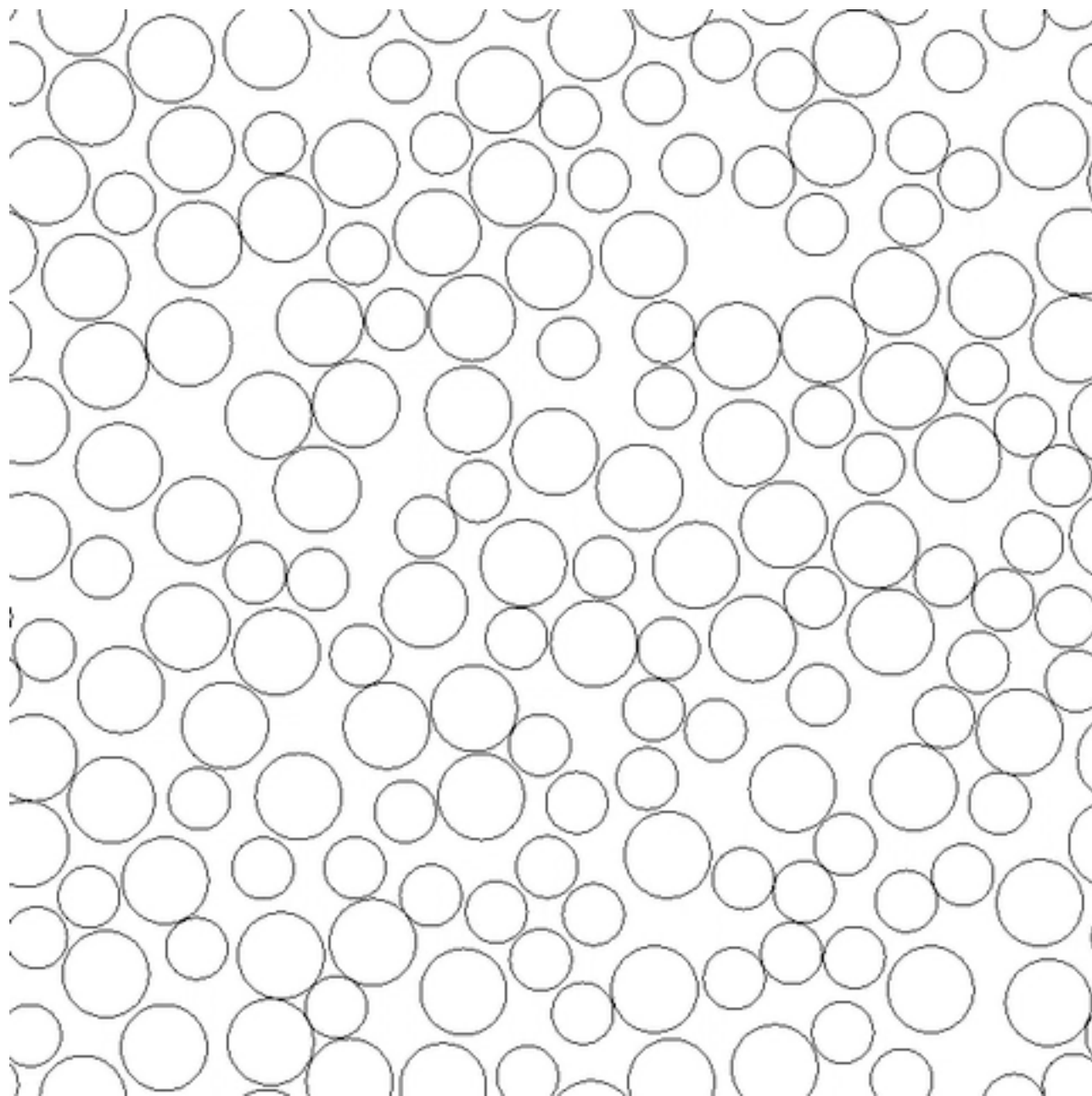


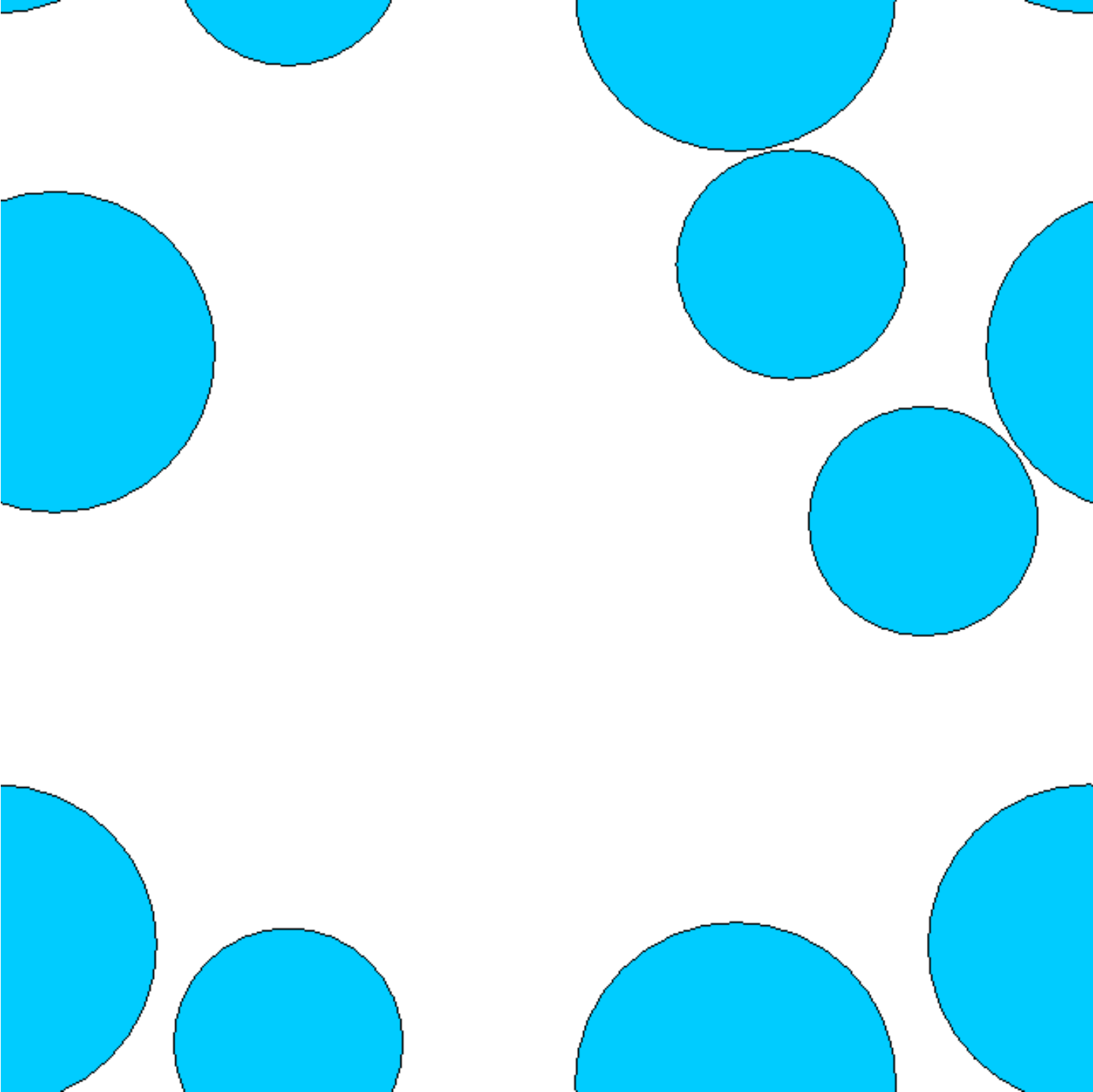
Figure 1.4: (a) The second invariant $q_2 = ((\text{Tr}D)^2 - \text{Tr}D^2)/2$ of the distance matrix D plotted versus the packing fraction ϕ for $N_c = 10^5$ bidisperse frictionless hard disk packings with $N = 6$ generated via the ‘basic’ Monte Carlo method (after $N_I = 10^5$ iterations) with one (blue xes) or two (green triangles) missing contacts $N_c^{\text{iso}} - N_c = 1$ or 2 relative to the isostatic value for frictionless disks. The MS packings with $N_c = N_c^{\text{iso}}$ are indicated by the filled red circles. Two configurations with $N_c^{\text{iso}} - N_c = 1$ that belong to a single geometrical family are labeled (b) and (c).

2. Lubachevsky-Stillinger Method

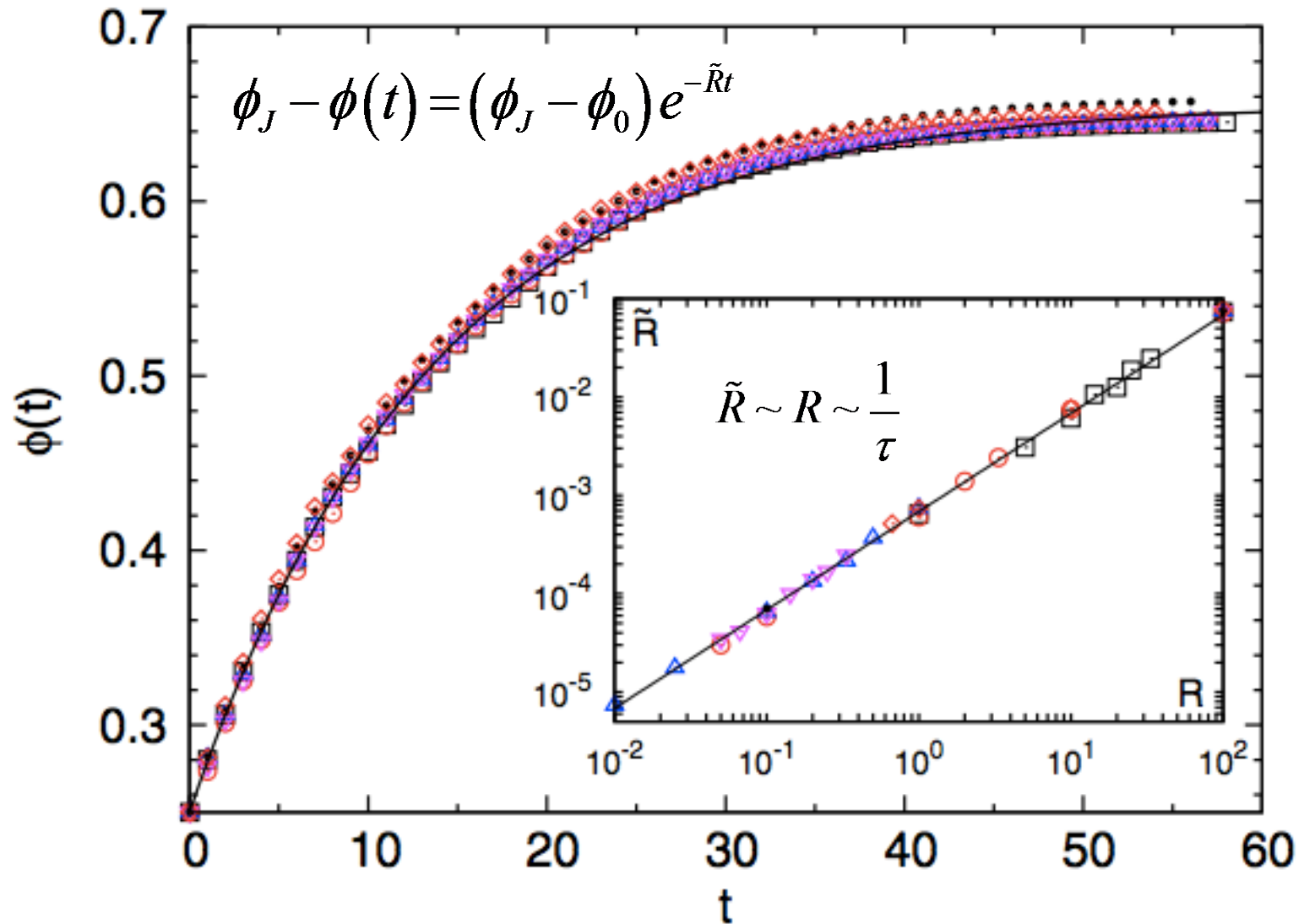
B. D. Lubachevsky and F. H. Stillinger, “Geometric properties of random disk packings,”
J. Stat. Phys. 60 (1990) 561

$\phi=0.6$

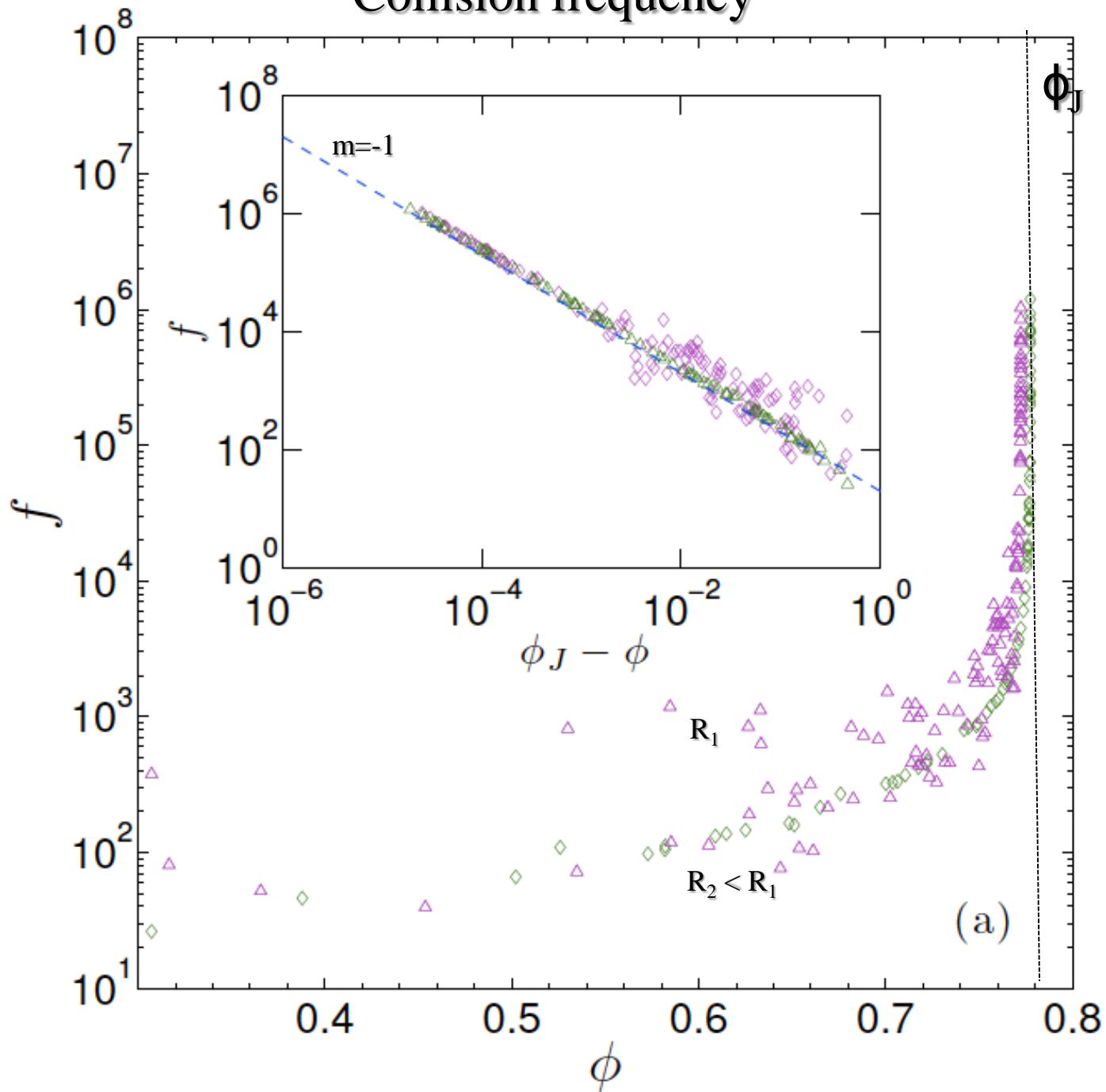




Lubachevsky-Stillinger Compression Protocol



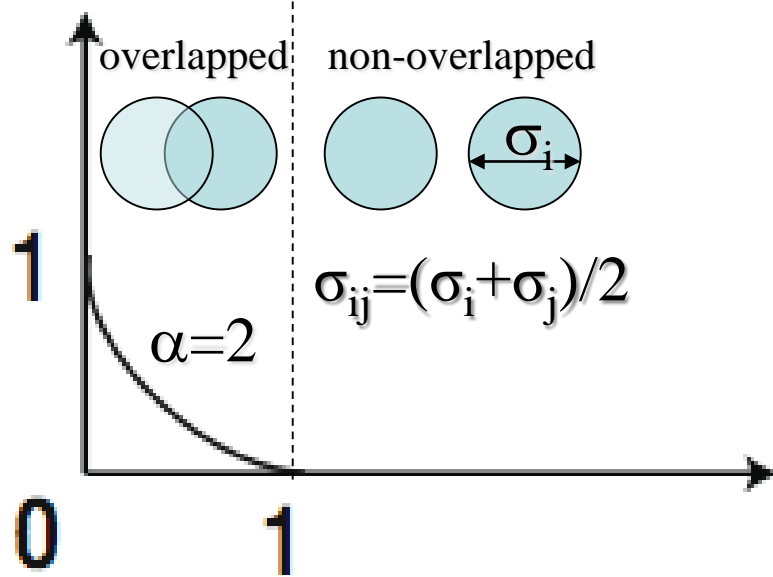
Collision frequency



3. Dissipative Molecular Dynamics Method

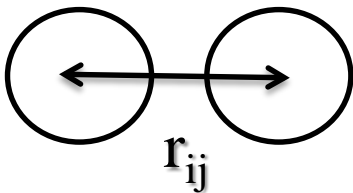
Purely repulsive soft interactions

$$V_{RS}(r_{ij})/\epsilon$$



$$V_{RS}(r_{ij}) = \frac{\epsilon}{\alpha} \left(1 - \frac{r_{ij}}{\sigma_{ij}}\right)^\alpha \Theta\left(1 - \frac{r_{ij}}{\sigma_{ij}}\right)$$

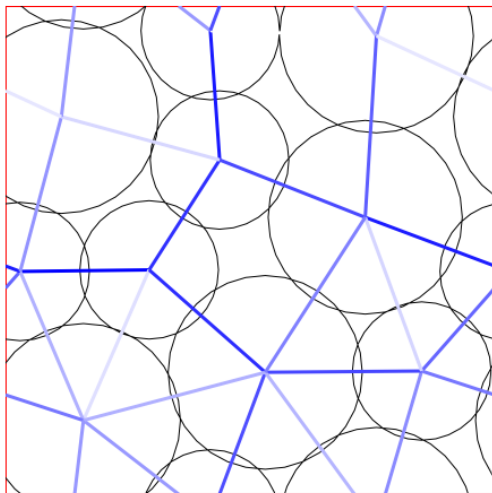
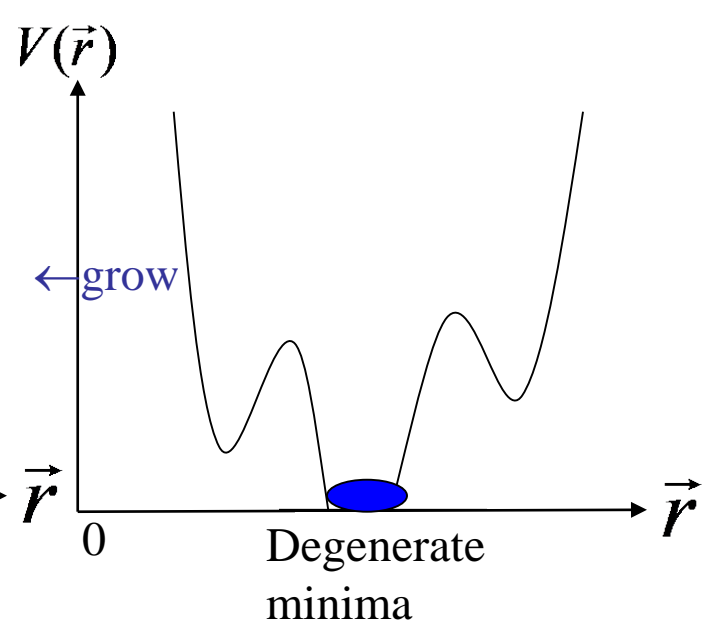
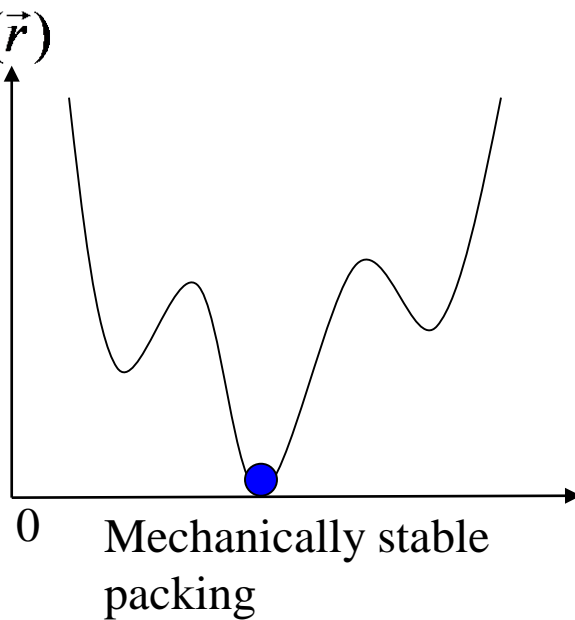
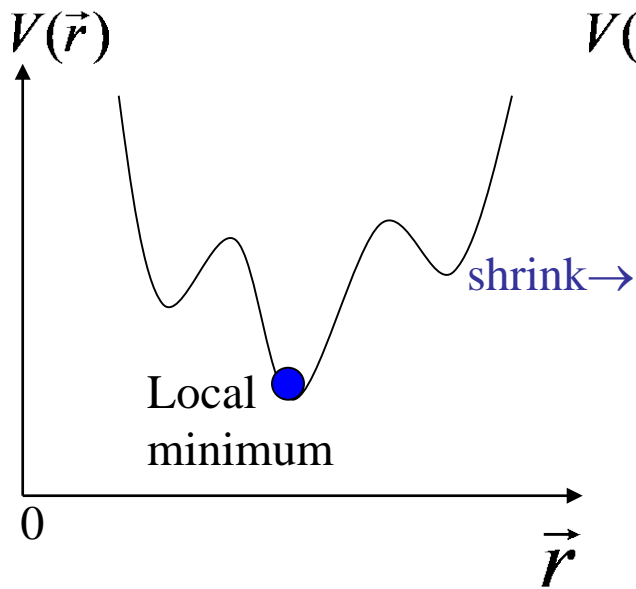
$$V = \frac{1}{N} \sum_{i>j} V_{RS}(r_{ij})$$



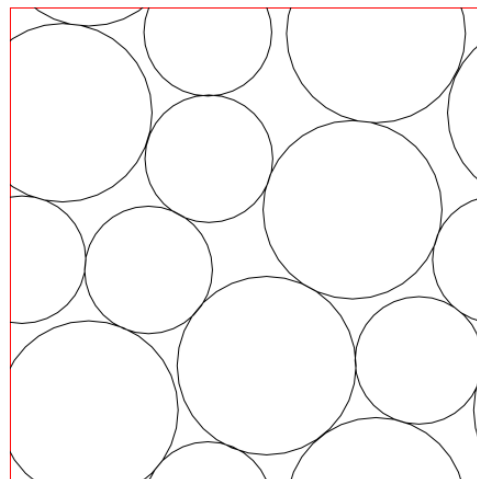
$N/2$ large, $N/2$ small with diameter ratio $\sigma_L/\sigma_S=1.4$

Notes

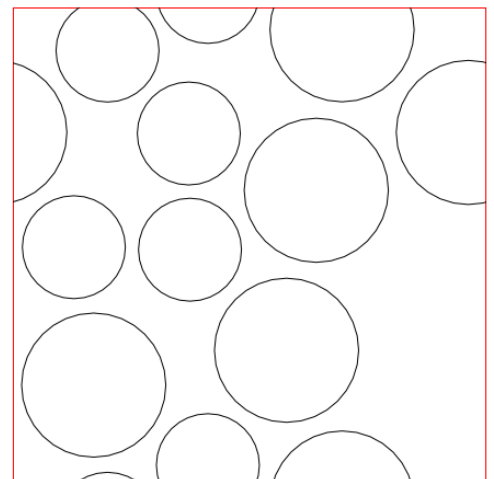
Potential Energy Landscape (PEL)



overlapped



Mechanically stable
packing



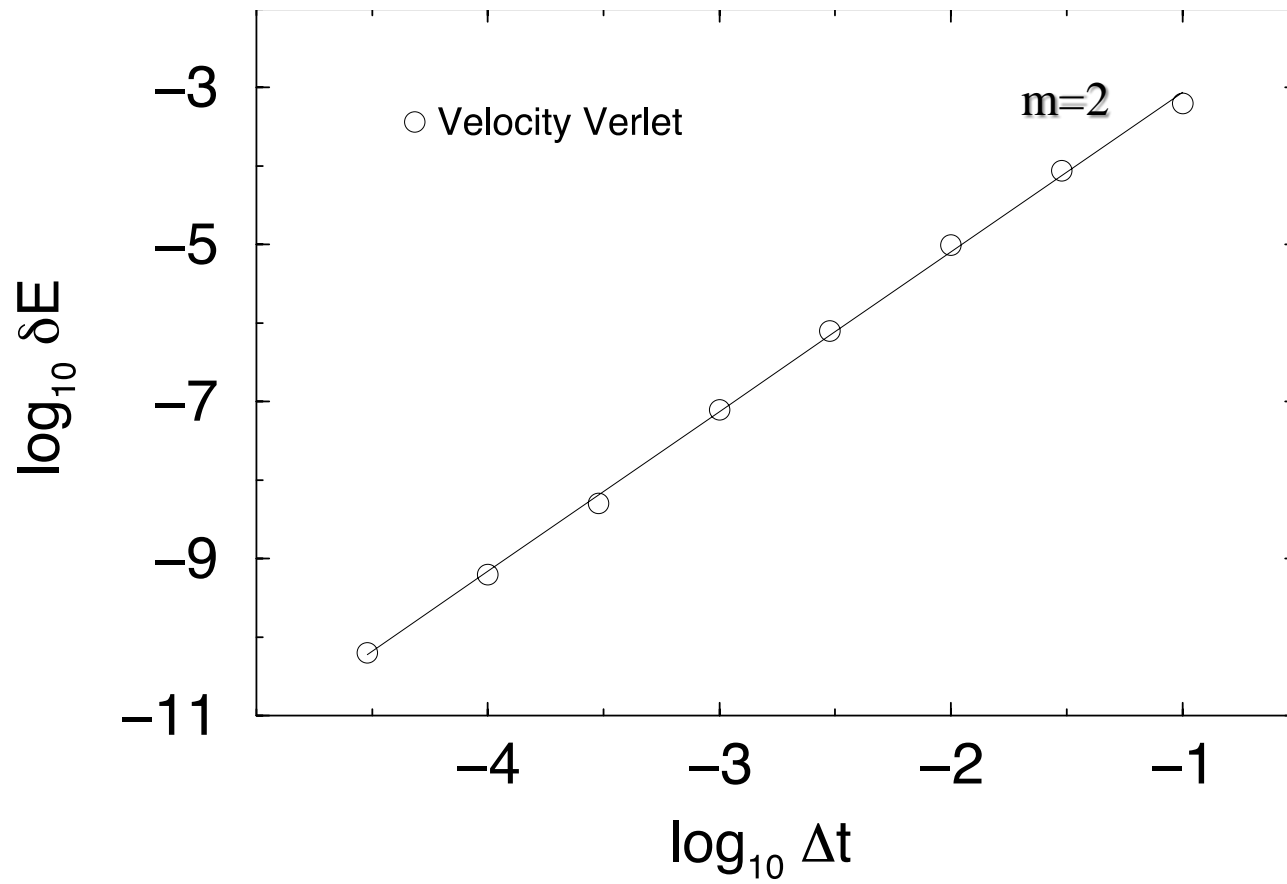
non-overlapped

Potential energy minimization

$$m\vec{a}_i = \sum_j \vec{F}(r_{ij}) - b\vec{v}_i$$

$$m\vec{a}_i = \sum_j \left(\vec{F}(r_{ij}) - b(\vec{v}_{ij} \cdot \hat{r}_{ij}) \hat{r}_{ij} \right)$$

Notes



Simulations

Integrator	Ensemble	N	E	T	P	ϕ
Velocity Verlet	NVE	64	0.64	0.0038 ± 0.0003	0.064 ± 0.003	0.6
Gear 4	NVE	64	0.64	0.0038 ± 0.0003	0.064 ± 0.002	0.6
Gear 5	NVE	64	0.64	0.0038 ± 0.0003	0.064 ± 0.002	0.6
Gear 6	NVE	64	0.64	0.0038 ± 0.0004	0.064 ± 0.002	0.6
Gaussian Constraint	NVT	64	0.63 ± 0.04	0.0037	0.063 ± 0.004	0.6
Nose-Hoover	NVT	64	0.63 ± 0.02	0.0037	0.063 ± 0.003	0.6

$$\frac{P\sigma^3}{\varepsilon} = \frac{\sigma^3}{\varepsilon L^3} \sum_{i>j} r_{ij} F_{ij}$$

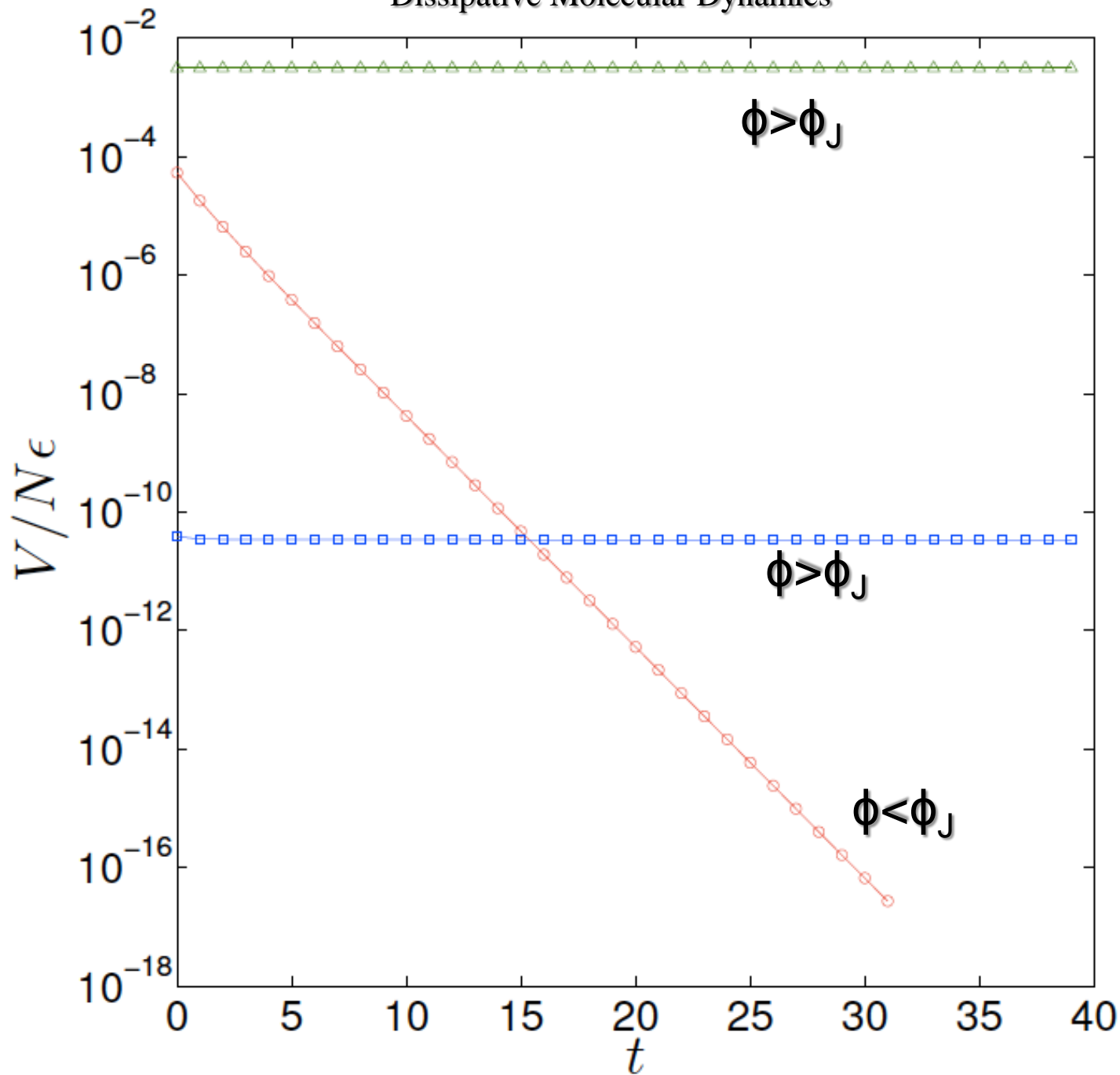
(E, <T>, ϕ)

(<E>, T, ϕ)

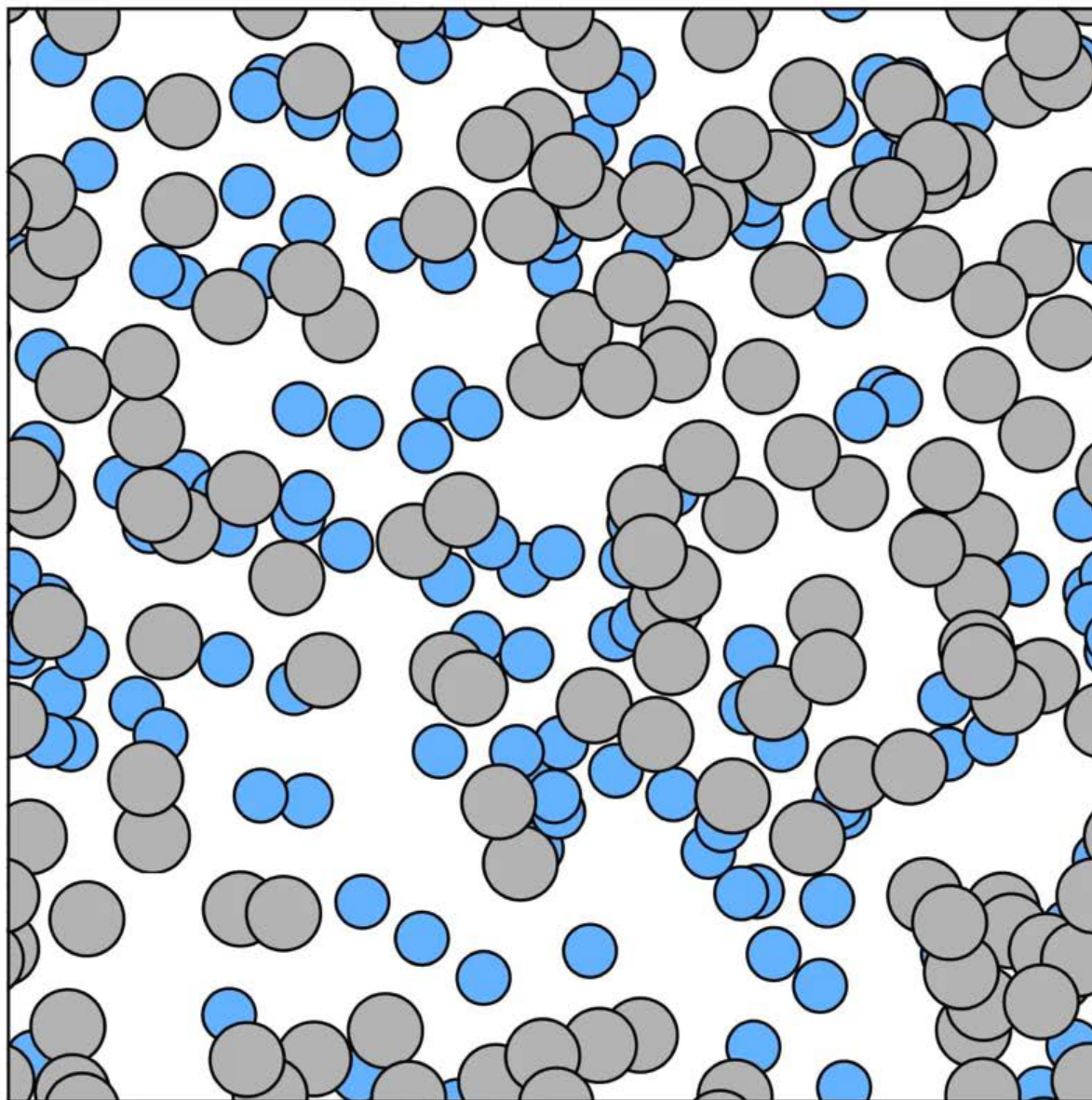
(P, < ϕ >)

(<P>, ϕ)

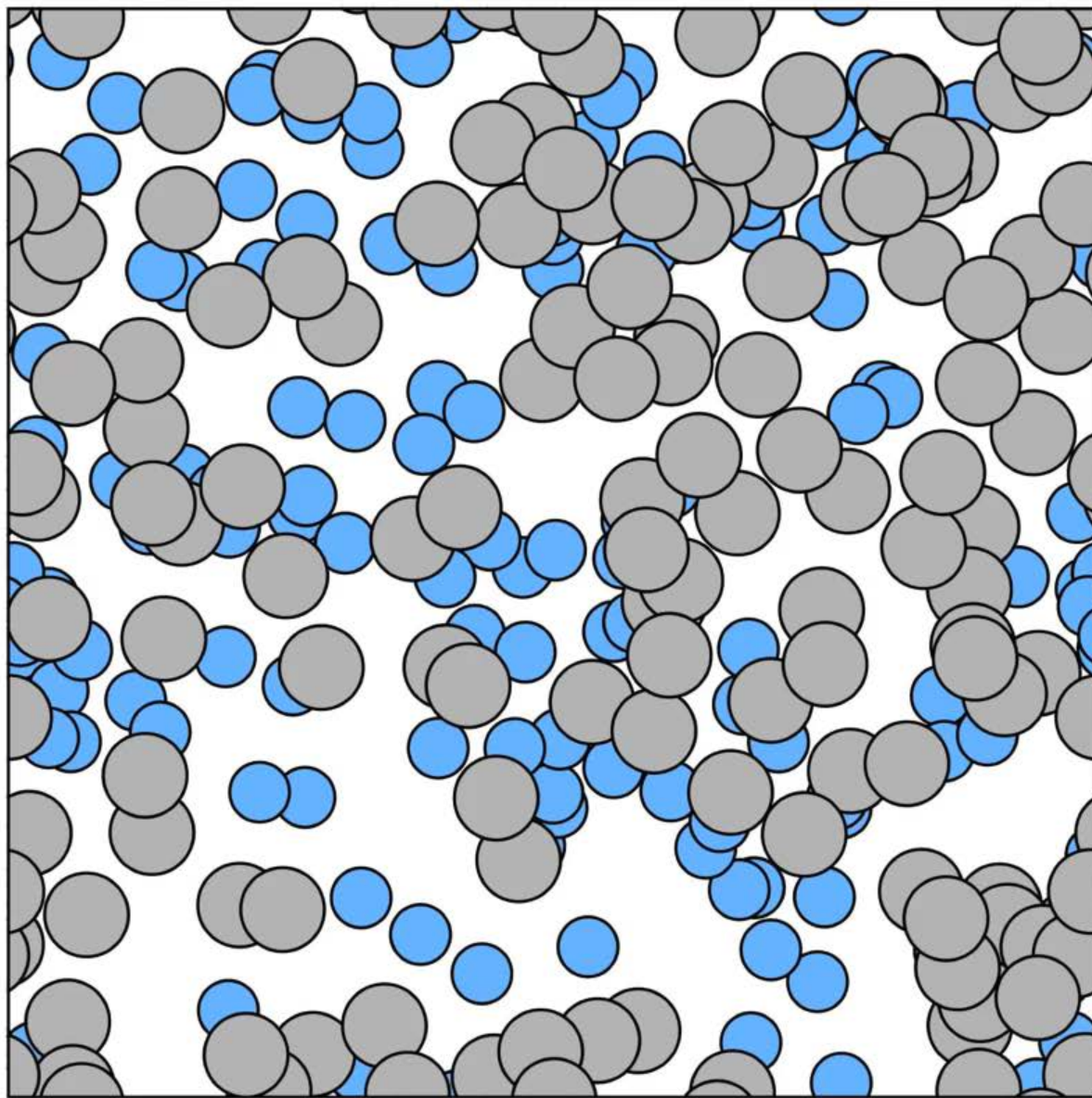
Dissipative Molecular Dynamics

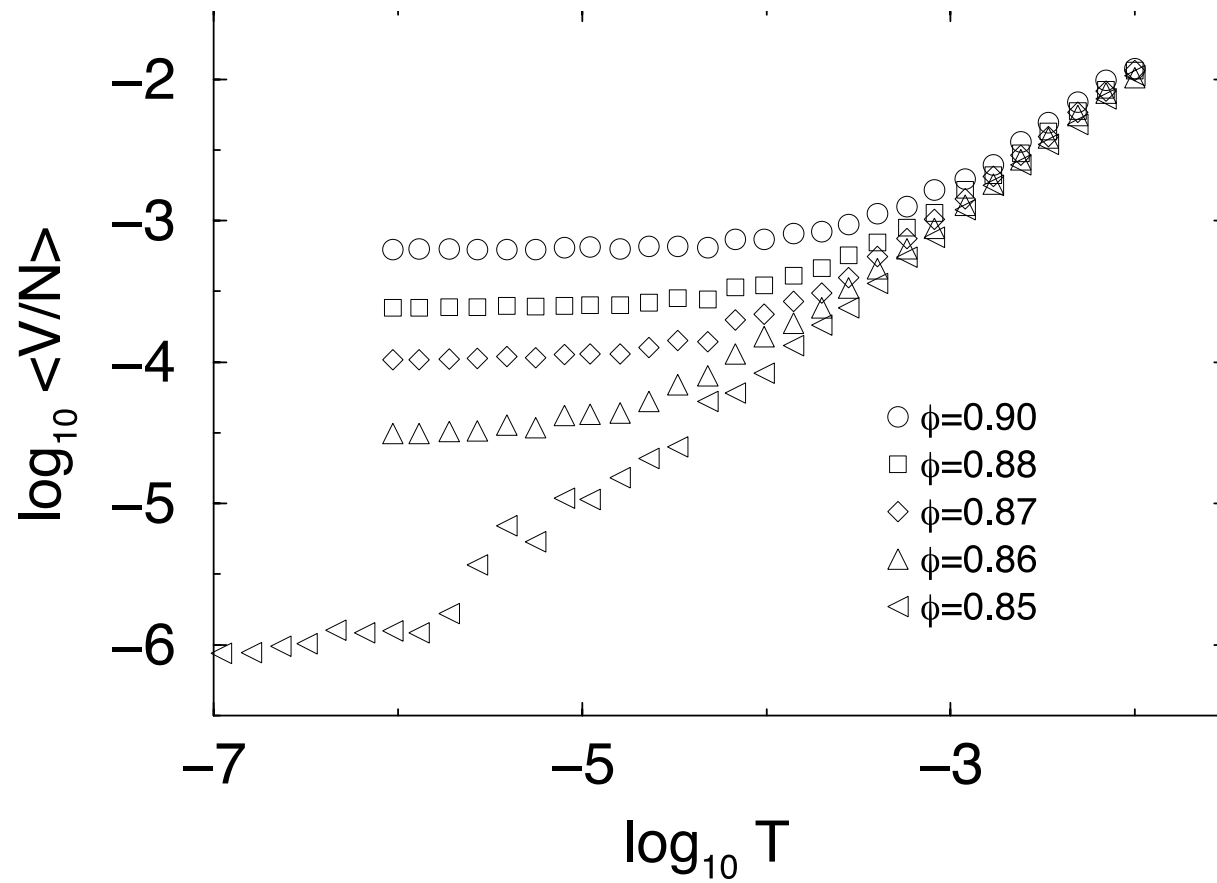


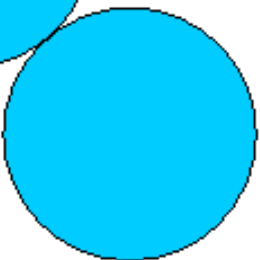
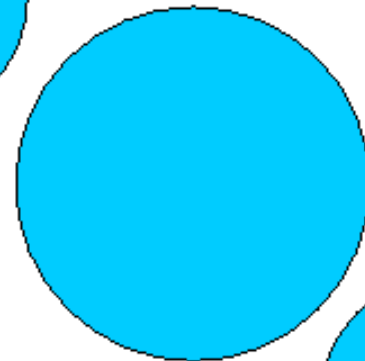
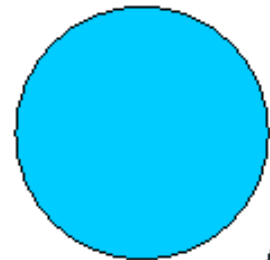
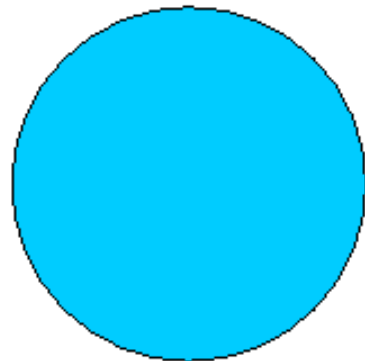
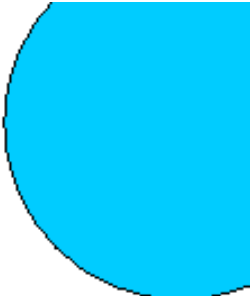
$\phi=0.7$

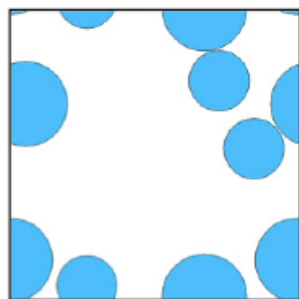


$\phi=0.9$

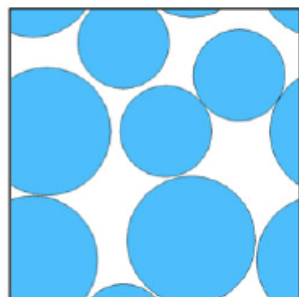




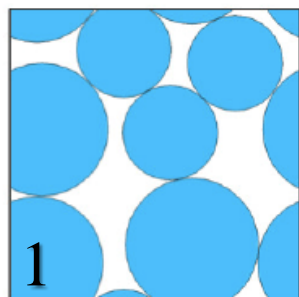




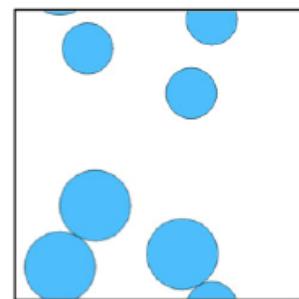
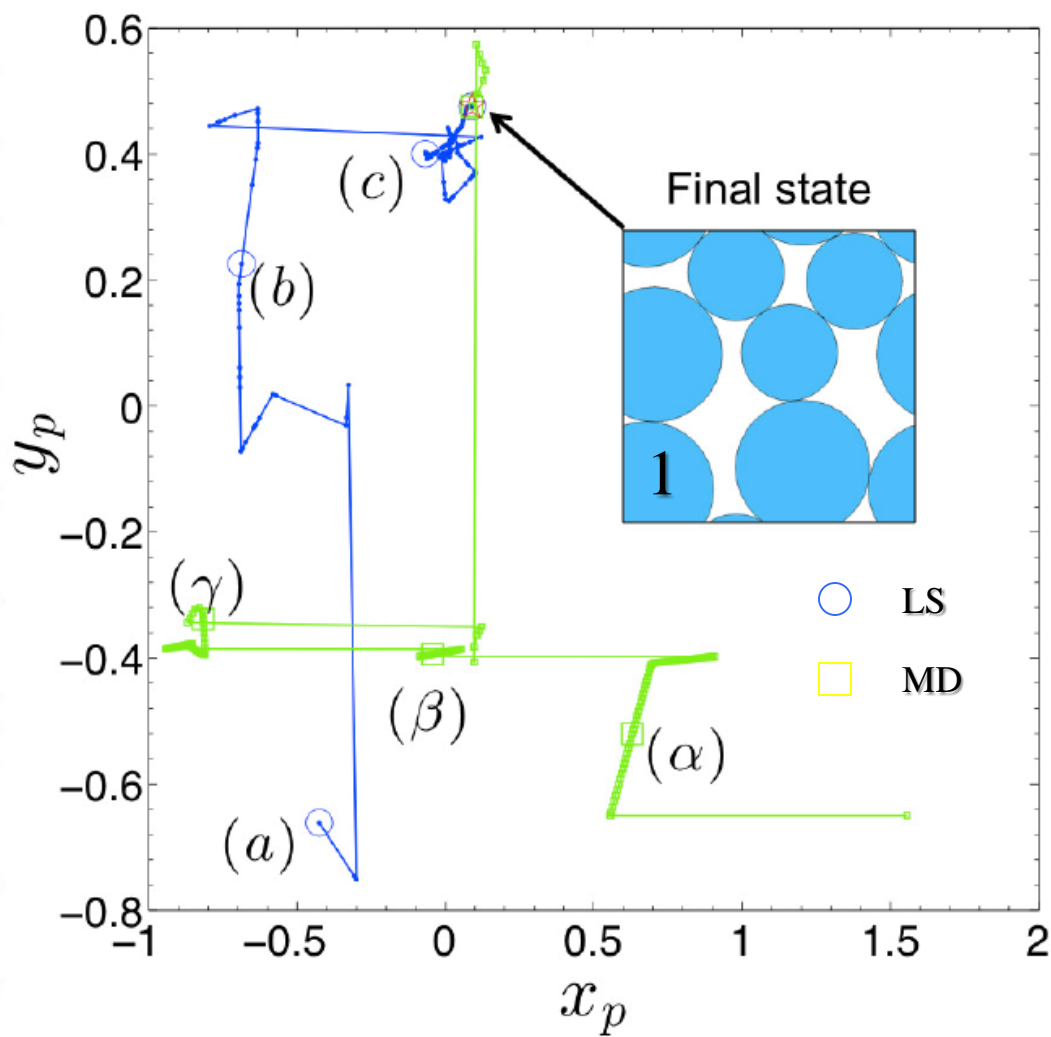
(a)



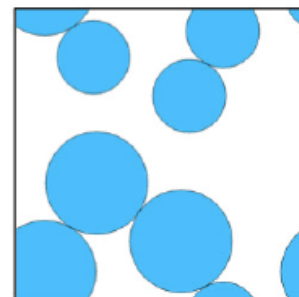
(b)



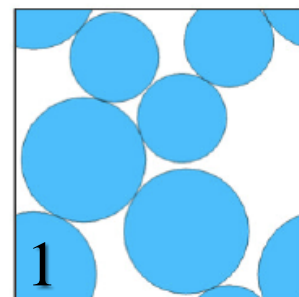
(c)



(alpha)



(beta)

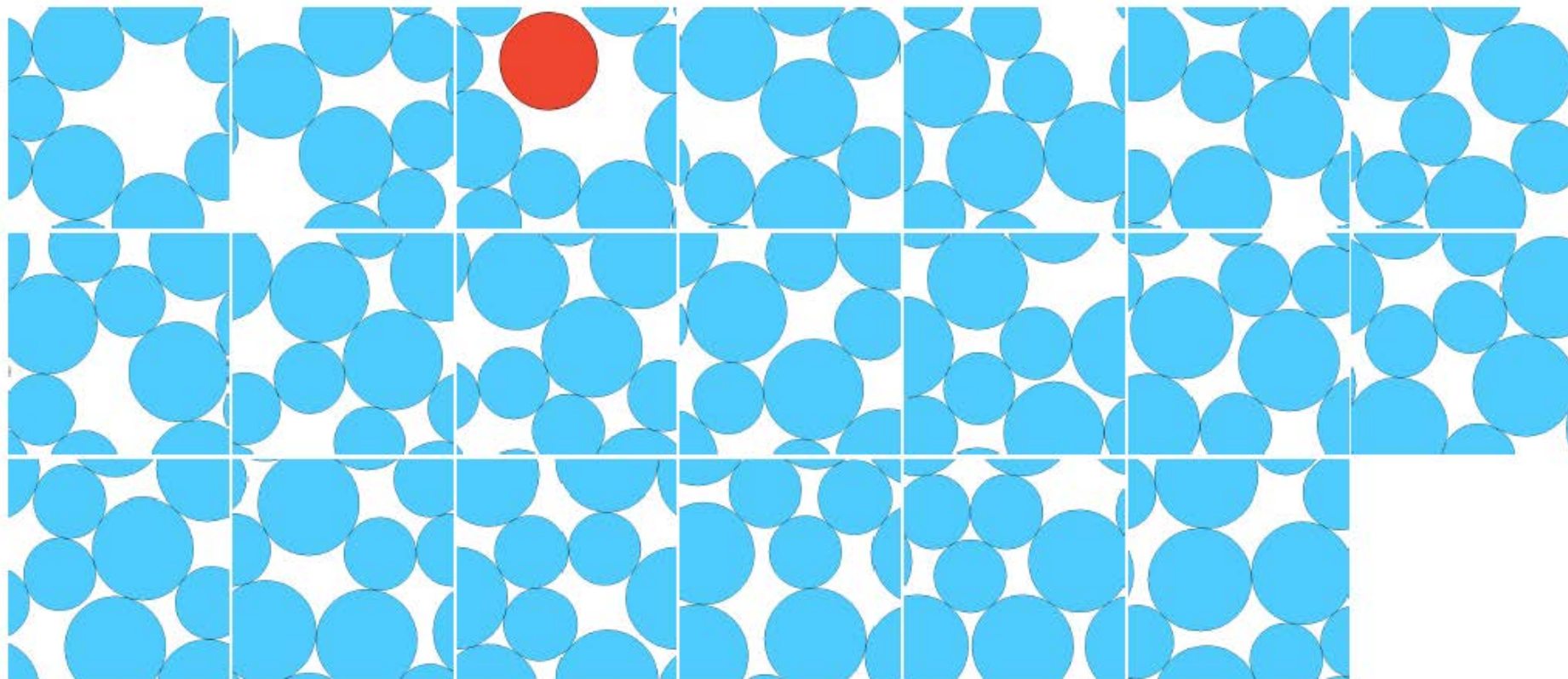


(gamma)

$$\vec{r}_p = \frac{1}{5} \sum_{i=2}^6 [(x_i - x_1) \hat{x} + (y_i - y_1) \hat{y}]$$

Isostatic packings for $N=6$; $N_c=11$

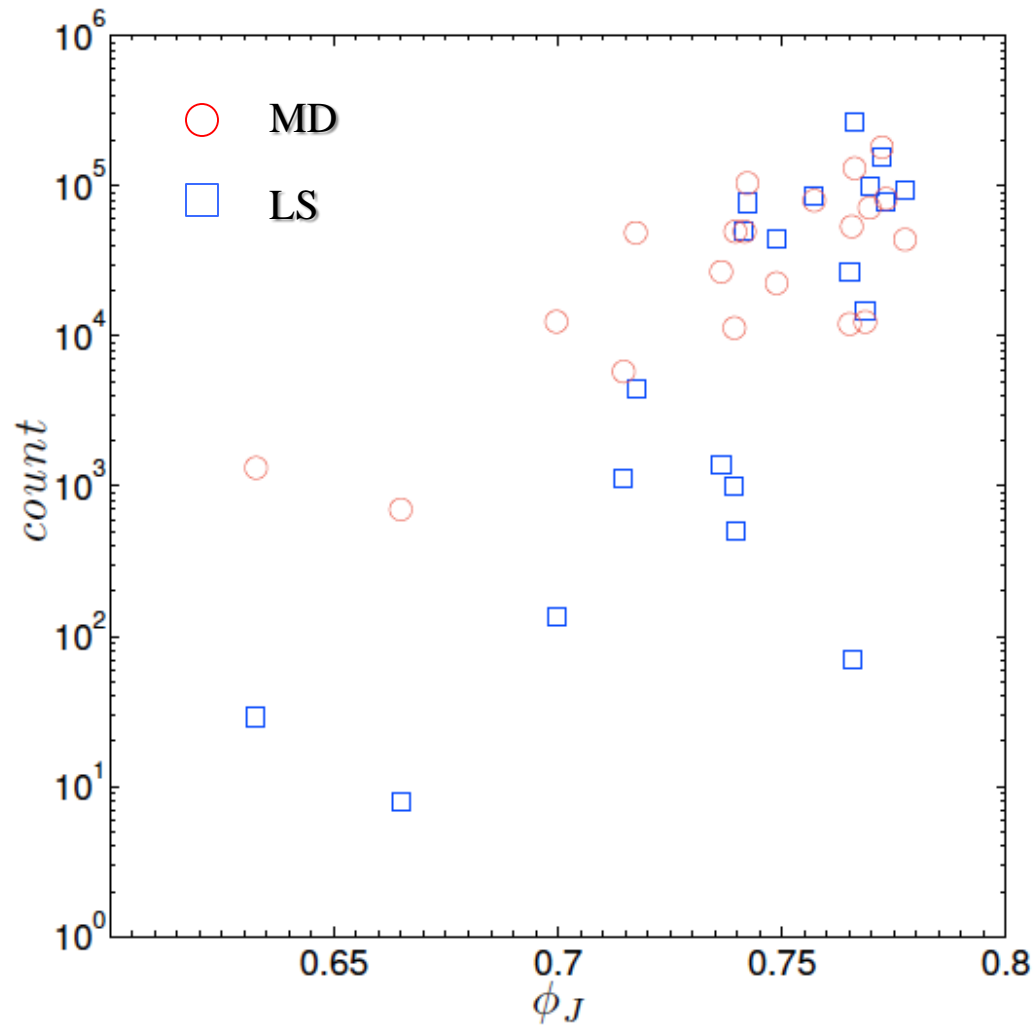
$\phi=0.633$

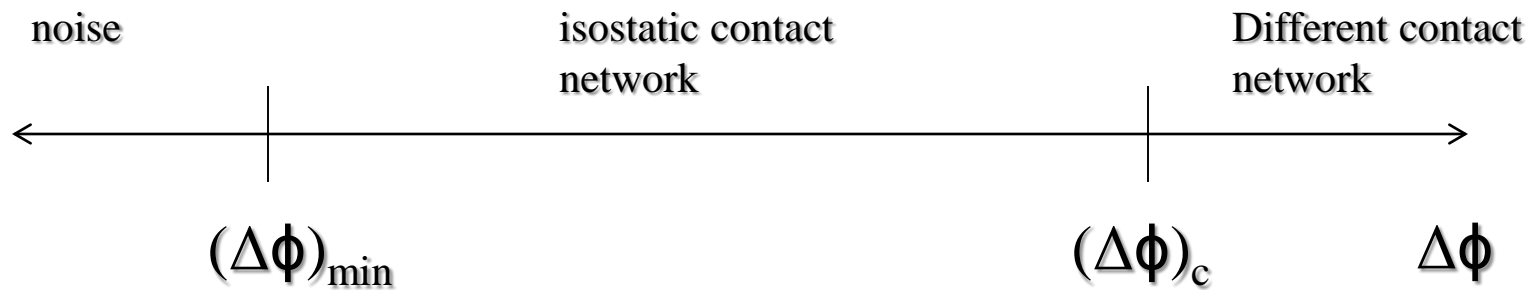


$\phi=0.772$

$\phi=0.778$

Frequency distribution for N=6 isostatic packings



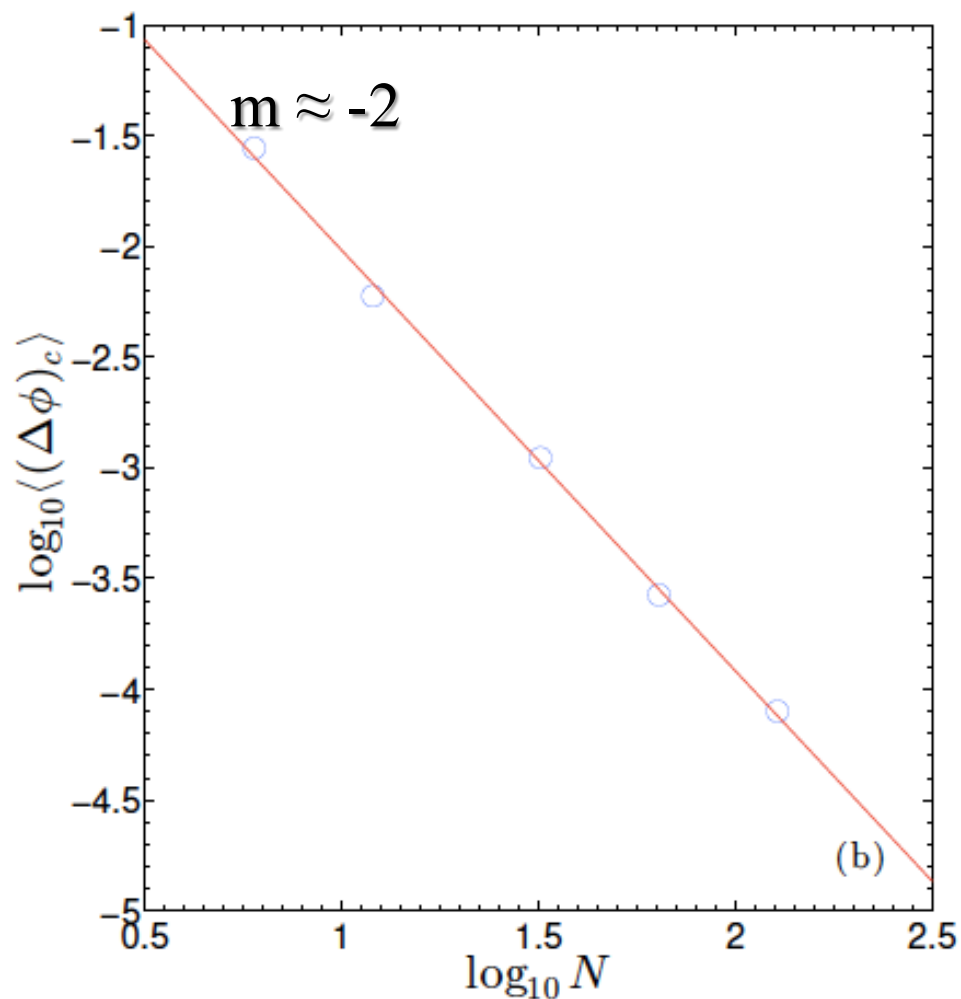
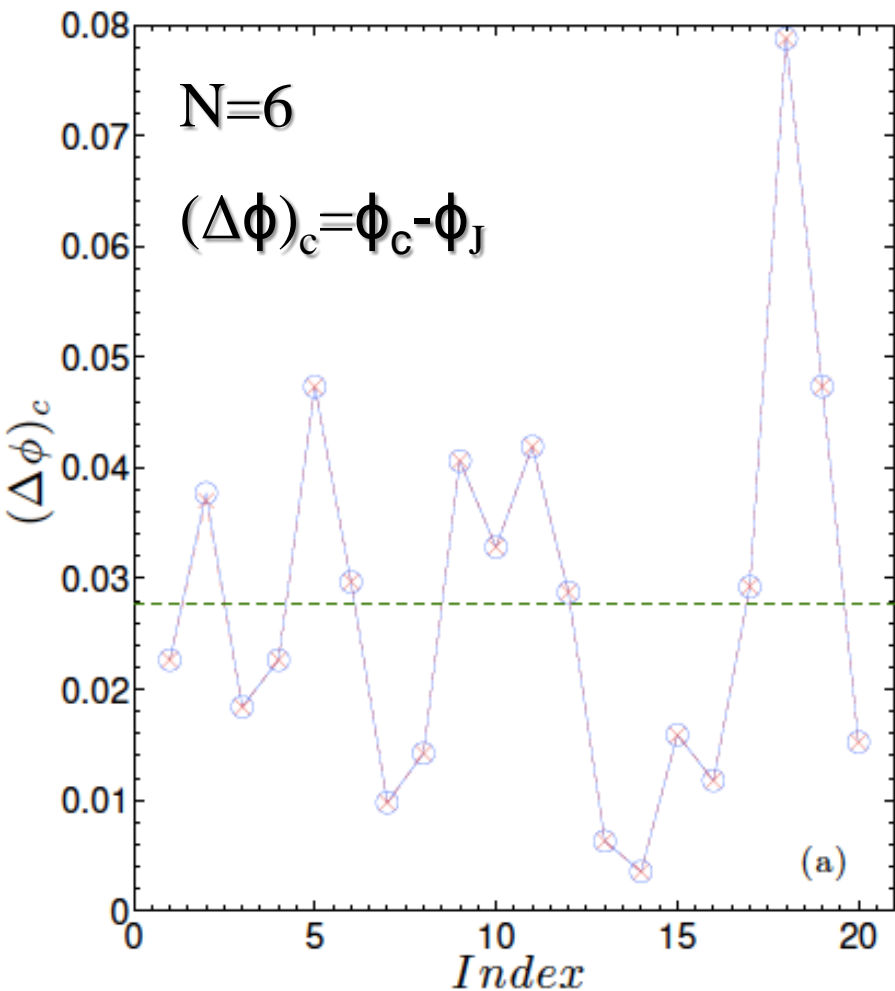


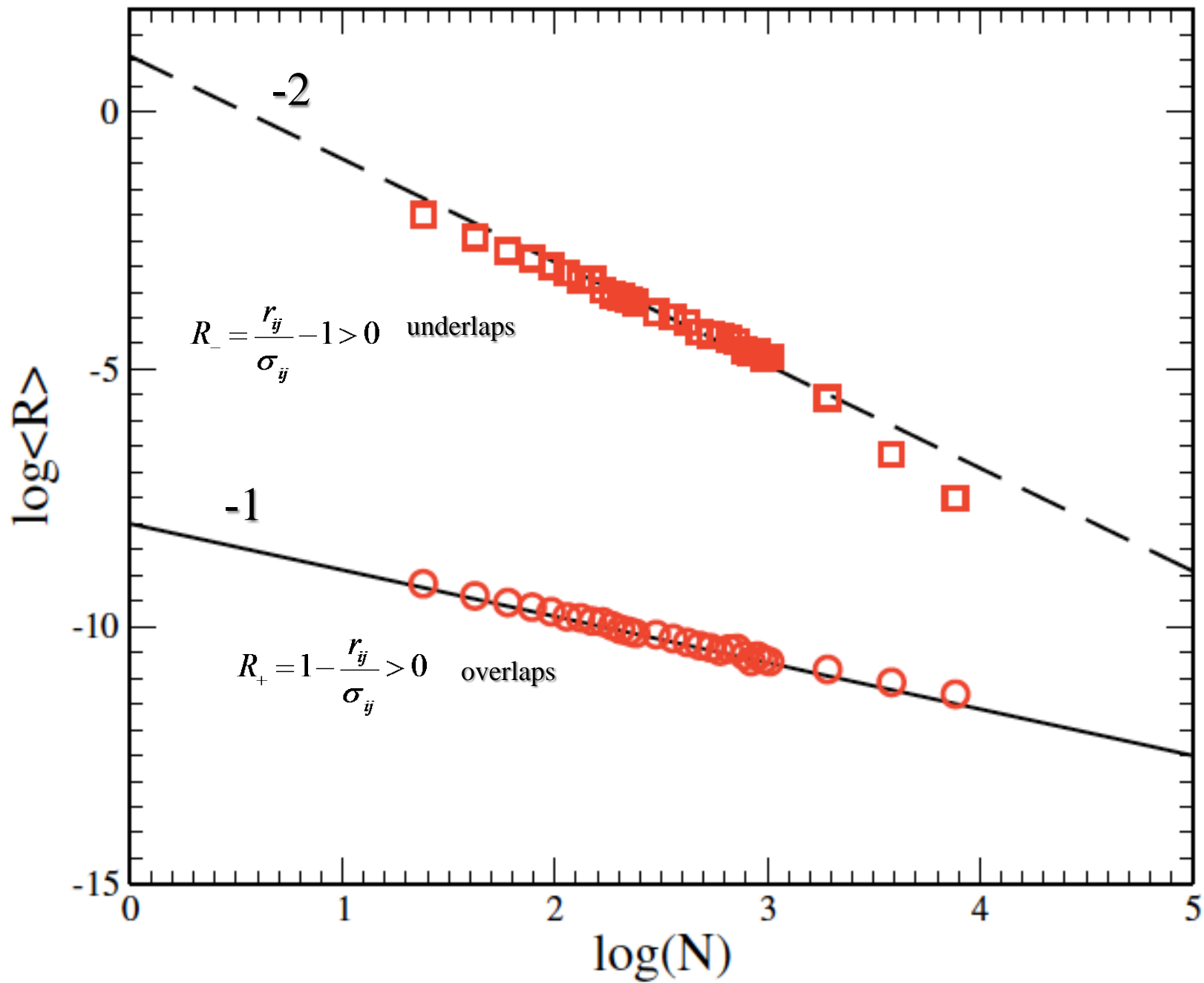
$$(\Delta\phi)_c^+ > (\Delta\phi)_c^- ?$$

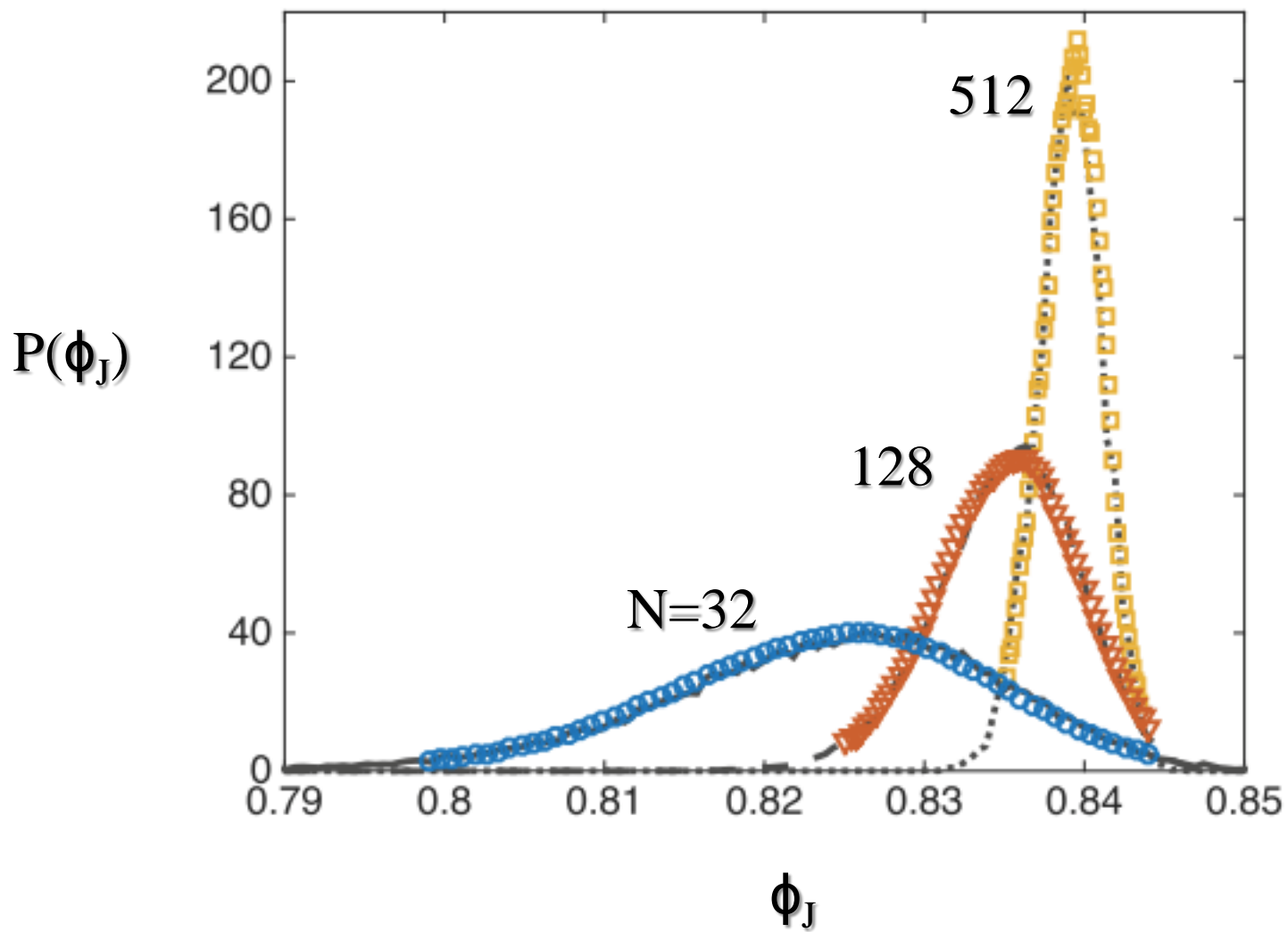
$\Delta\phi_c^+ > 0$; soft particles

$\Delta\phi_c^- < 0$; hard particles

Dissipative MD method







What have we learned so far?

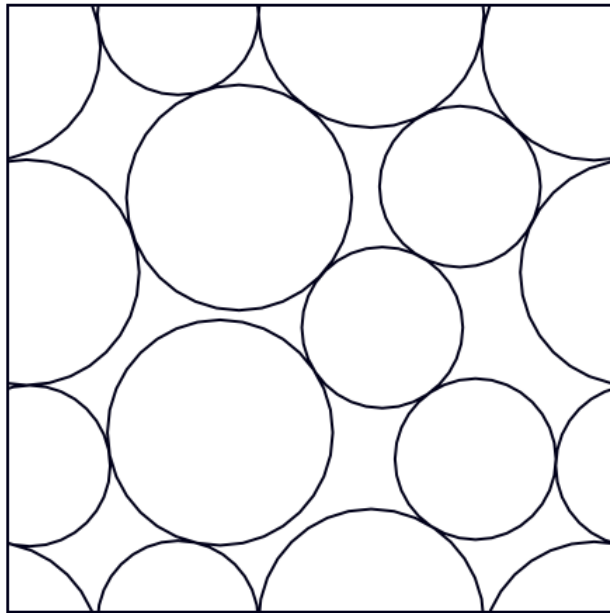
- Hard and soft sphere methods yield same *isostatic* packings, but probabilities depend on protocol
- Isostatic packings are points in configuration space
- Hypostatic packings form higher dimensional structures in configuration space

Edwards' Hypothesis for Granular Packings

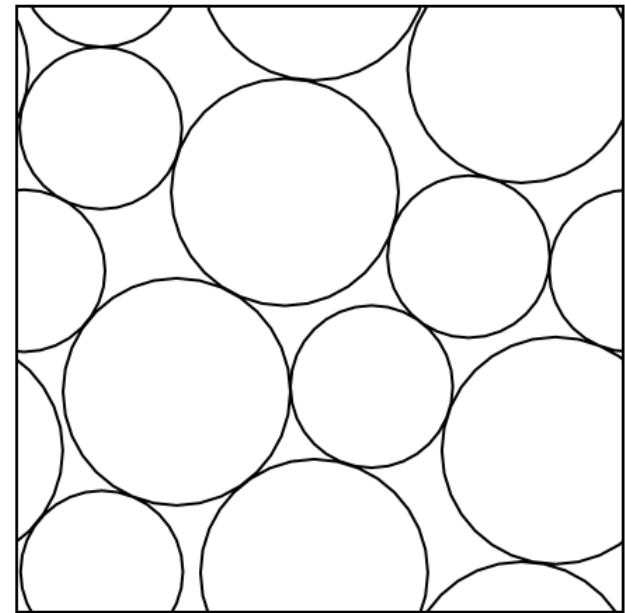
“for a given volume all [jammed] configurations are equally probable”

S. F. Edwards and R. B. S. Oakeshott, “Theory of Powders”, *Physica A* 157 (1989) 1080

...but often jammed packings are not equally likely!



rare



10^6 more frequent

Experimental protocol to generate frictionless MS packings

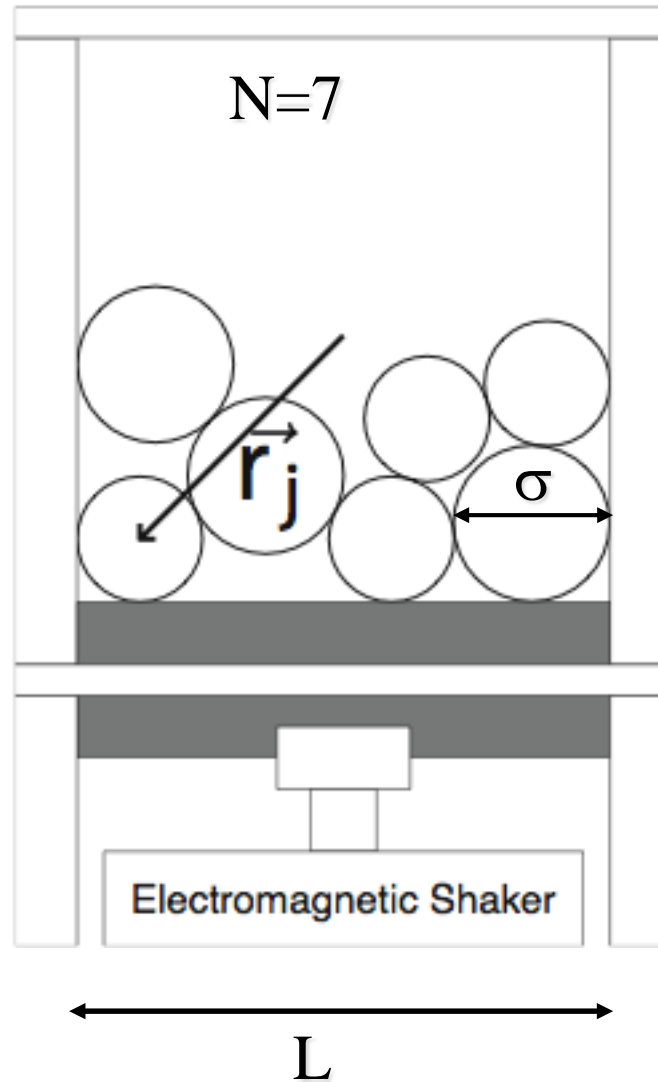
$(N+1)/2$ small particles
 $(N-1)/2$ large particles

- Plastic or steel particles

- shake and settle

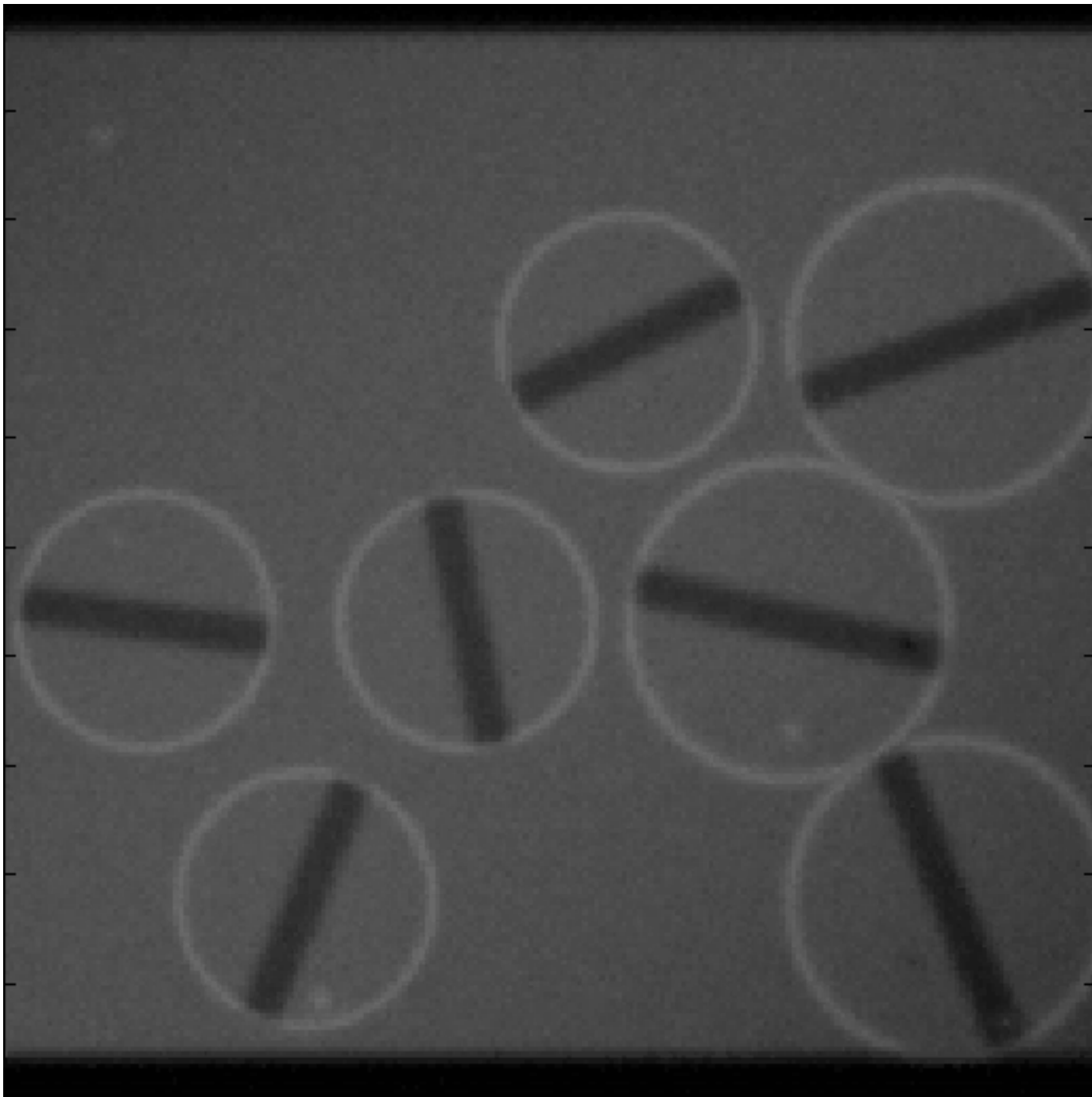
- add low amplitude, high frequency vibrations to excite particle rotation and remove frictional contacts

- repeat 10^6 times to create an ensemble of static packings



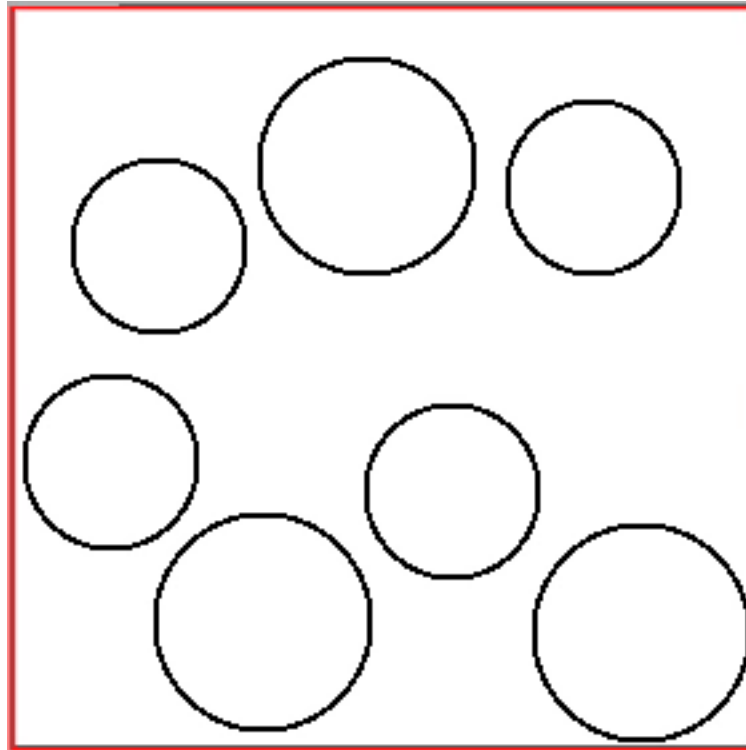
$$\frac{\sigma_L}{\sigma_S} = 1.25$$

$$\frac{L}{\sigma_S} = 4.25$$



1 cm

Deposition Algorithm in Simulations



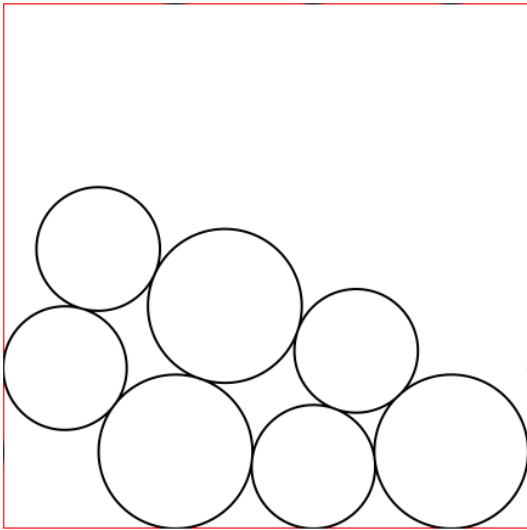
$$\bar{g} = \frac{m_s g}{k \sigma_s}$$

$$U = \frac{1}{2} \sum_{\langle i,j \rangle} k \sigma_{ij} \left(1 - \frac{r_{ij}}{\sigma_{ij}} \right)^2 \theta \left(1 - \frac{r_{ij}}{\sigma_{ij}} \right)$$

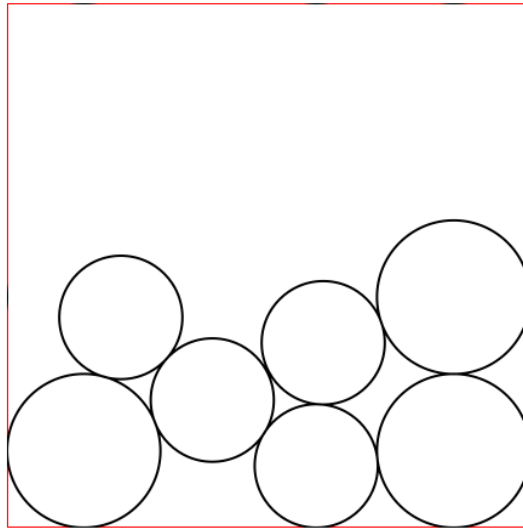
$$\sigma_{ij} = \frac{(\sigma_i + \sigma_j)}{2}$$

- All geometric parameters identical to those for experiments
- Terminate algorithm when $F_{\text{tot}} < F_{\text{max}} = 10^{-14}$
- Vary random initial positions and conduct $N_{\text{trials}} = 10^8$ to find ‘all’ mechanically stable packings for small systems $N=3$ to 10.

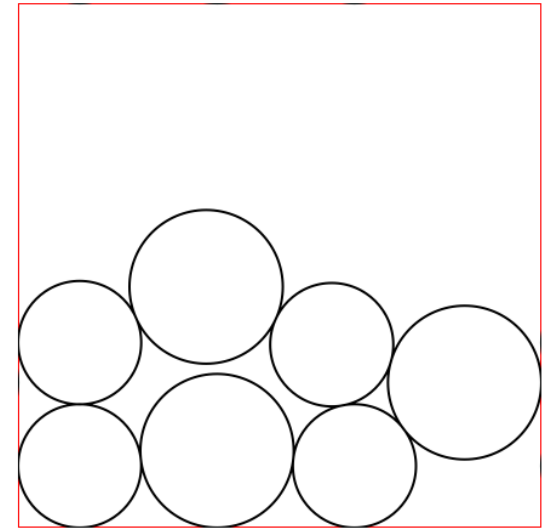
Mechanically Stable Frictionless Packings



1



2

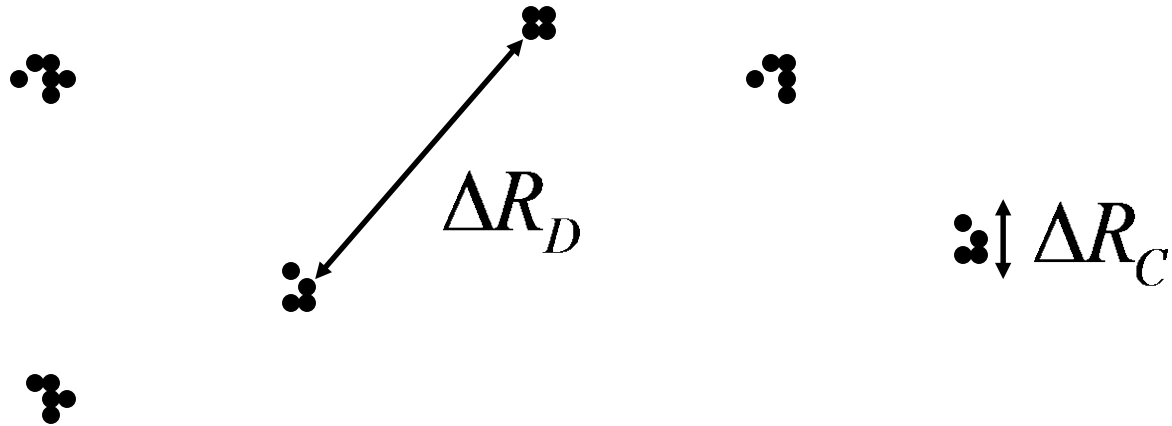


3

- Distinct MS packings distinguished by particle positions $\{\vec{r}_i\}$

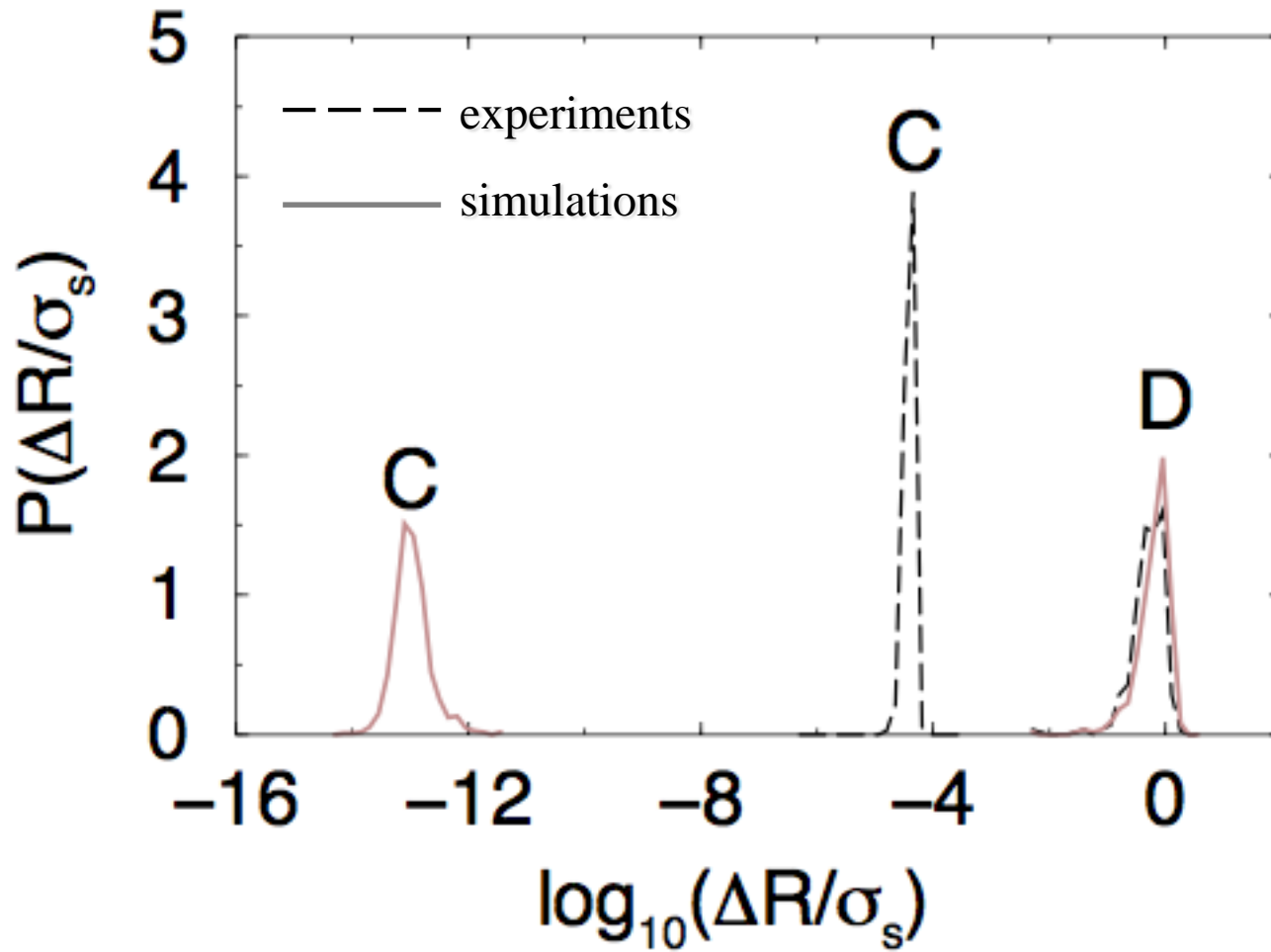
Configuration Space of Mechanically Stable Packings

$$R = \{ \vec{r}_1, \vec{r}_2, \dots, \vec{r}_N \}$$



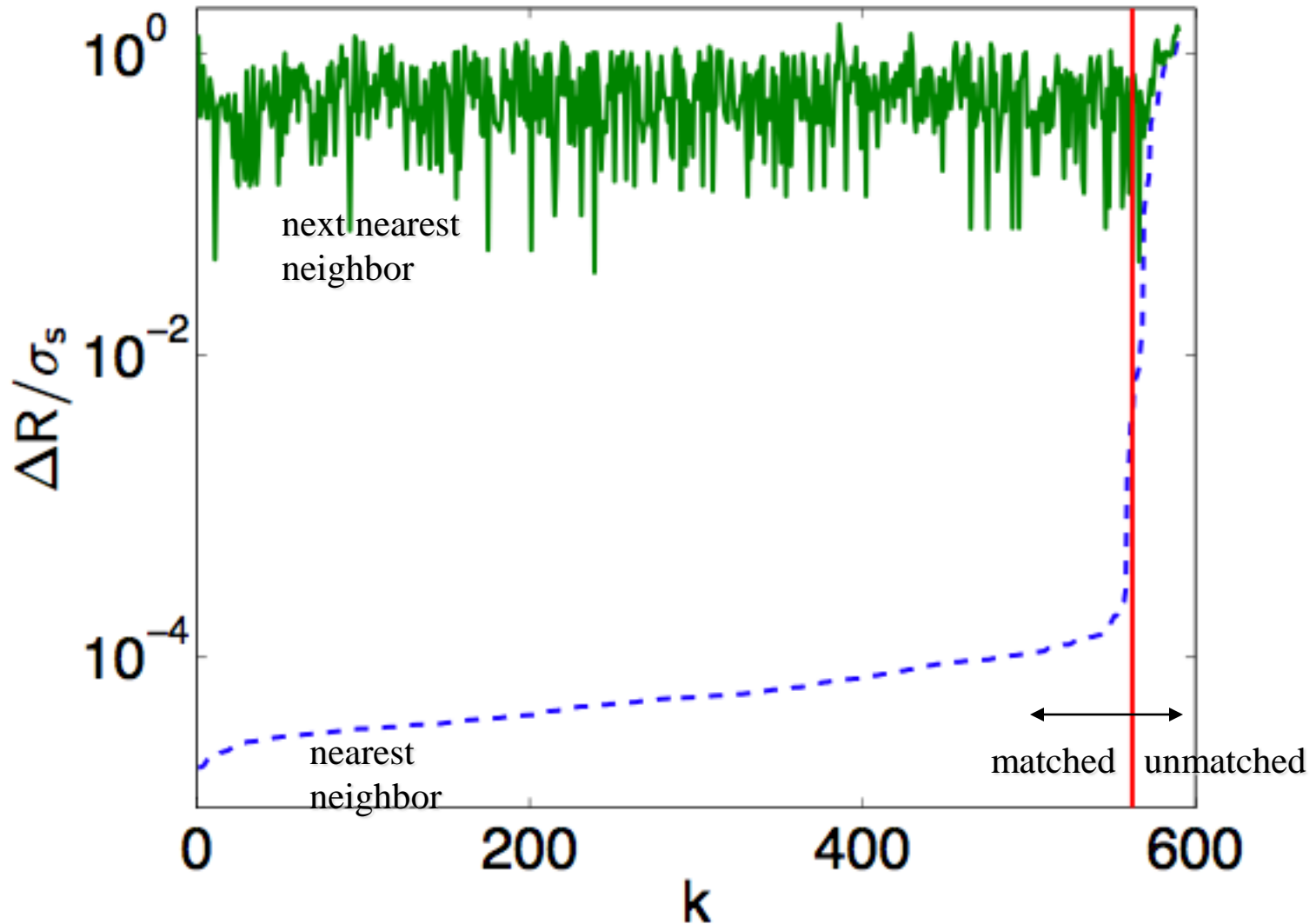
- ΔR_D = distance in configuration space between distinct MS packings
- ΔR_C = error in measuring distinct MS packings

Separation in Configuration Space



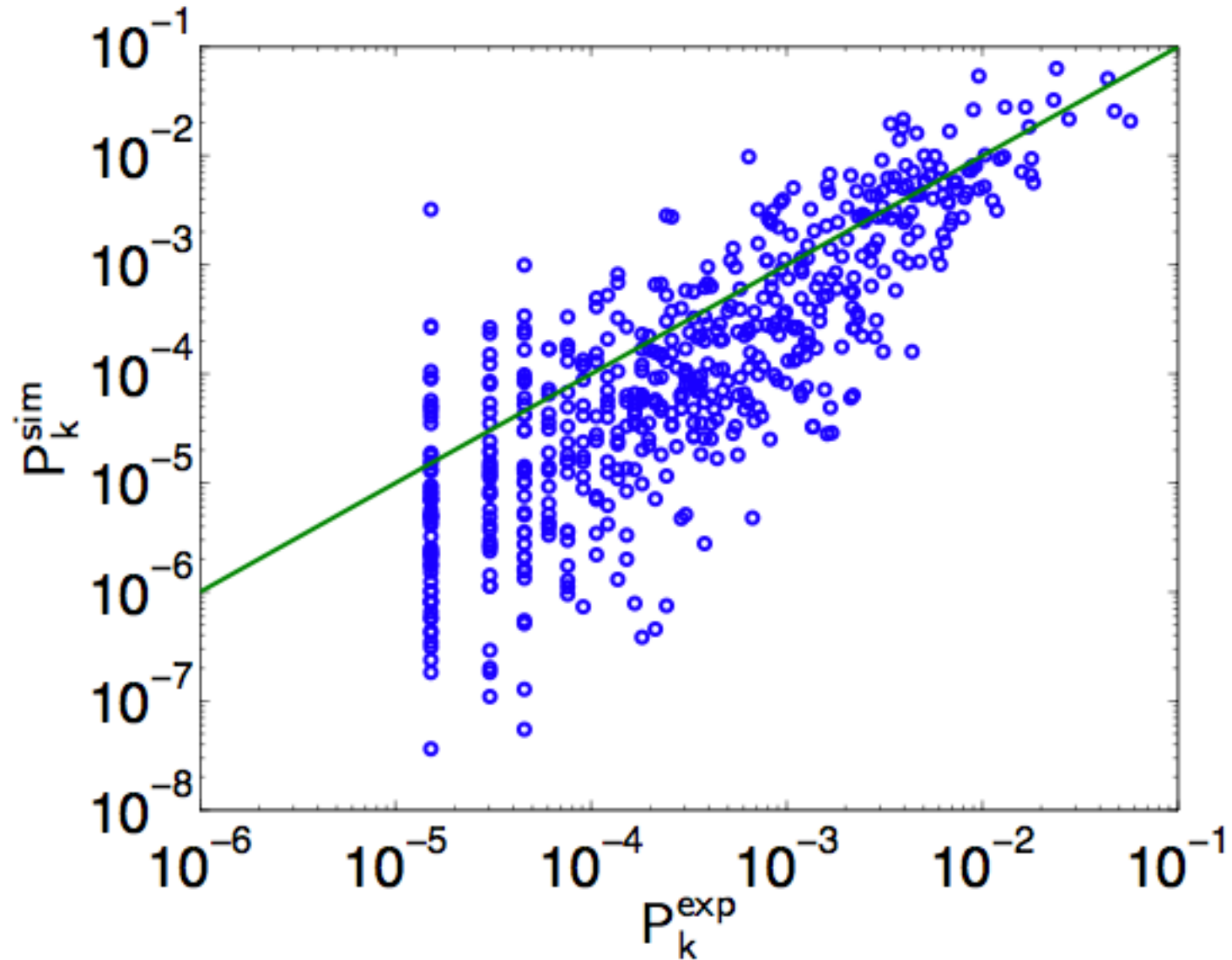
- MS frictionless packings are discrete points in configuration space

How is the quantitative agreement between sims and exps?



- 95% of distinct MS packing match; others are unstable in sims

MS Packing Probabilities Are Robust

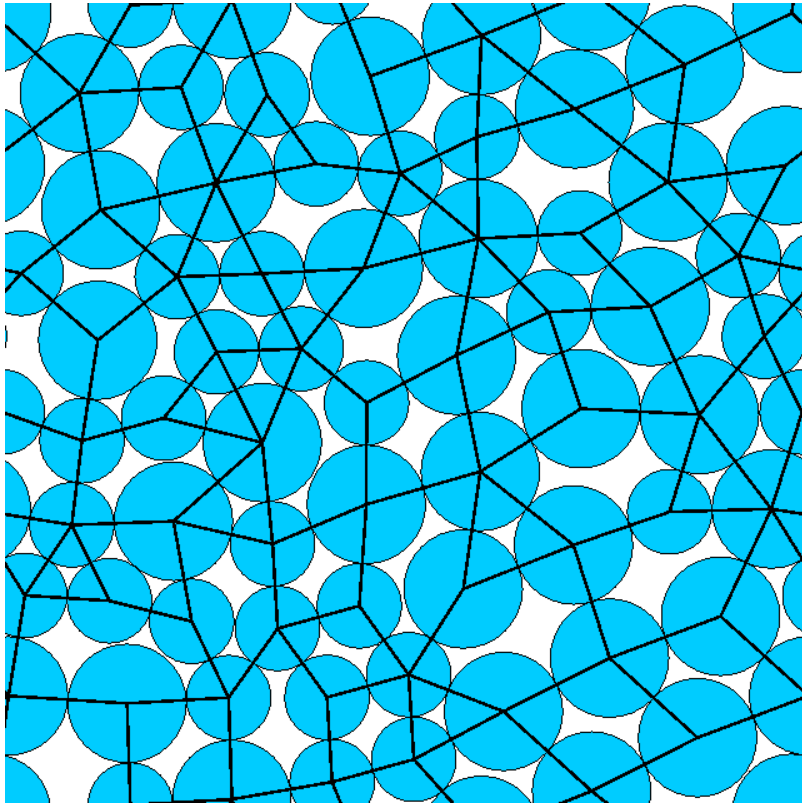


- Rare MS packings in expts are rare in sims; frequent MS packings in expts are frequent in sims

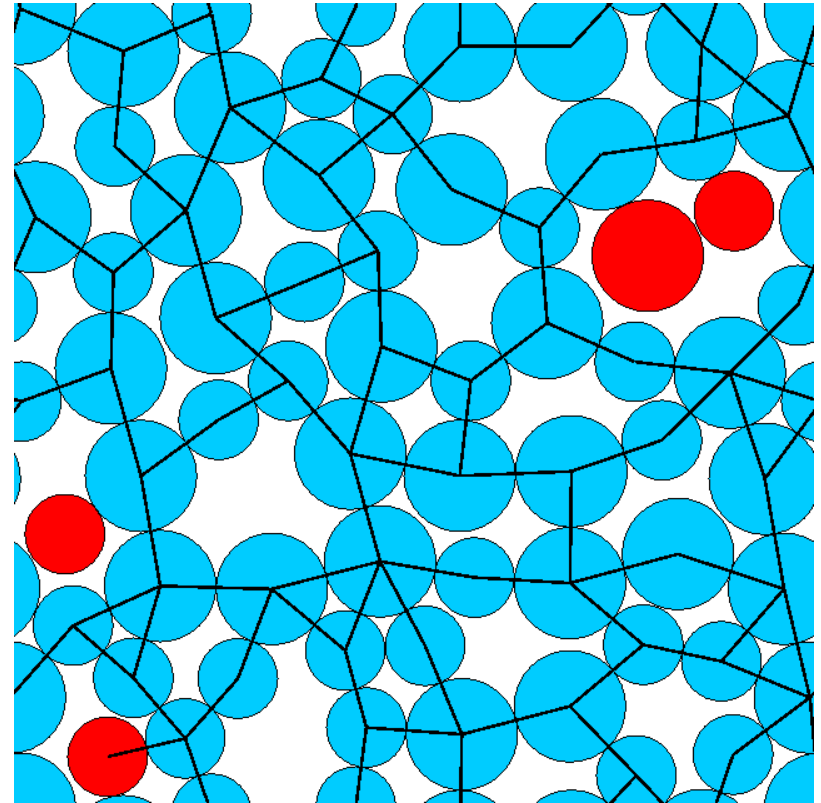
Frictional Packings

Key Points

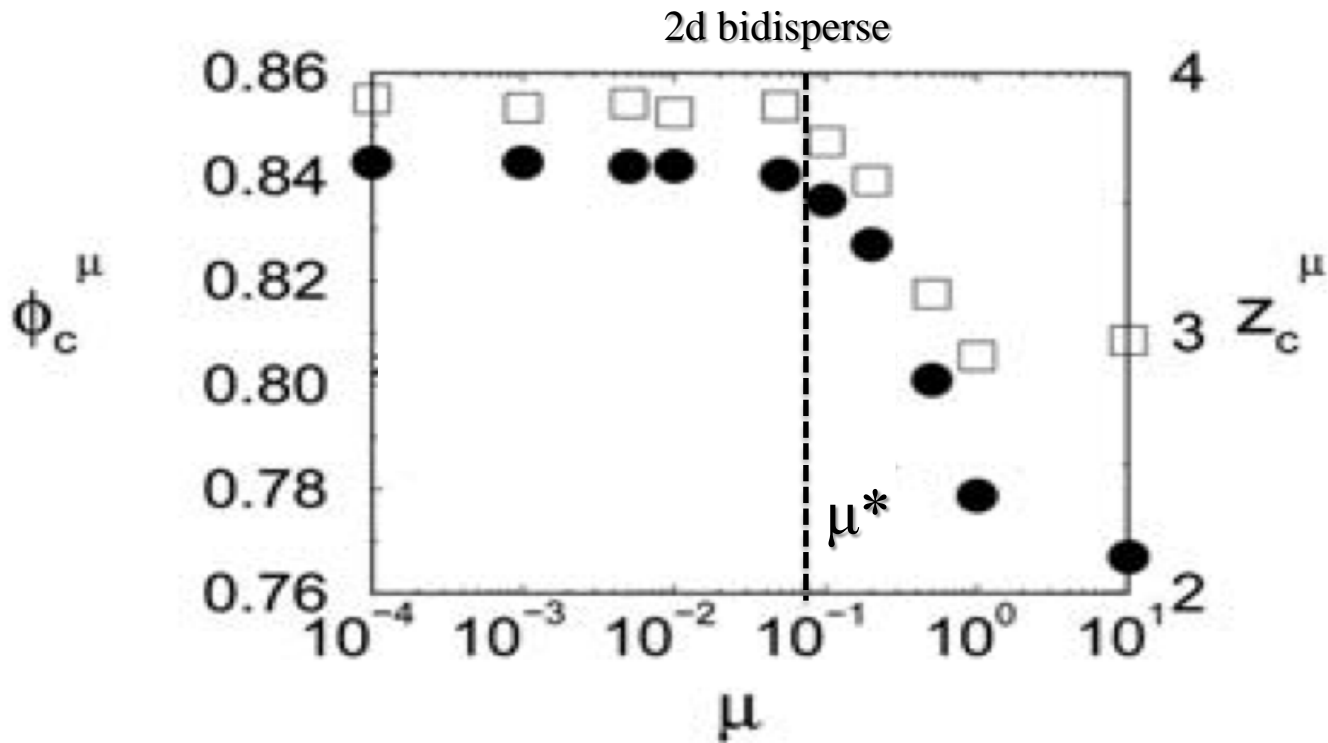
- Frictionless packings at jamming onset occur as *points* in configuration space with $N_c = N_c^0$ and $\phi = \phi_J$
- Frictional packings at jamming onset occur as finite dimensional subspaces in configuration space with $N_c < N_c^0$ and $\phi < \phi_J$
- Probability to obtain a particular frictionless packing at jamming onset is determined by fraction of *initial conditions* that “are collected” by that packing
- Probability to obtain frictional packing with a given number of contacts is proportional to the volume of configuration space occupied by admissible packings



small μ ; $\langle z \rangle = 4$; $\phi_J \sim 0.84$



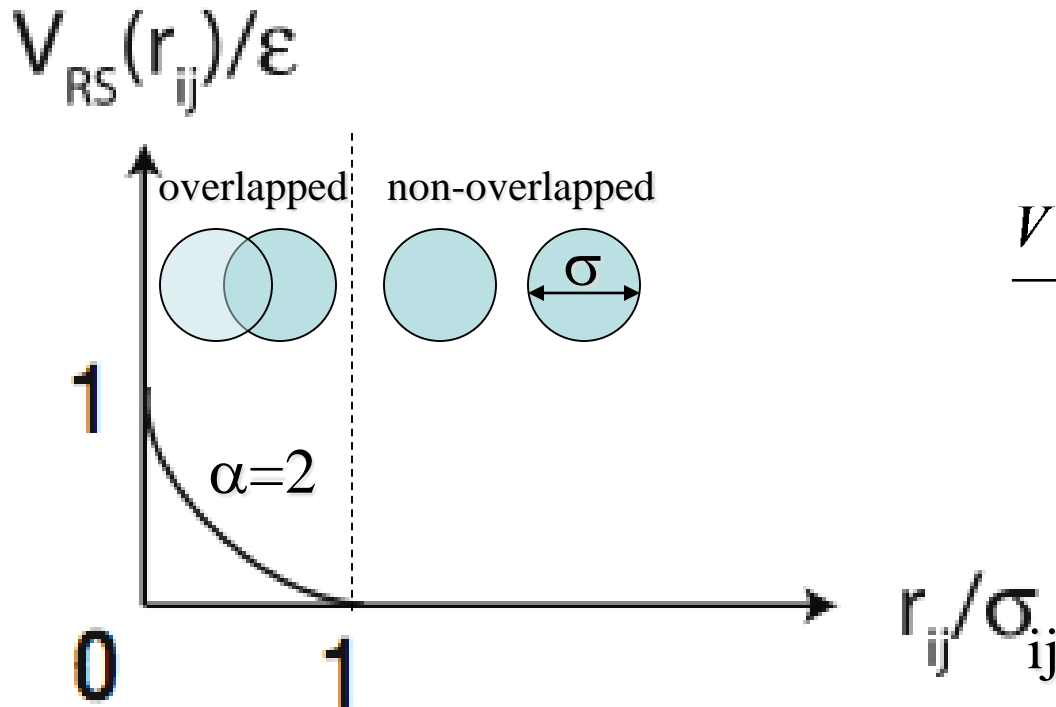
large μ ; $\langle z \rangle \sim 3$; $\phi_J \sim 0.76$



What is the characteristic μ^* above which static packings transition from frictionless to frictional? Does this crossover depend on N ? How does μ^* depend on packing-generation protocol?

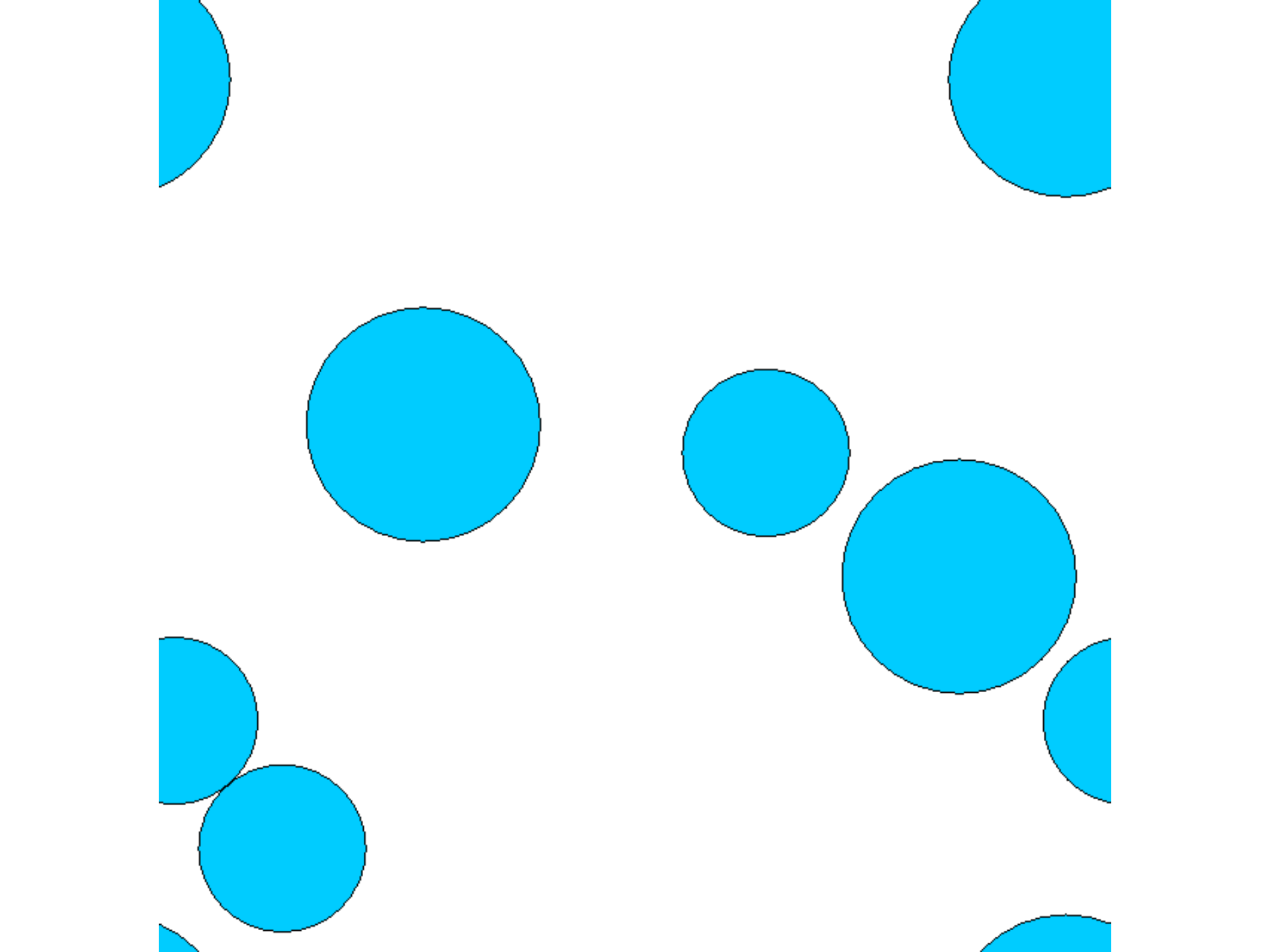
Can we predict the structural and mechanical properties of frictional packings using frictionless packings?

Contact Interactions



$$\frac{V(r_{ij})}{\epsilon} = \alpha^{-1} \left(1 - \frac{r_{ij}}{\sigma_{ij}}\right)^{\alpha} \theta\left(1 - \frac{r_{ij}}{\sigma_{ij}}\right)$$

Total potential energy $V = \sum_{\langle i,j \rangle} V(r_{ij})$

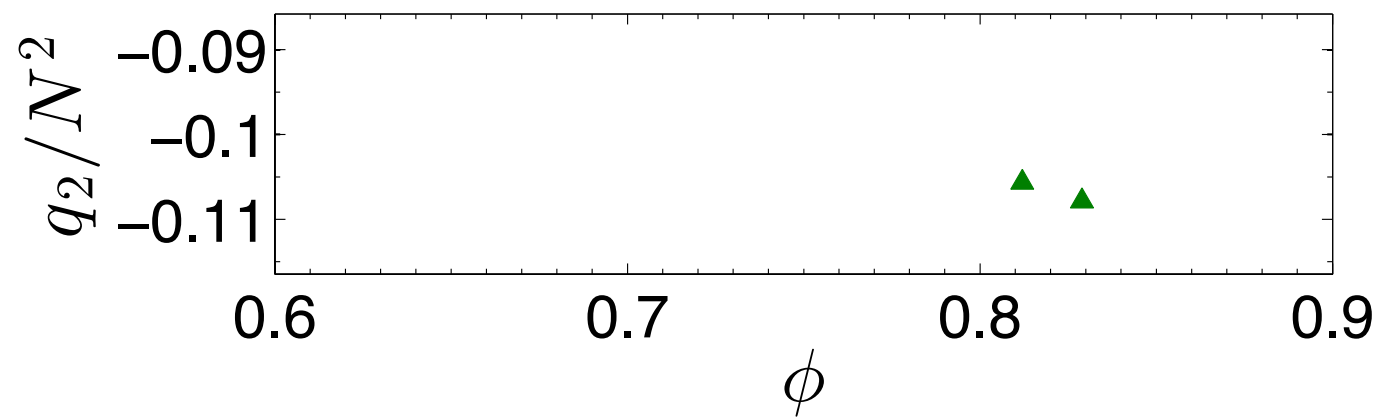
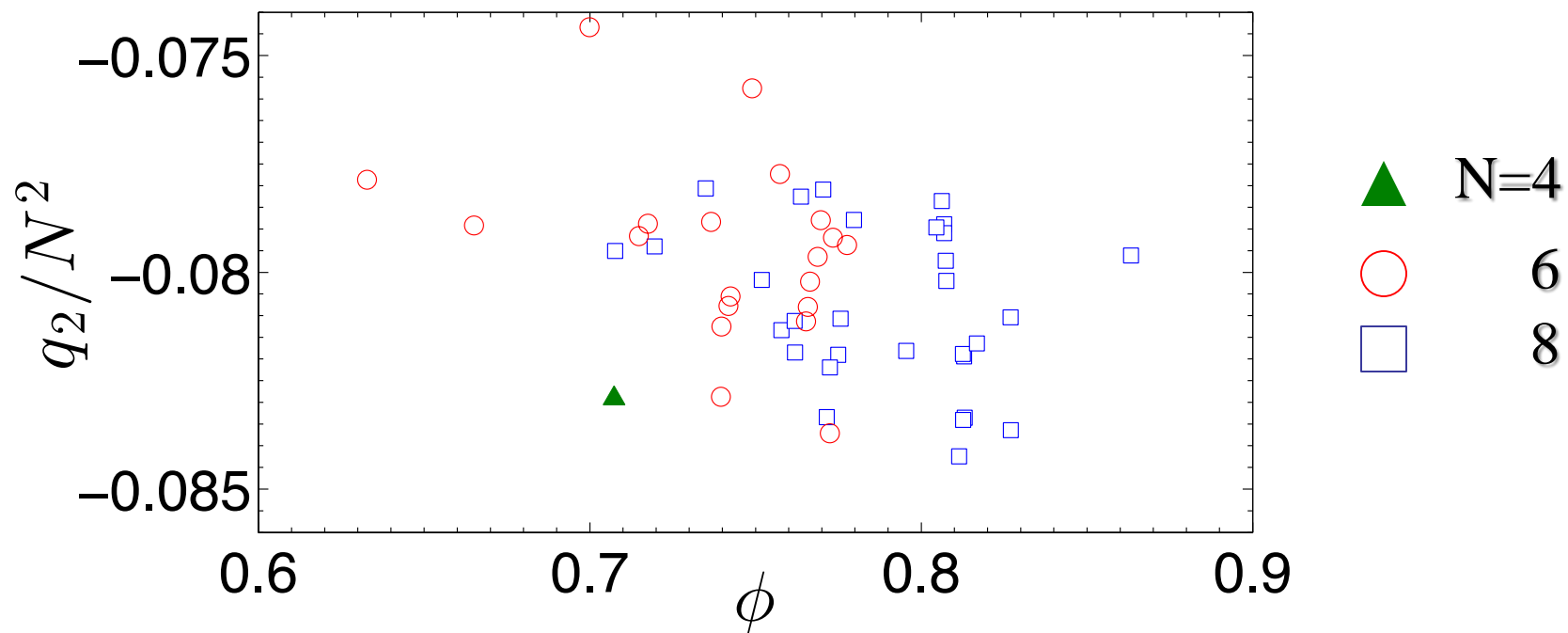


Classification of Packings

Distance matrix $D_{ij} = \left| \vec{r}_i - \vec{r}_j \right|$ particles i, j

Second invariant $q_2 = \frac{1}{2} \left((TrD)^2 - Tr(D^2) \right)$

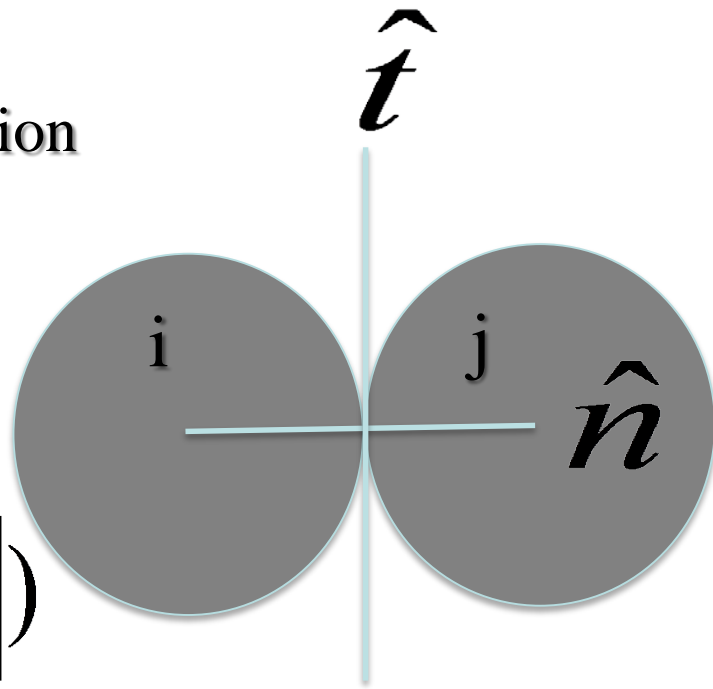
Distance Matrix for Frictionless Packings



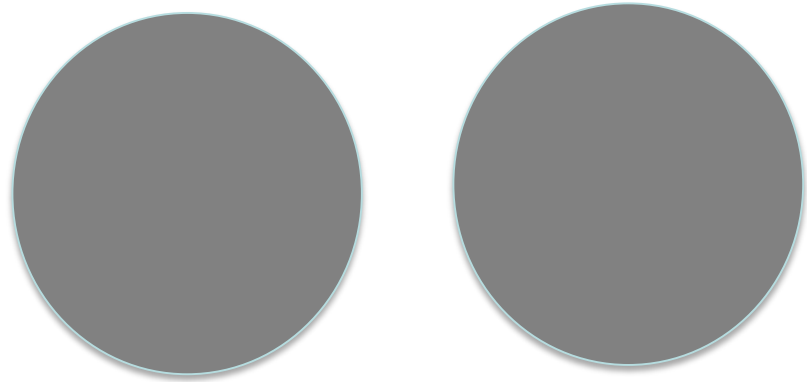
Cundall-Strack Model for Friction

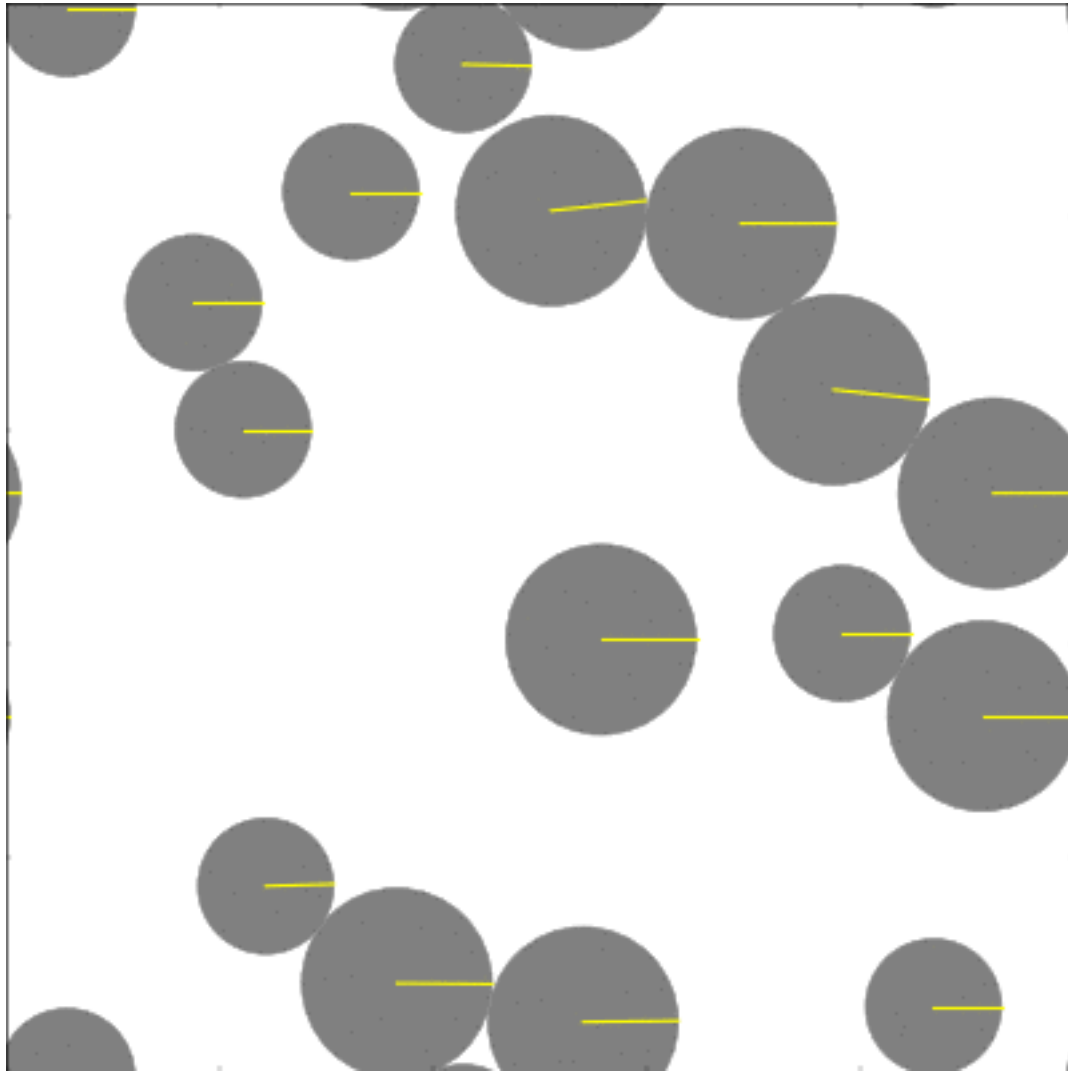
$$F_n^{ij} = k_n (\sigma - r_{ij})$$

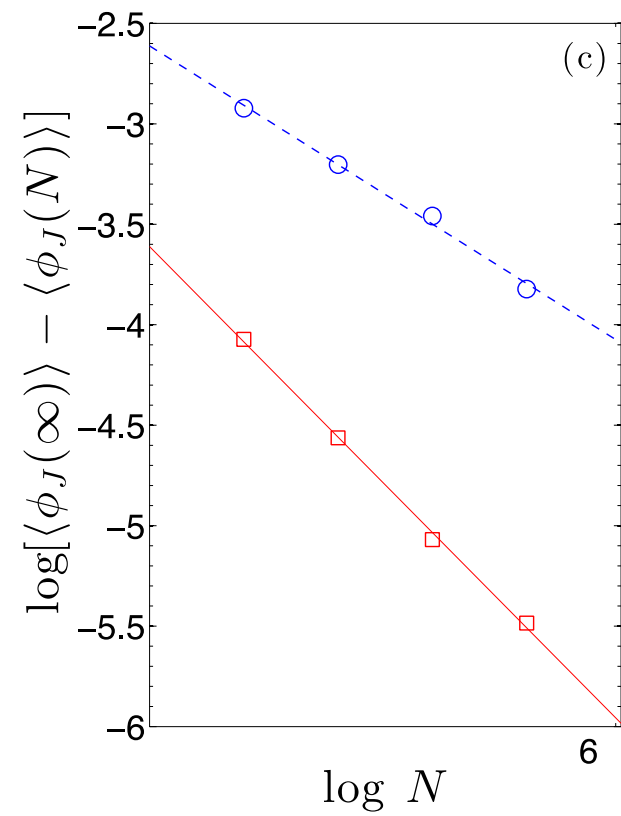
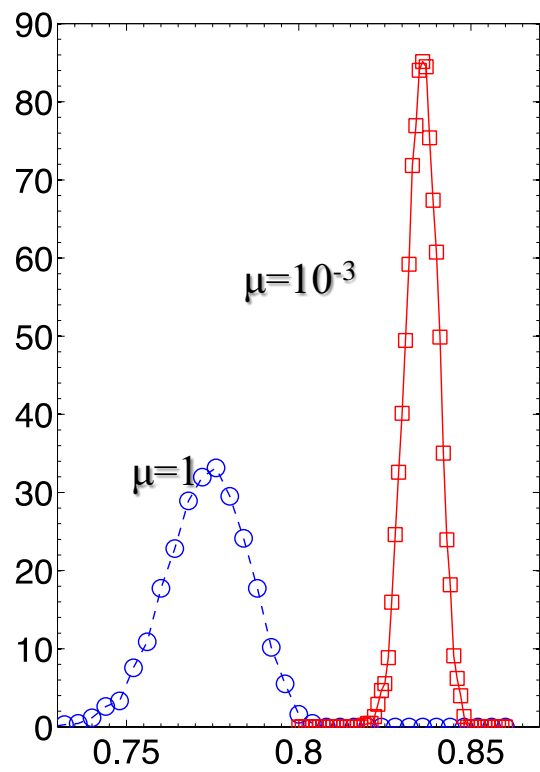
$$F_t^{ij} = \min(|k_t \Delta u_t|, \mu |F_n^{ij}|)$$



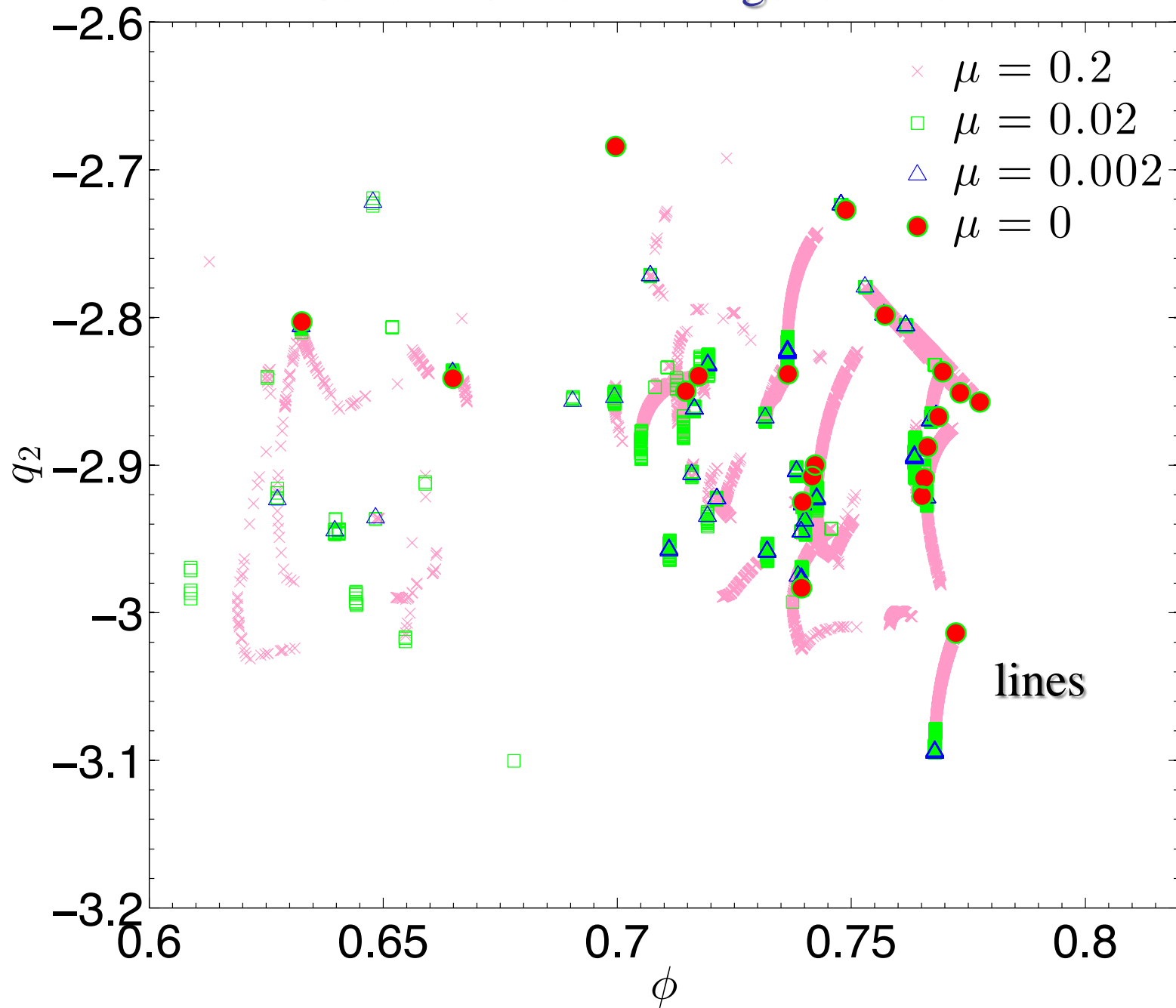
$$F_{n,t}^{ij} = 0$$





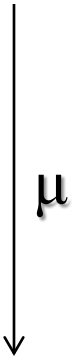


Cundall-Strack Packings for N=6

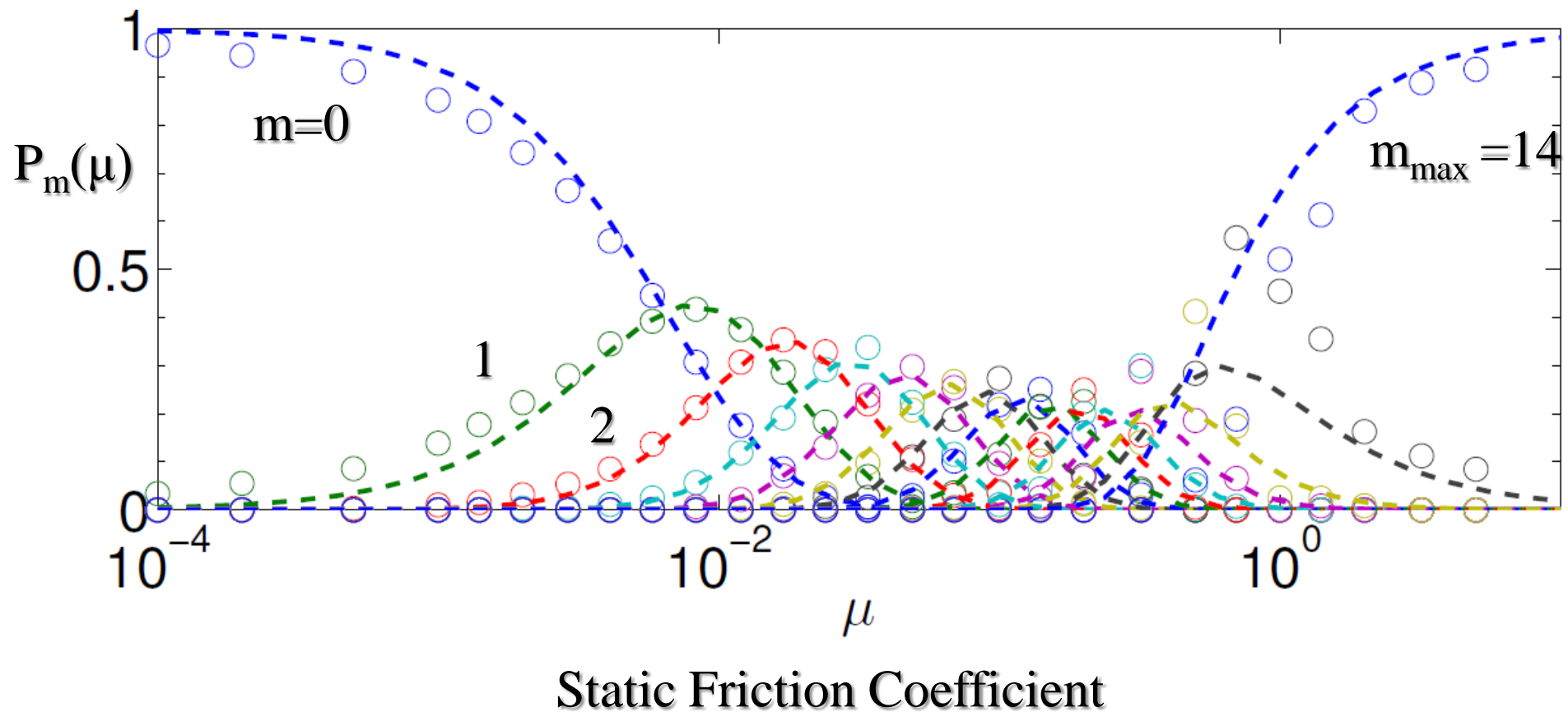


Packings of frictional particles are saddle packings of frictionless particles

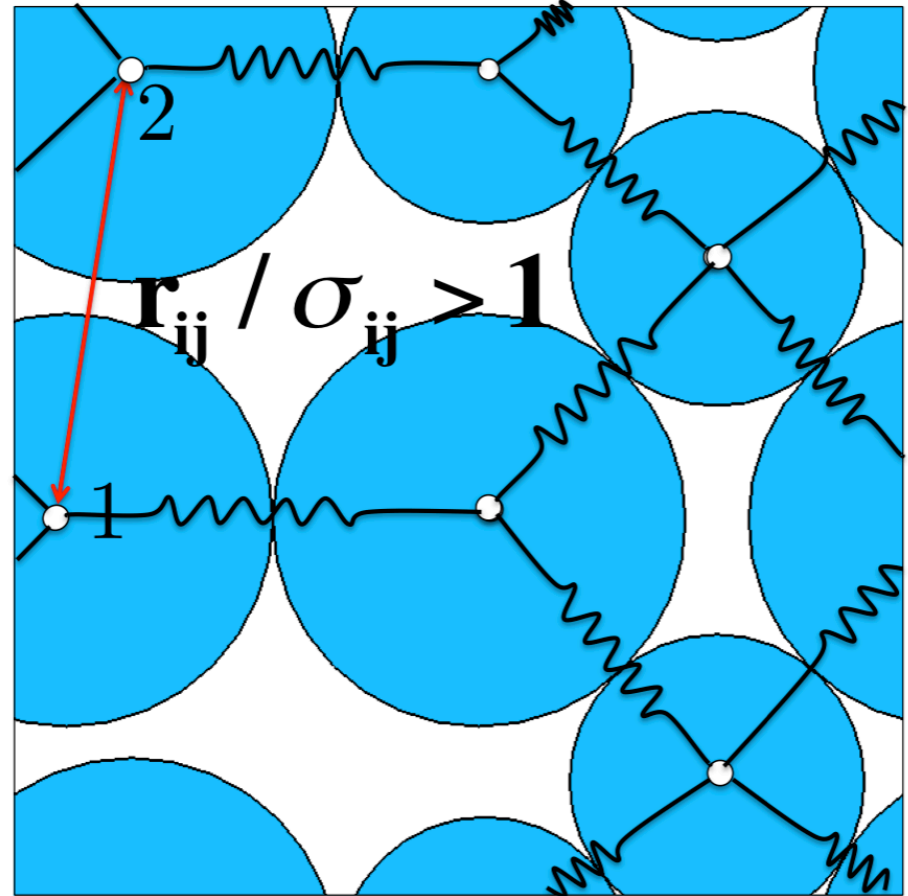
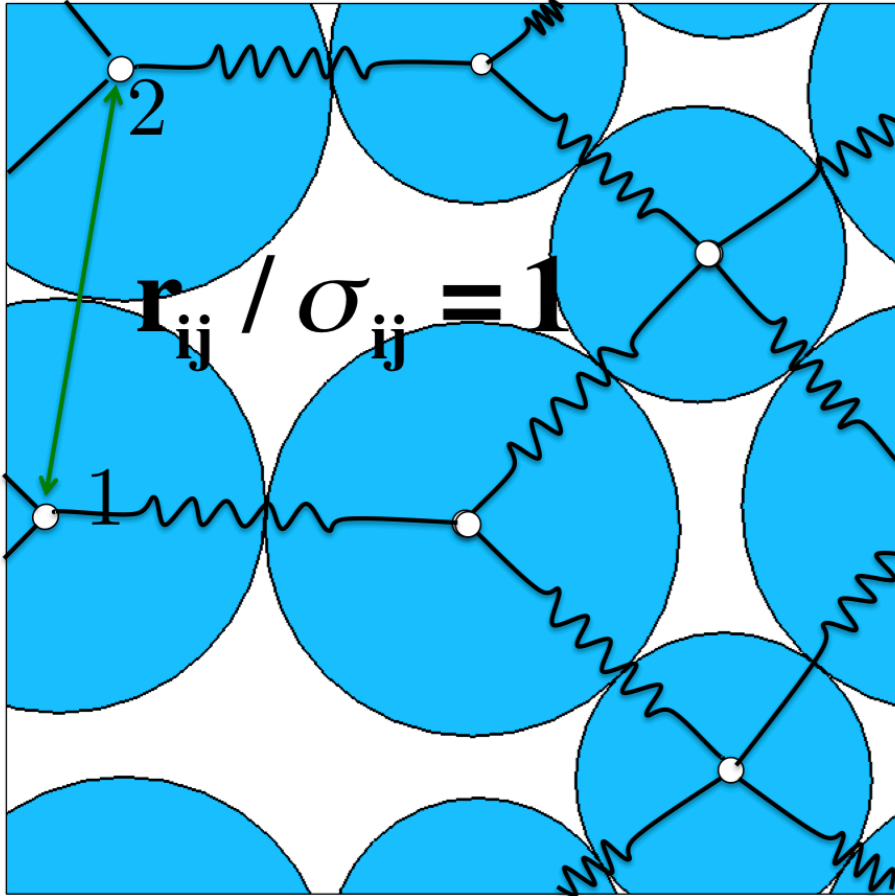
Saddle number (m)	$N_c^{iso} - N_c$	N_c
0	0	$N_c = 2N - 1$
1	1	.
.	.	.
.	.	.
.	.	.
$N/2 - 1$	$N/2 - 1$	$N_c = 3/2N$



Probability of m^{th} Order Saddles For $N=30$ Frictional Packings

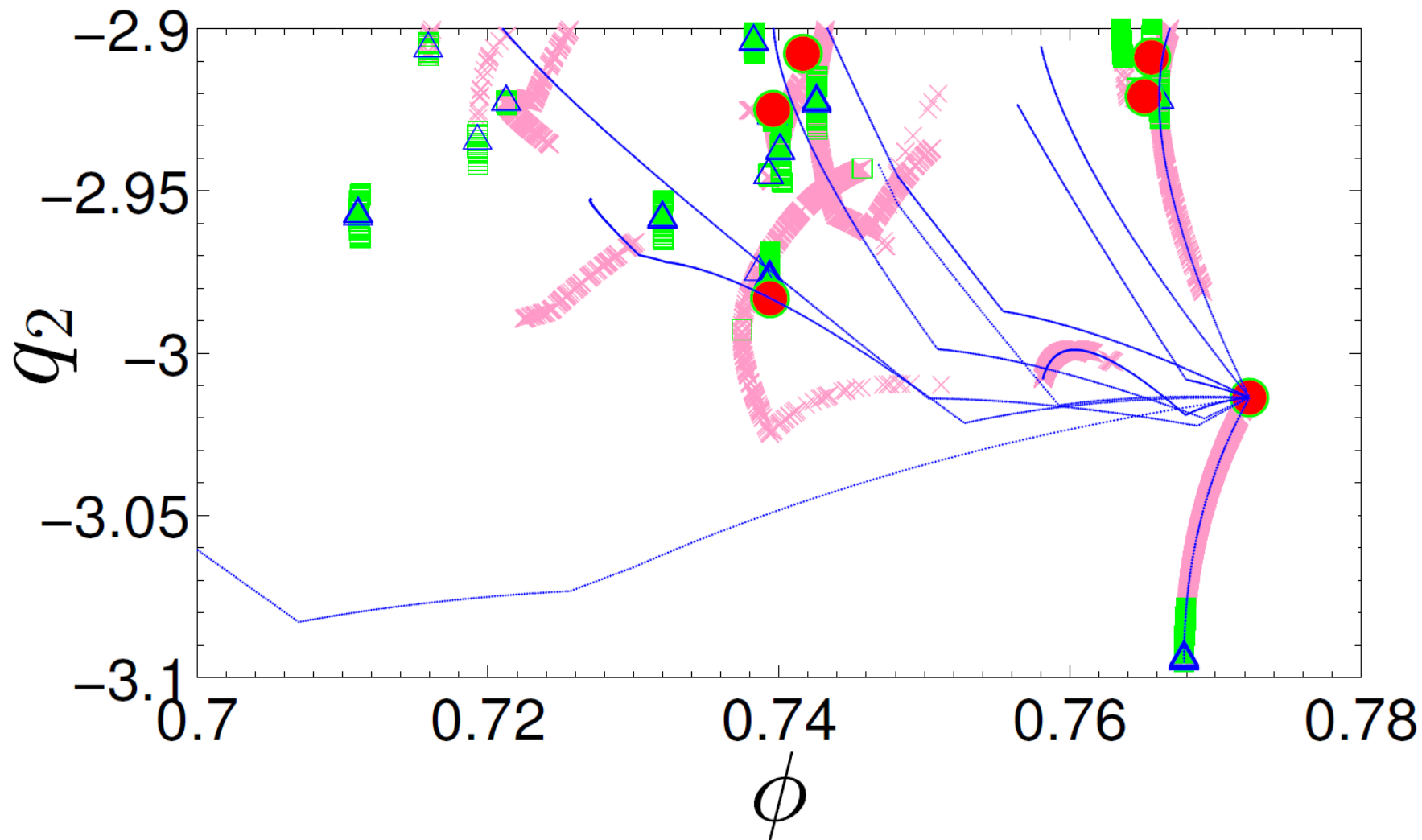


Spring Model



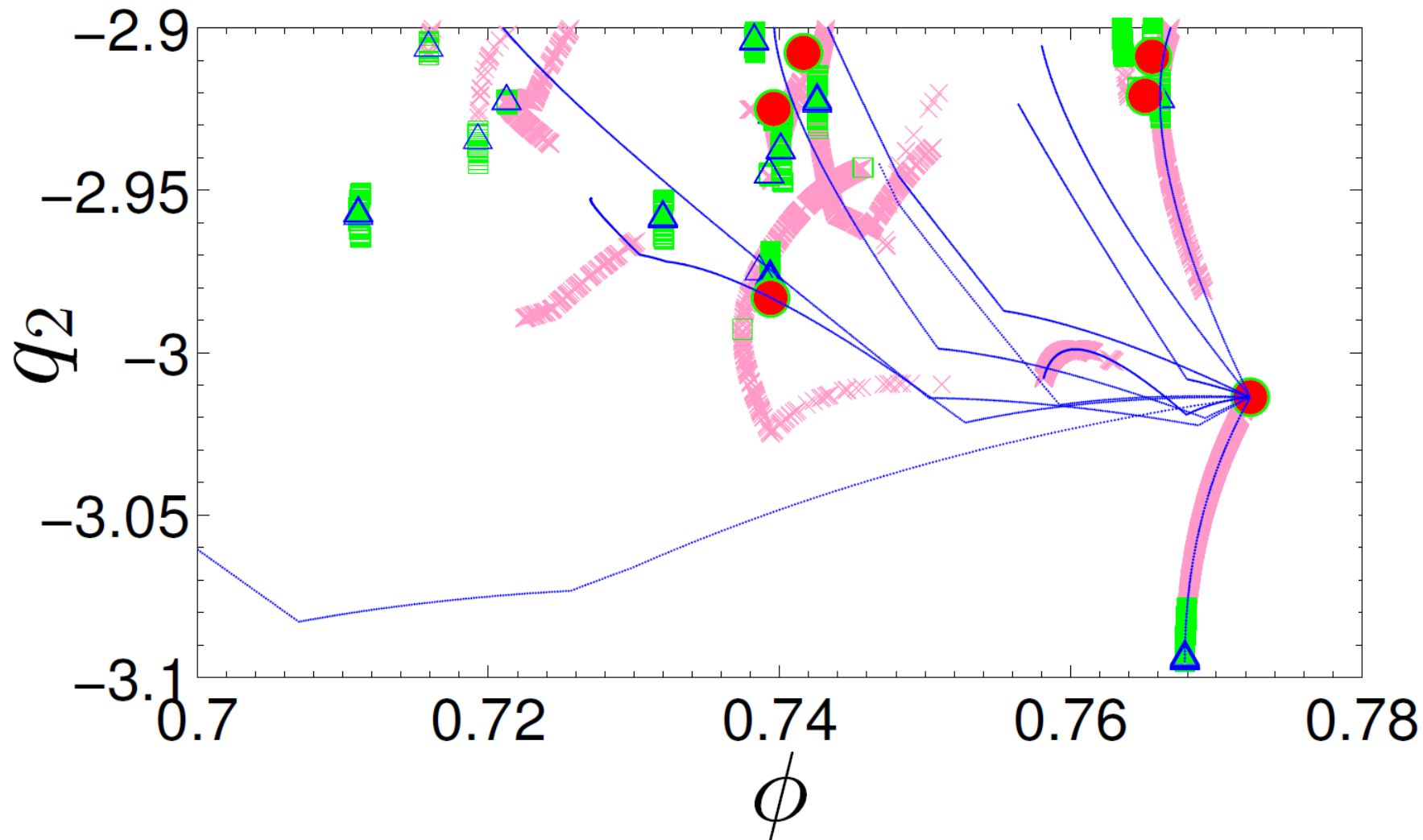
Cundall-Strack Frictional Packings

1st Order Saddles Enumerated

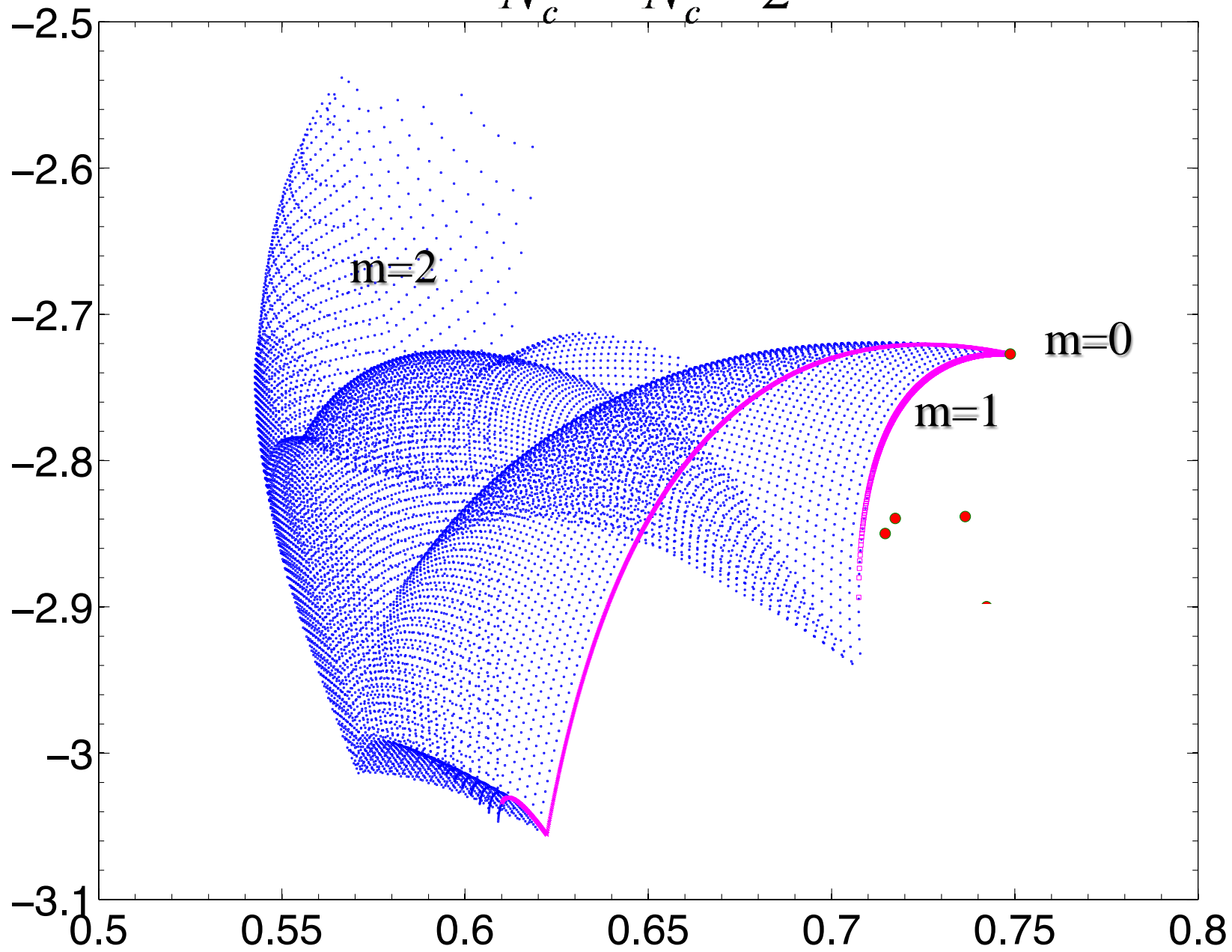


Cundall-Strack Frictional Packings

1st Order Saddles Enumerated

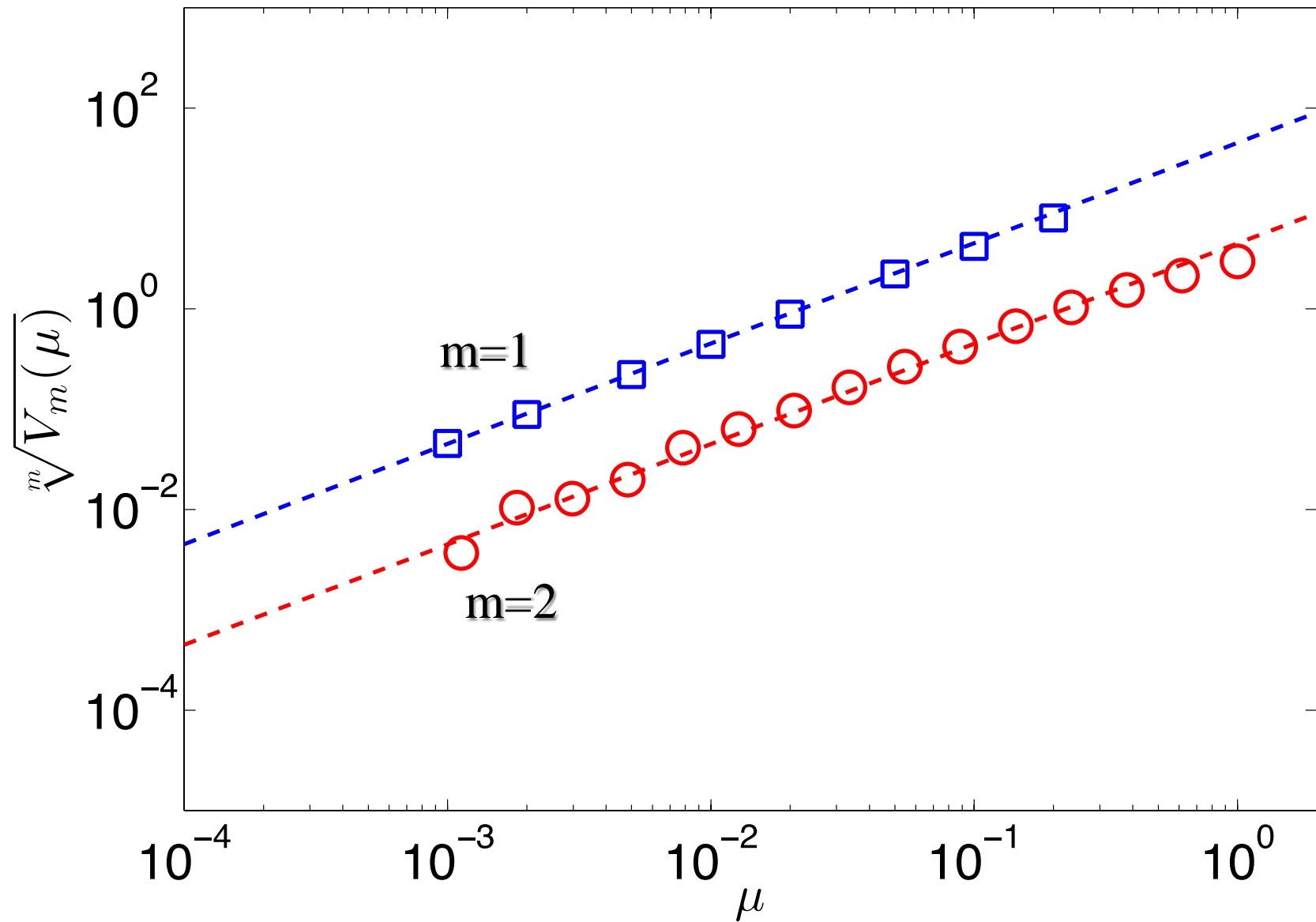


$$N_c^{iso} - N_c = 2$$



Theoretical description for $P_m(\mu)$

- Enumerate all $m=0, 1, 2, \dots$ packings
- Calculate volume of configuration space $V_m(\mu)$ for a given m where packings are stabilized by $\mu' \leq \mu$ with $F_n^{ij} > 0$ and $|F_t^{ij}| \leq \mu |F_n^{ij}|$
- Find that $V_m(\mu) \sim \mu^m$



Theoretical description for $P_m(\mu)$

$$Z_m(\mu) \propto V_m(\mu) \delta^{2N-1-m}$$

$$\frac{Z_m(\mu)}{Z_0(\mu)} \propto \left(\frac{l(\mu)}{\delta} \right)^m$$

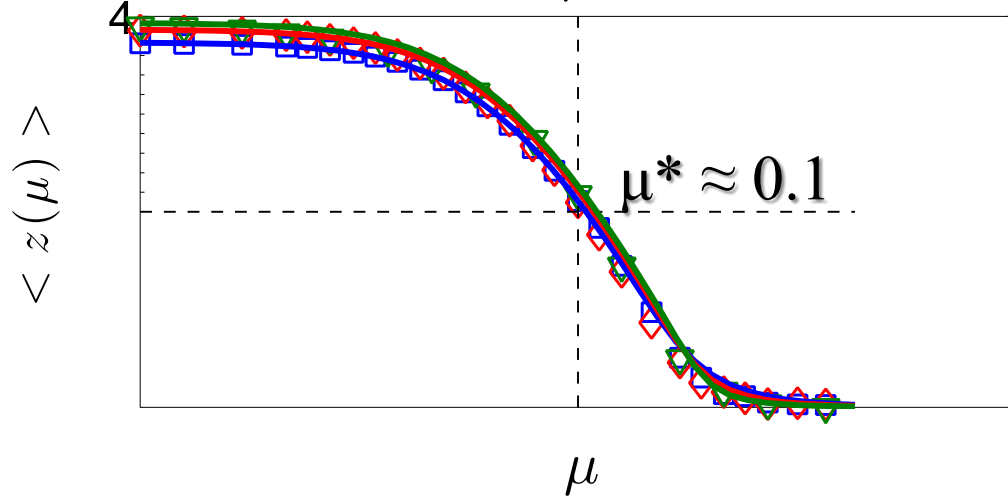
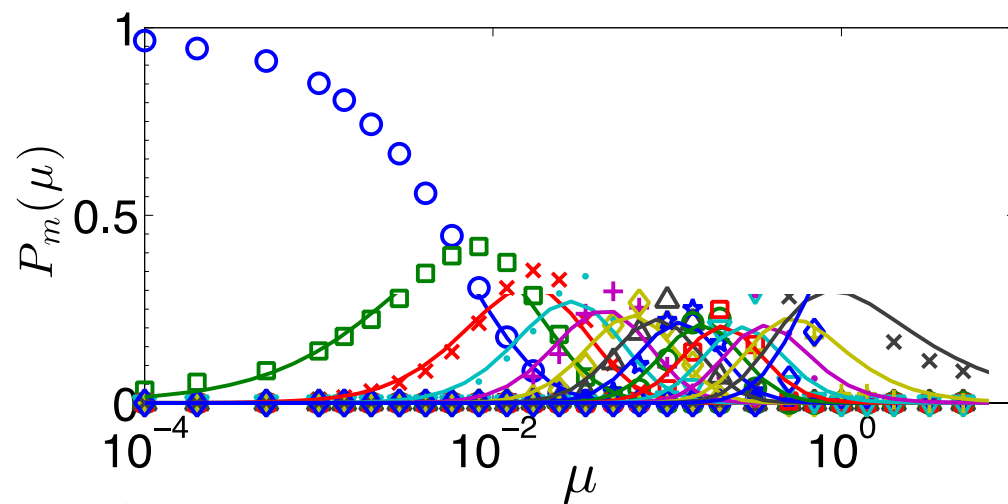
$$P_m(\mu) = \frac{A_m \mu^m}{\sum_{m=0}^{m_{\max}} A_m \mu^m} = \frac{a_m \mu^m}{1 + \sum_{m=1}^{m_{\max}} a_m \mu^m}$$

$$A_m \approx N_s(N) N_b(N, m)$$

m=0

m=14

N=30



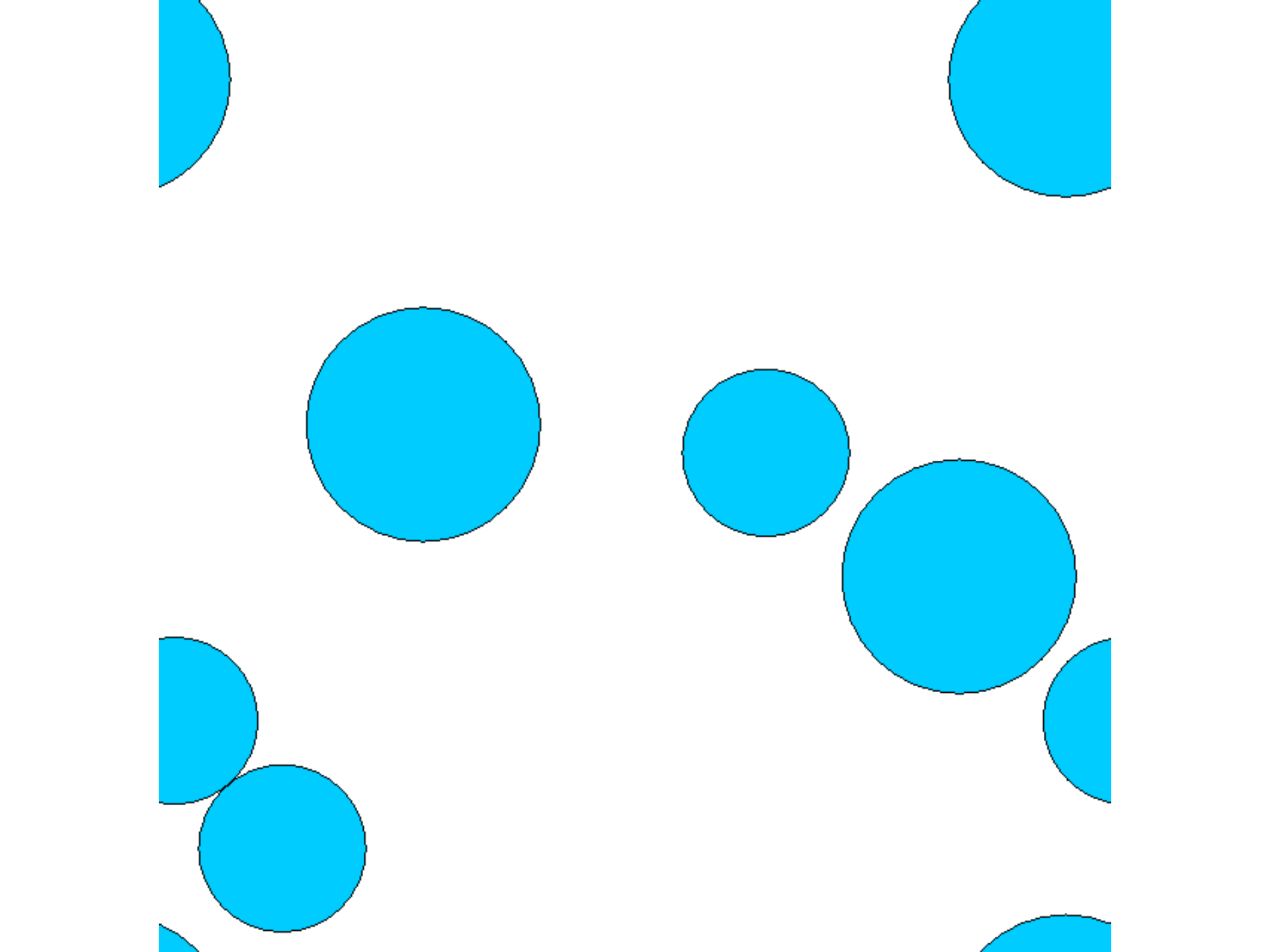
N=30, 64, 128

Conclusions

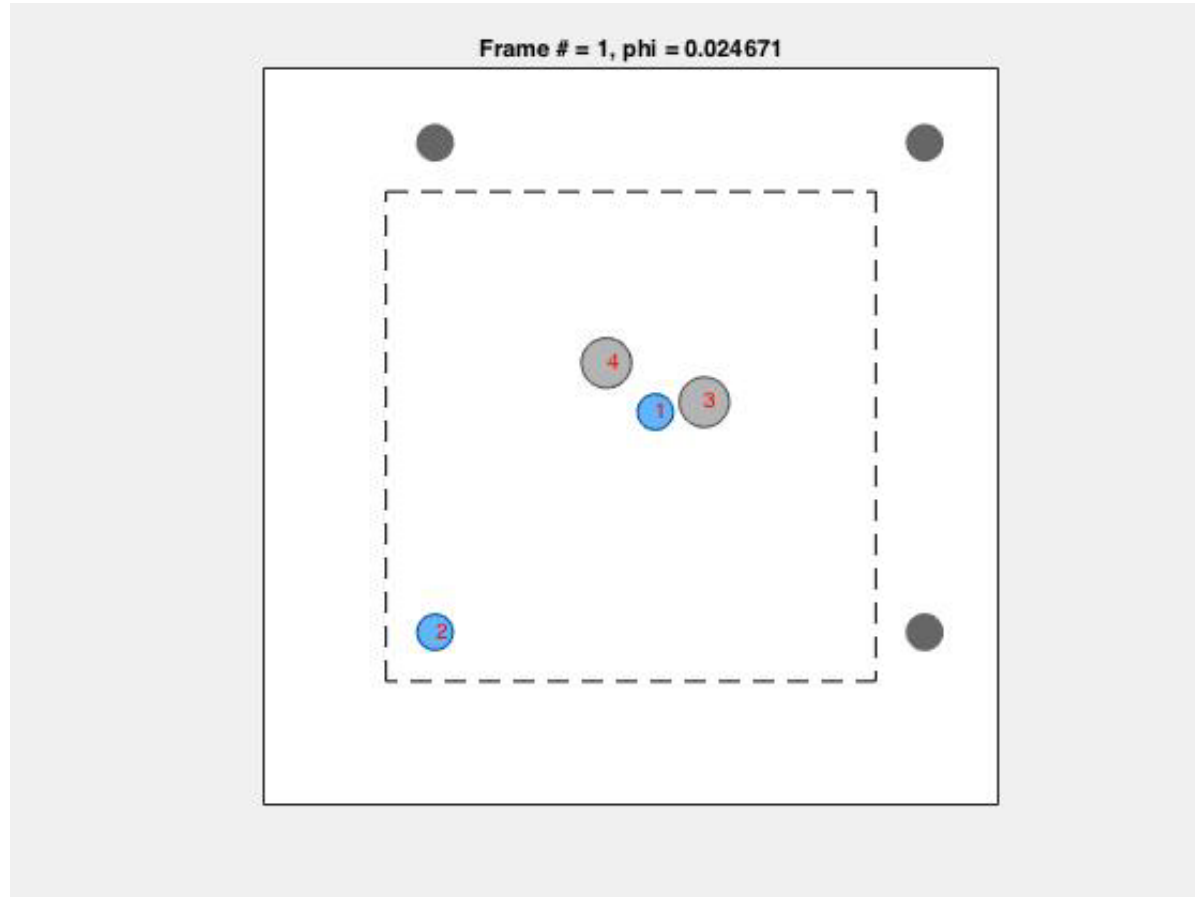
1. Frictional packings can be organized by saddle order m .
1. Frictional packings occur as geometrical families in dimension m .
1. Can predict $\langle z \rangle(\mu)$ in large systems using enumeration of packings in small systems.
4. Similar theoretical description holds for $m < 0$ for overcompressed frictionless packings.
5. How does $\langle z \rangle(\mu)$, $\phi_J(\mu)$ depend on packing-generation protocol?

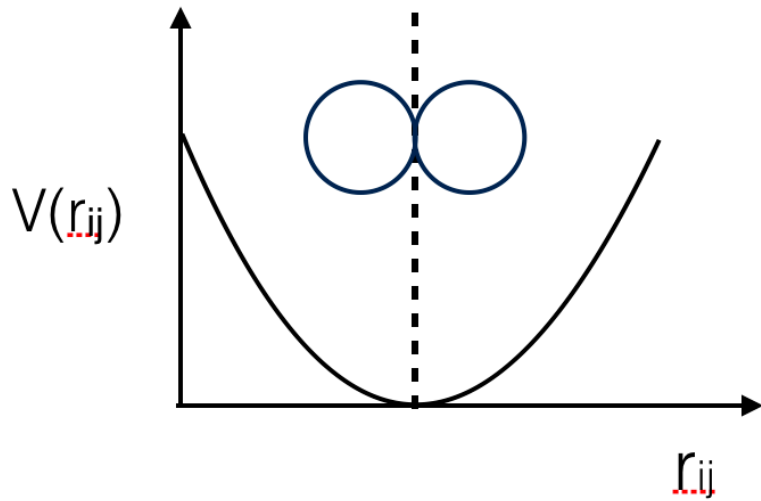
How do we calculate $P(N_c, \phi)$?

T. Bertrand, R. P. Behringer, B. Chakraborty, CSO, and M. D. Shattuck, "Protocol dependence of the jamming transition," *Phys. Rev. E* **93** (2016) 012901. $N_c = N_c^0$

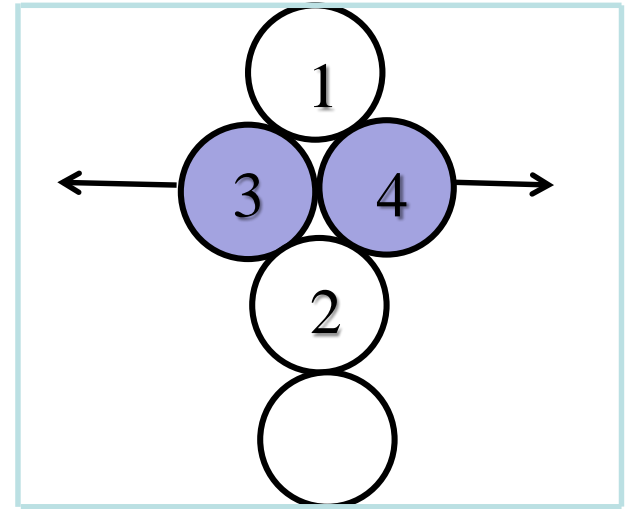


Protocol Dependence



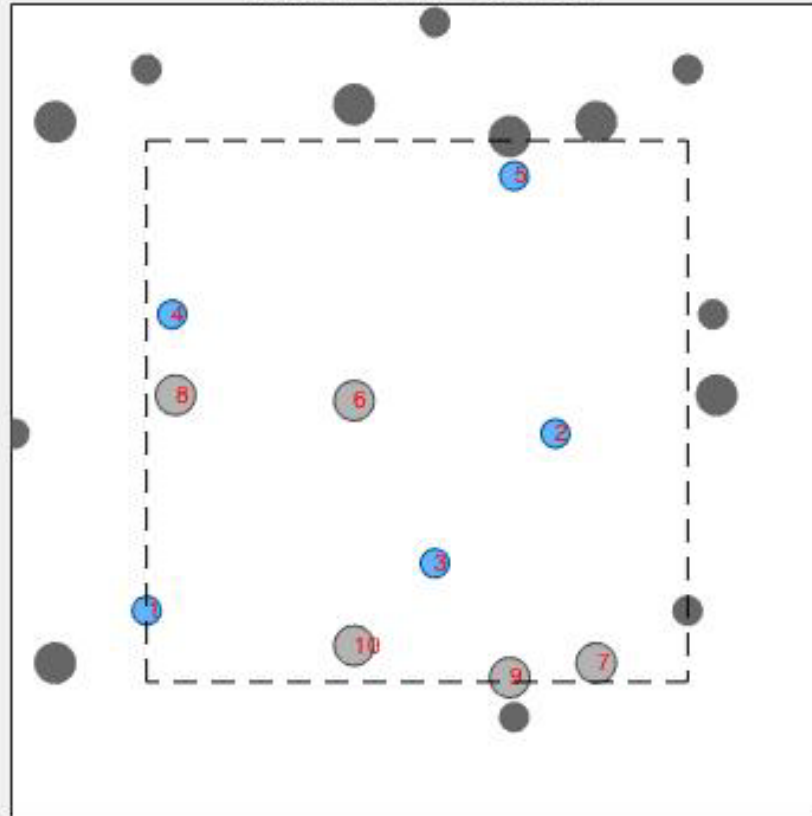


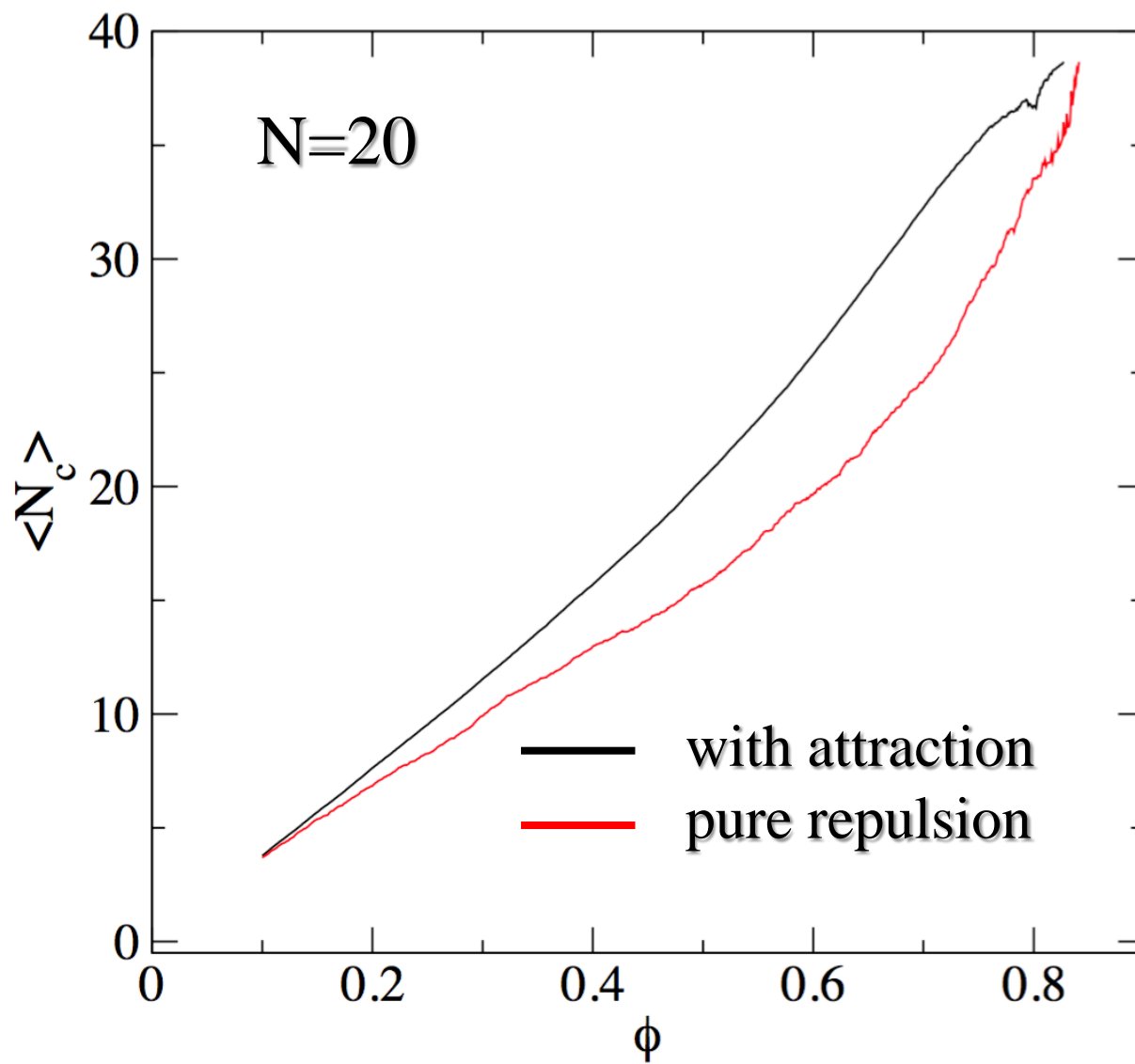
After contact forms,
initiate double-sided spring

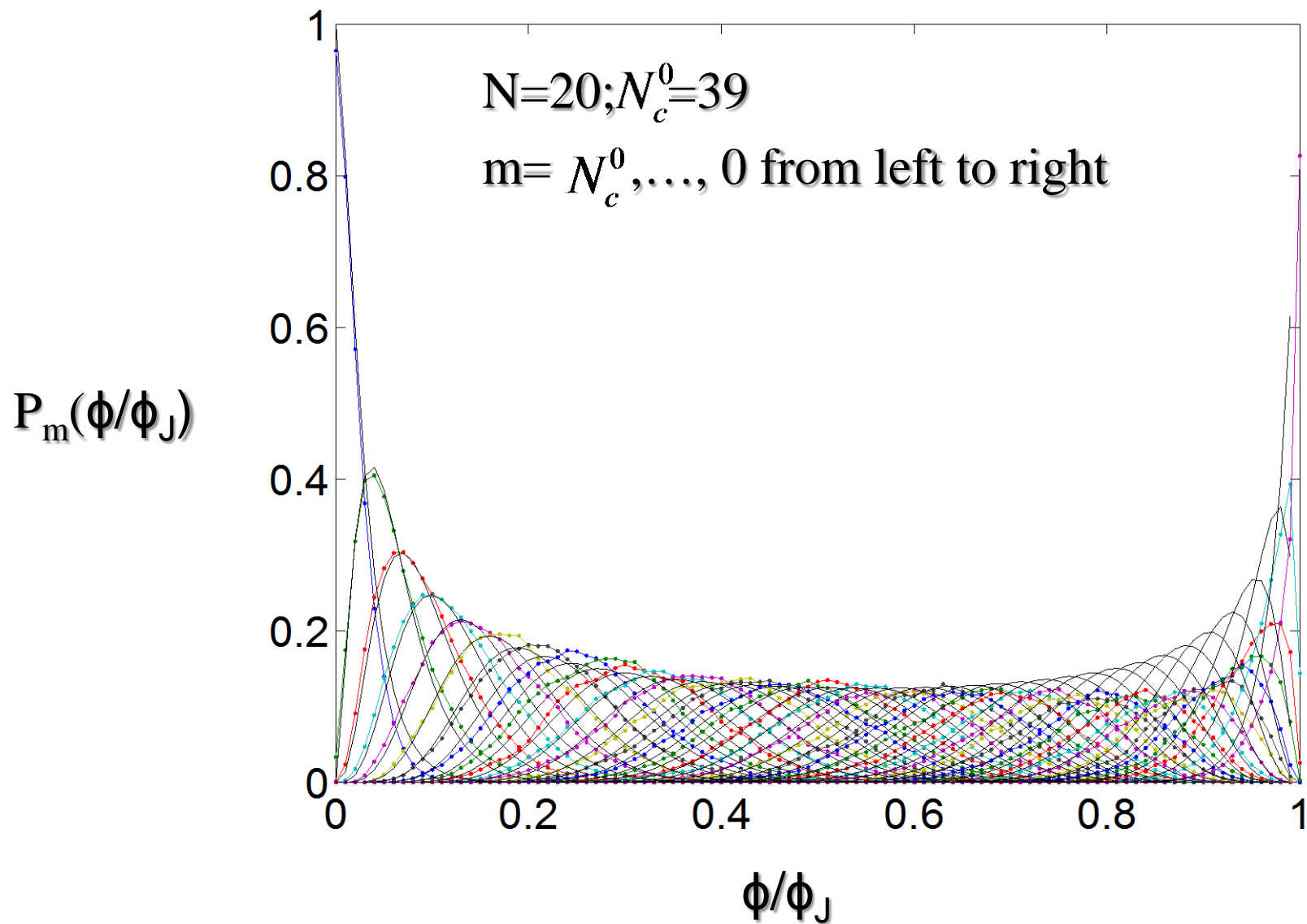


Break double-sided spring
between 3 and 4 when spring
becomes stretched after
energy minimization

Frame # = 1, $\phi = 0.032002$





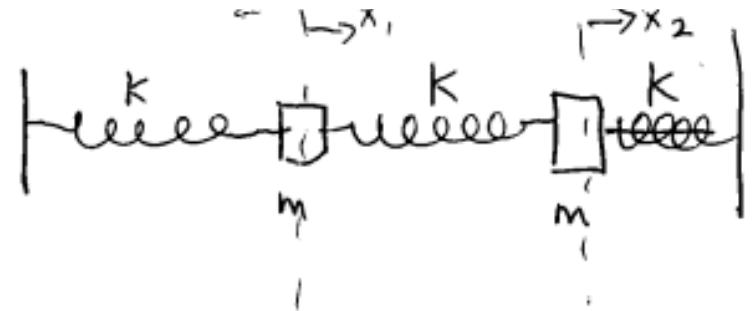


Normal modes

$$\omega_0^2 = \frac{k}{m}$$

$$m\ddot{x}_1 = -kx_1 + k(x_2 - x_1)$$

$$m\ddot{x}_2 = -k(x_2 - x_1) - kx_2$$



$$x_1 = A_1 \cos(\omega t - \phi)$$

$$x_2 = A_2 \cos(\omega t - \phi)$$

$$0 = (\bar{\omega}^2 - 2)A_1 + A_2$$

$$0 = (\bar{\omega}^2 - 2)A_2 + A_1$$

$$\bar{\omega} = \frac{\omega}{\omega_0}$$

$$\omega^2 = 1 \quad \omega^2 = 3$$

$$x_1(t) = A_1 \cos \omega_0 t - \phi_1 + A_2 \cos \sqrt{3} \omega_0 t - \phi_2$$

$$x_2(t) = A_1 \cos \omega_0 t - \phi_1 - A_2 \cos \sqrt{3} \omega_0 t - \phi_2$$

$$A_1, A_2, \phi_1, \phi_2$$

How many initial conditions: two for x_1 , two for x_2

Dynamical Matrix

$$D_{ij}^r = \left. \frac{\partial^2 V(\vec{r})}{\partial r_i \partial r_j} \right|_{\vec{r}=\vec{r}_0}$$

d N- d eigenvalues; $(\omega_i^d)^2 > 0$.

Sources of nonlinearities in particulate media

- *Breaking existing contacts and forming new contacts (contact clapping/thermal fluctuations)*

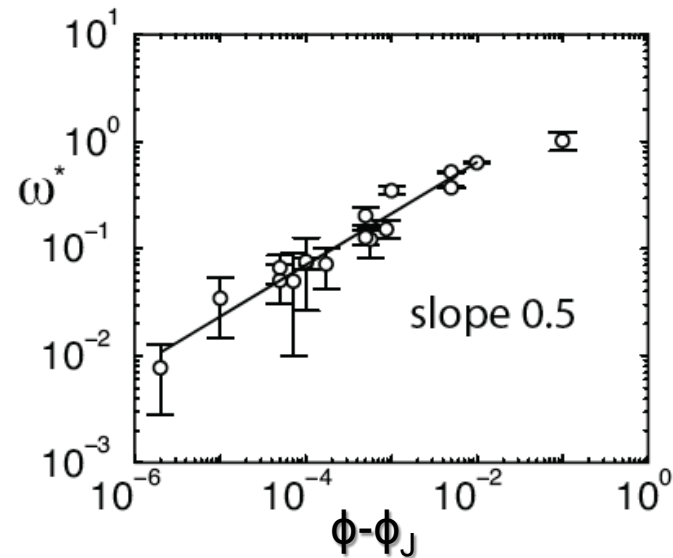
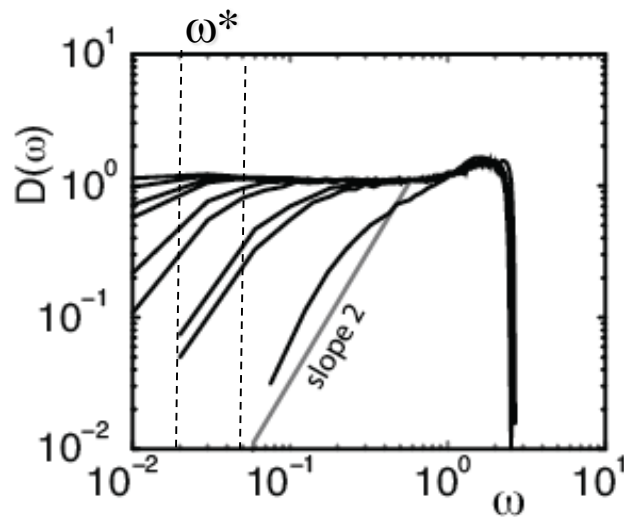
- Nonlinear interaction potential
- Explicit dissipation from normal contacts
- Sliding and rolling friction

Contact Interactions

$$\frac{V(r_{ij})}{\varepsilon} = \alpha^{-1} \left(1 - \frac{r_{ij}}{\sigma_{ij}} \right)^\alpha \theta \left(1 - \frac{r_{ij}}{\sigma_{ij}} \right)$$

- Several nonlinear contributions

Density of vibrational modes assuming linear response



- Formation of plateau in $D(\omega)$ (excess of low-frequency modes) as $\Delta\phi \rightarrow 0$
- $\omega^* \sim \Delta z \sim \Delta\phi^{0.5}$ responsible for anomalous structural/mechanical properties of athermal systems *as well as boson peak/anomalous thermal conductivity in glasses*

The FPU paradox

The original idea, proposed by Enrico Fermi, was to simulate the one-dimensional analogue of atoms in a crystal: a long chain of particles linked by springs that obey Hooke's law (a linear interaction), but with a weak nonlinear correction (quadratic for the FPU- α model or cubic for the FPU- β model), see Figure 1.

A purely linear law for the springs guarantees that energy given to a single 'normal' mode always remains in that mode (see caption of Figure 2 for the definition of normal modes in terms of atom displacements from their equilibrium positions).

Fermi, Pasta and Ulam thought that, due to the nonlinear correction, the energy introduced into the lowest frequency mode $k = 1$ should have slowly drifted to the other modes, until the equipartition of energy, a consequence of ergodicity, would have been reached. The beginning of the calculation indeed suggested that this was the case. Modes $k = 2, k = 3, \dots$, were successively excited, reaching a state close to equipartition, as shown in Figure 2. However, by accident, one day, they let the program run longer. When they realized their oversight and came back to the computer room, they noticed that the system, after remaining in the near equipartition state for a while, had then departed from it. To their great surprise, after 157 periods of the mode $k = 1$, almost all the energy (all but 3%) was back to this mode. Further calculations, performed later with faster computers, showed that the same phenomenon repeats many times, and that a *super-recurrence* exists, at which the initial state is recovered with an even higher accuracy (see Ford, 1992 and Weissert, 1997 for a historical account).

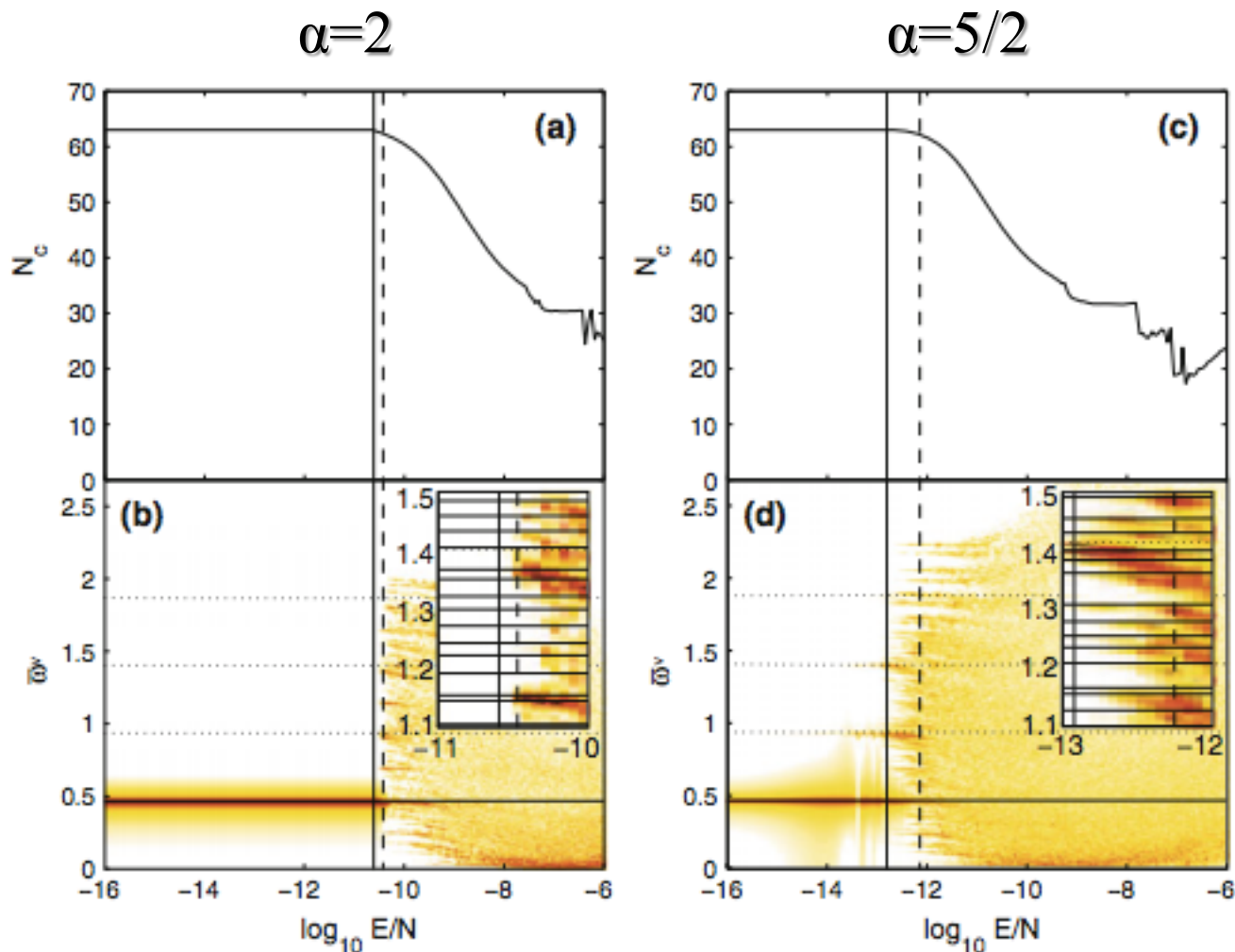
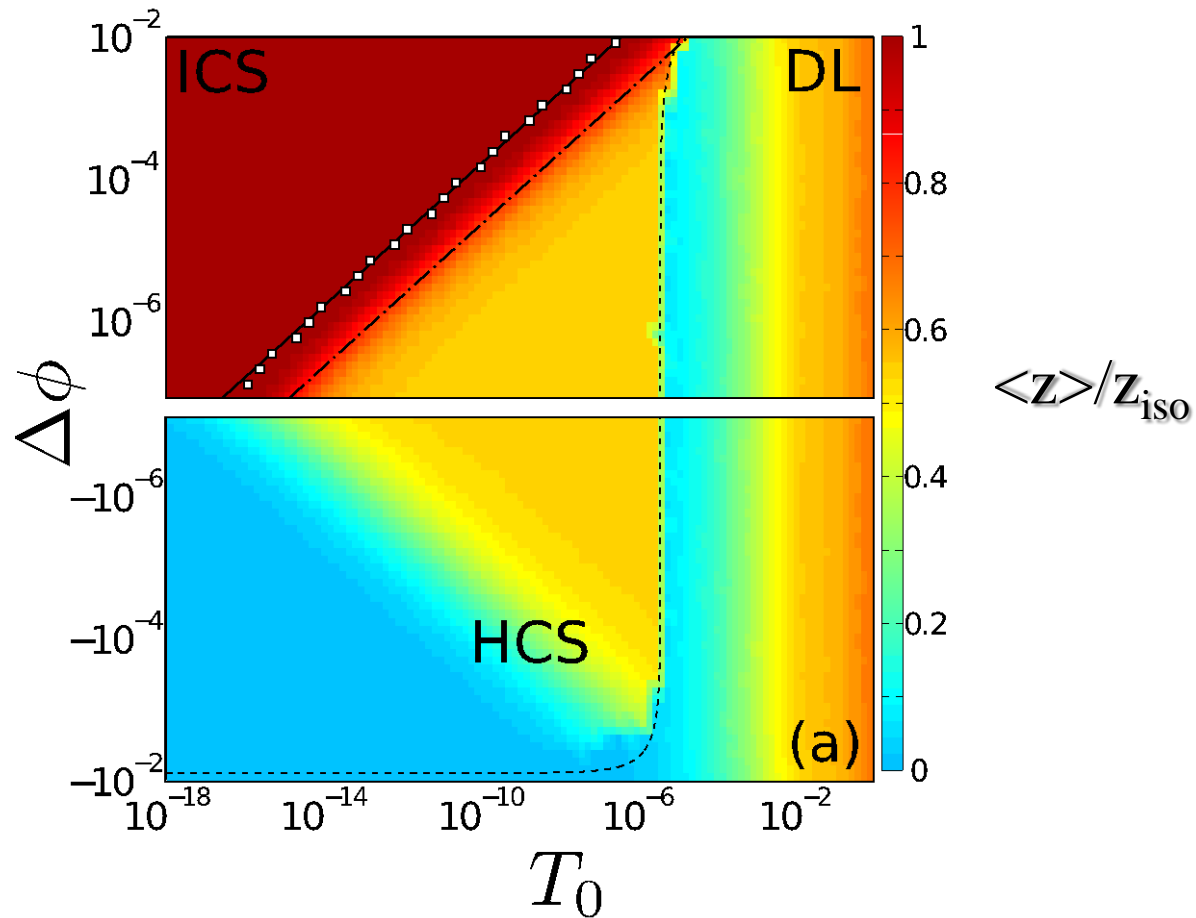


Fig. 3 Time-averaged number of contacts N_c (**a**, **c**) and color-scale plot of $\log_{10} D(\bar{\omega}^\nu)$ (**b**, **d**) for static packings of $N = 32$ bidisperse disks perturbed along a single eigenmode (mode 12) as a function of the perturbation energy E/N . At $E = 0$, the packing possesses the isostatic number of contacts $2N' - 1 = 63$. In **b**, **d**, the *solid horizontal line* represents the frequency of the driving frequency ω_{12} and the *dotted horizontal lines* indicate harmonics of the driving frequency,

$2\omega_{12}$, $3\omega_{12}$, and $4\omega_{12}$. The *vertical solid* and *dashed lines* indicate the energies E_c above which the first contact breaks and E_1 above which there is on average one contact missing from the zero-temperature configuration. The *inset* shows a close-up of the region between E_c/N and E_1/N , where the *solid horizontal lines* give the dynamical matrix frequencies. The left (*right*) columns show the results for purely repulsive linear (Hertzian) spring interactions

Time-averaged contact number

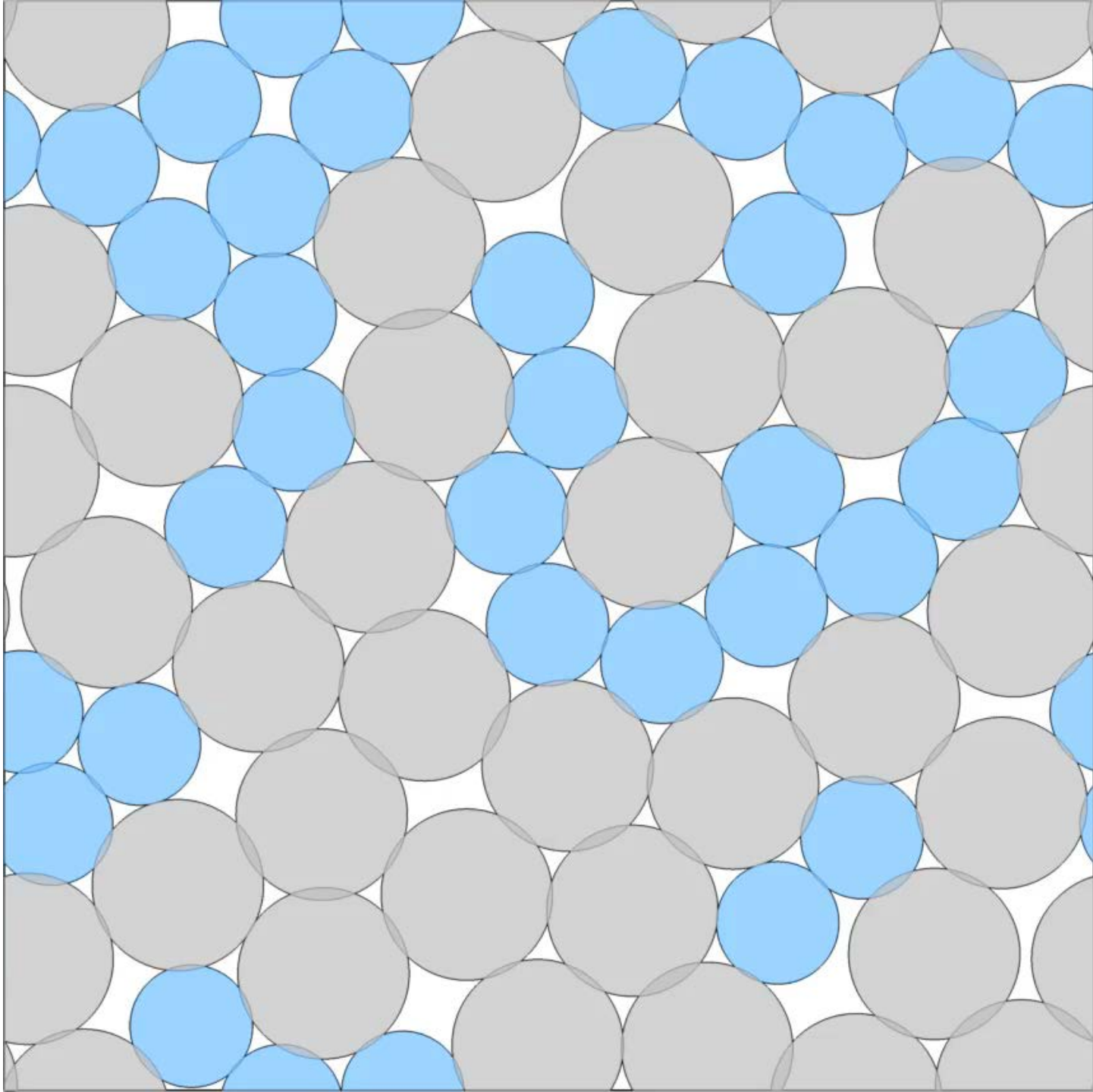
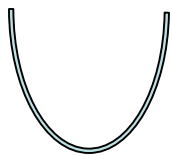


----- Glass line; $\tau_r \rightarrow \infty$

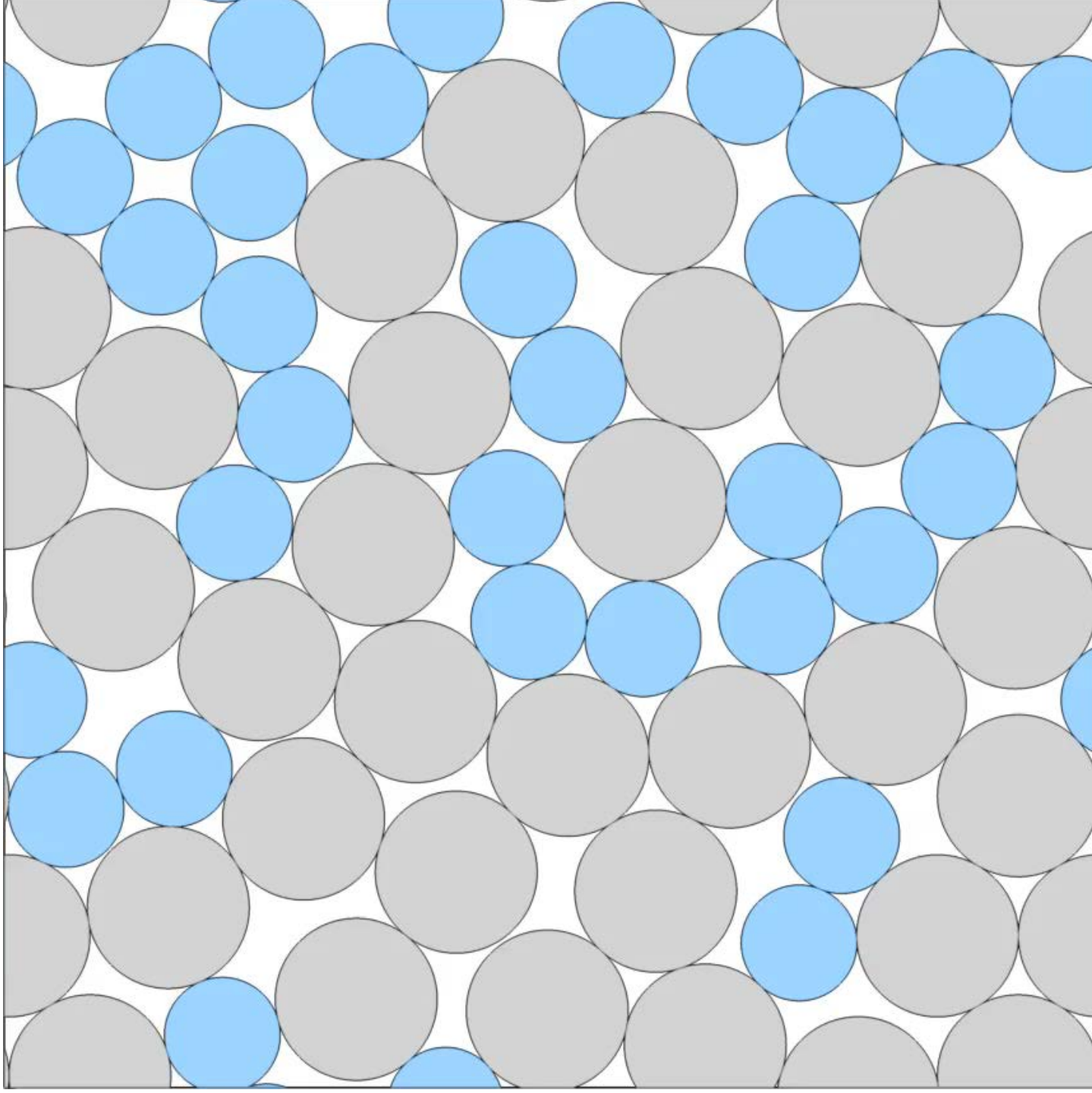
----- Transition between ICS and HCS

○○○ Strictly harmonic line

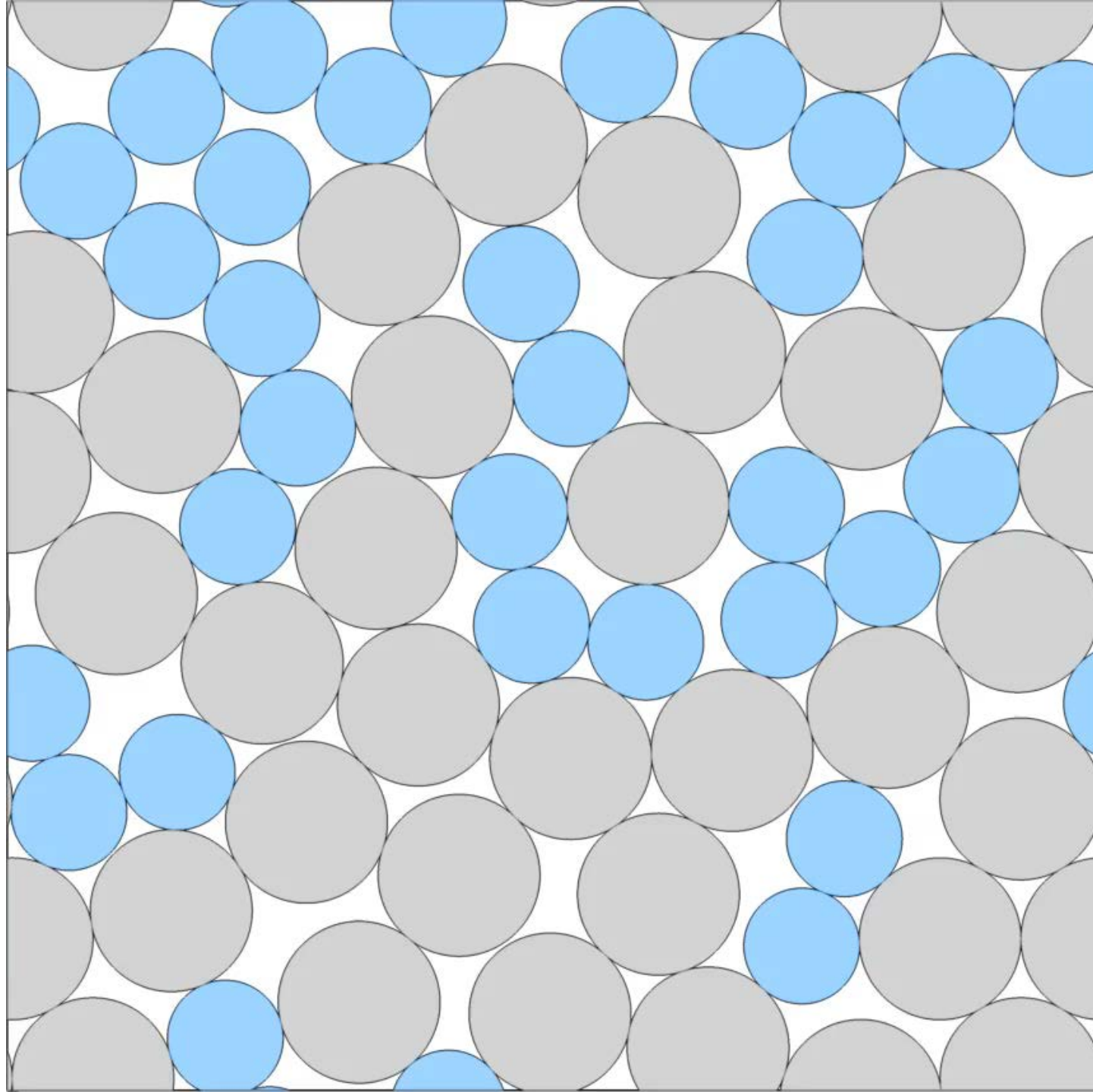
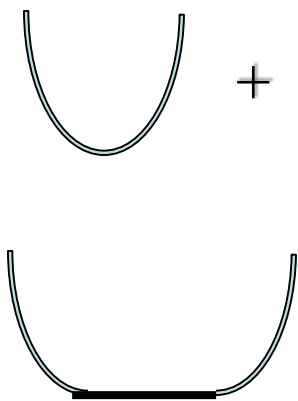
ICS

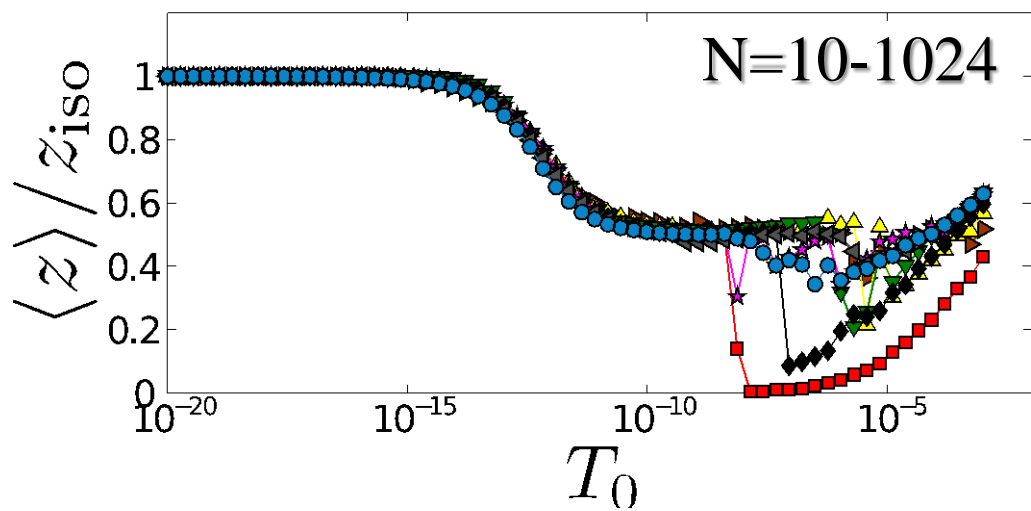
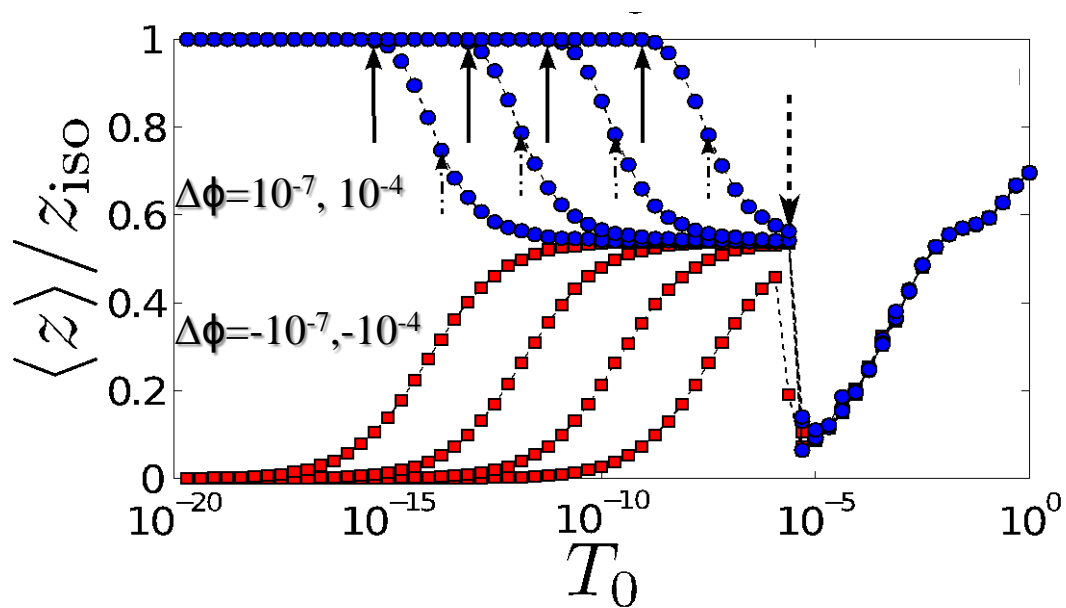


DL



HCS





Measurements of vibrational modes

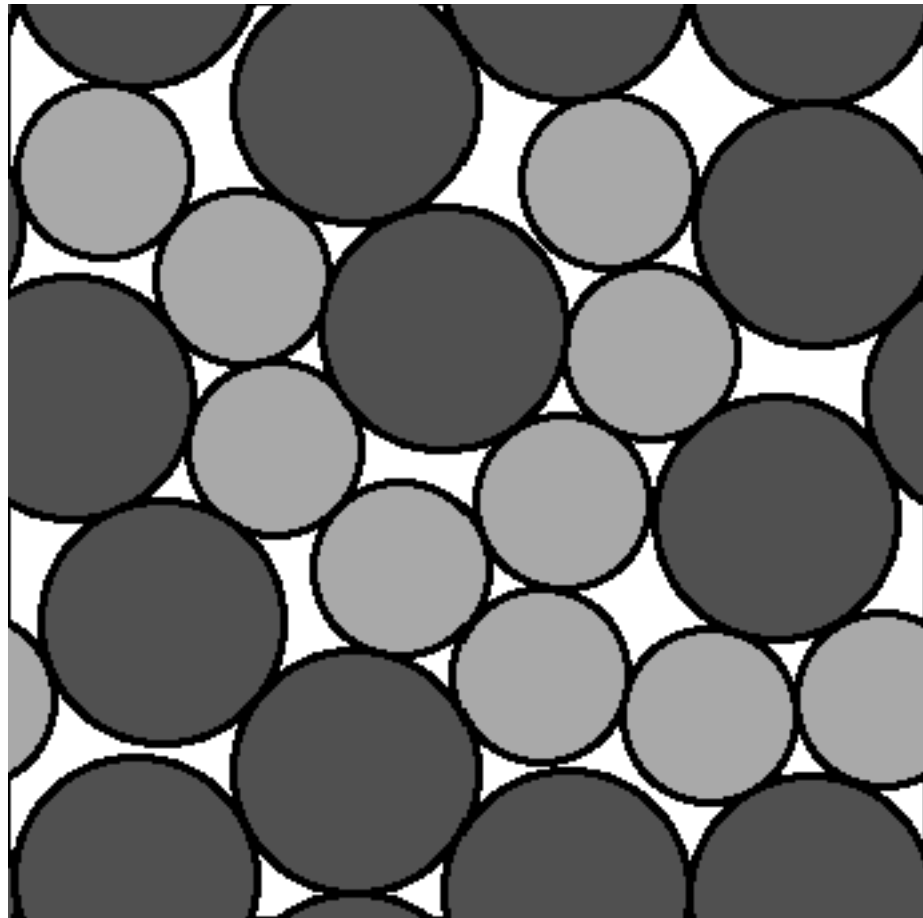
$$1. \quad D_{ij}^r = \frac{\partial^2 V(\vec{r})}{\partial r_i \partial r_j} \Big|_{\vec{r}=\vec{r}_0} \quad d \text{ N- d eigenvalues; } d^r_i = (\omega^d_i)^2 > 0.$$

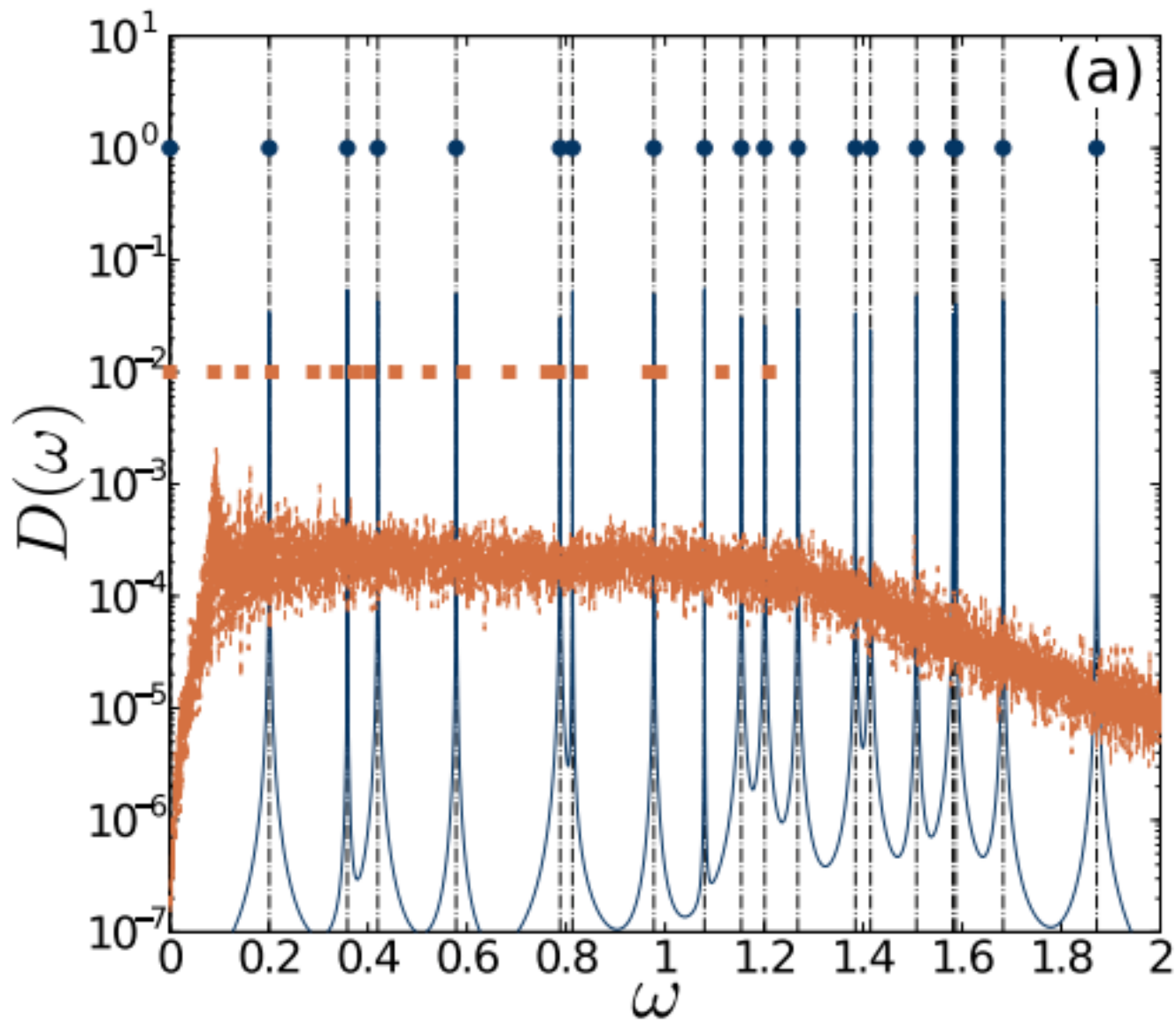
$$2. \quad D_{ij}^s(\omega^s) = E_{ik} C_{kj}^{-1} \quad d \text{ N- d eigenvalues; } d^v_i = (\omega^v_i)^2 > 0.$$

$$C_{ij} = \left\langle \left(r_i - \langle r_i \rangle \right) \left(r_j - \langle r_j \rangle \right) \right\rangle$$

$$E_{ik} = m \langle v_i v_k \rangle$$

$$3. \quad D_{vacf}(\omega^v) = \int e^{i\omega t} \langle \vec{v}(t) \cdot \vec{v}(0) \rangle dt \quad \text{Continuous function}$$





Solid lines: vacf
Vertical dashed lines: DM
Symbols: covariance

$$N=10$$

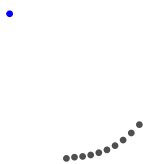
$$\Delta\phi=10^{-6}$$

$$\Delta\phi>0$$

$$\Delta\phi<0$$

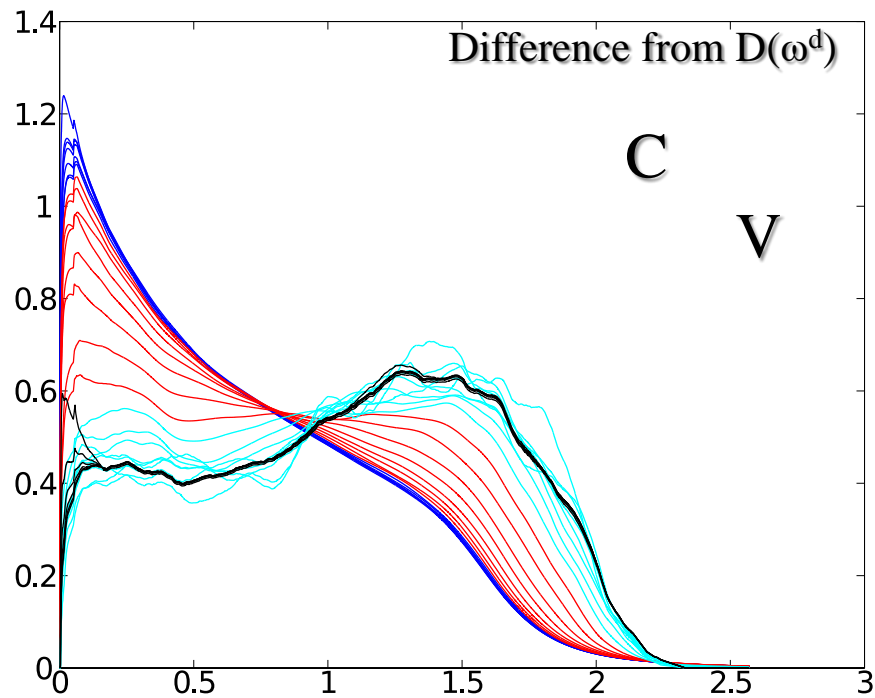
$$\Delta\phi=-10^{-6}$$

Covariance matrix



$N=128; \Delta\phi=10^{-6}$

Velocity autocorrelation function



Density of vibrational modes for HCS

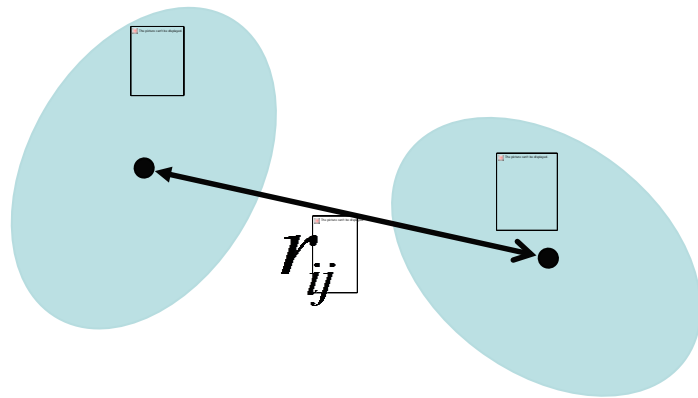
Summary

1. HCS 'phase' with $z/z_{\text{iso}} \sim 0.5$, new and non-unique density of vibrational modes that appears to persist in large-system limit
2. HCS is different from ICS
3. Normal modes do not persist in jammed solids, e.g. continuous set of frequencies develops

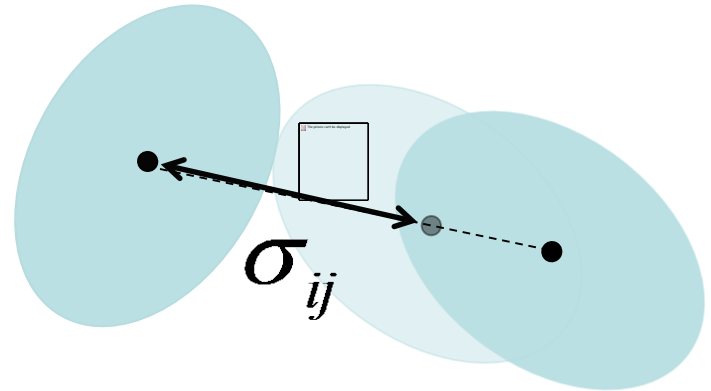
Non-spherical particles

Most current computational studies use hard-particle
Monte Carlo

Pairwise Repulsive Interactions: True Contact Distance



$$V(r_{ij}) = 0$$



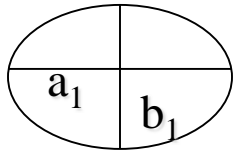
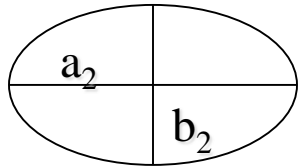
$$V(r_{ij}) > 0$$

$$V(r_{ij}) = \begin{cases} \frac{\epsilon}{\alpha} \left(1 - \frac{r_{ij}}{\sigma_{ij}}\right)^\alpha & r < \sigma_{ij} \\ 0 & r \geq \sigma_{ij} \end{cases}$$

$\alpha=2$; linear springs

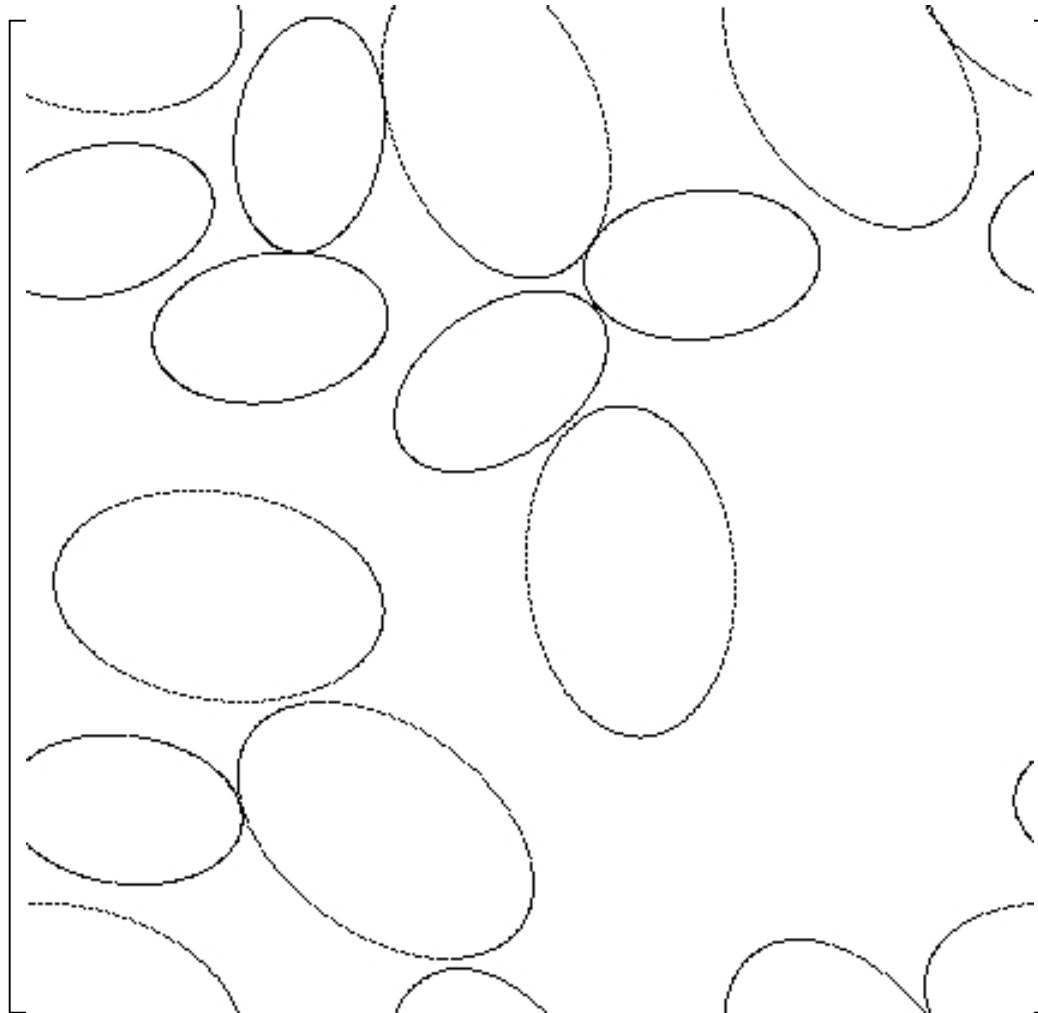
Packings of ellipse-shaped particles

bidisperse



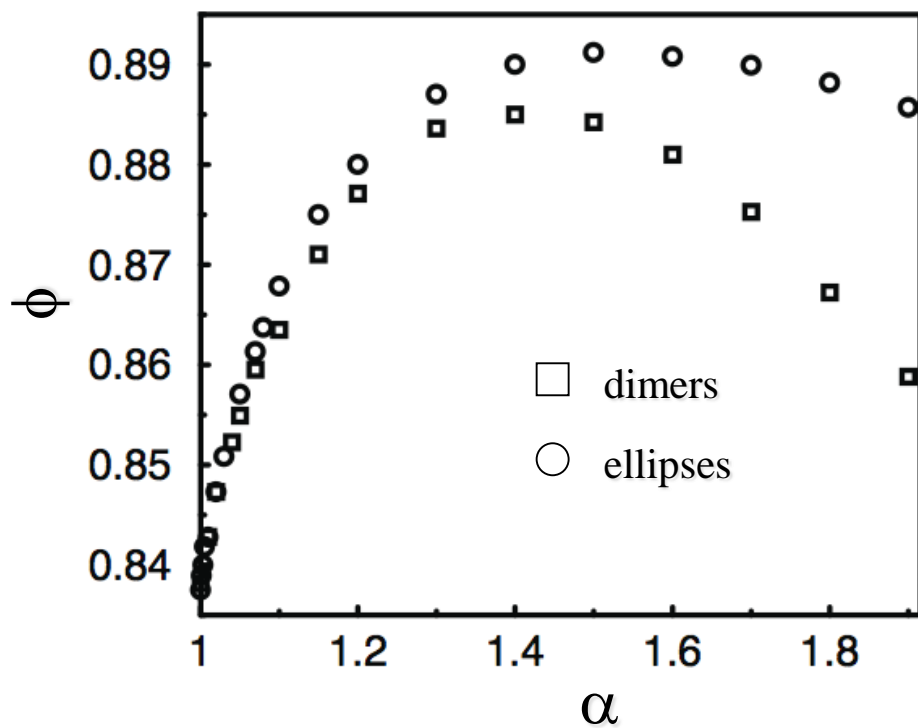
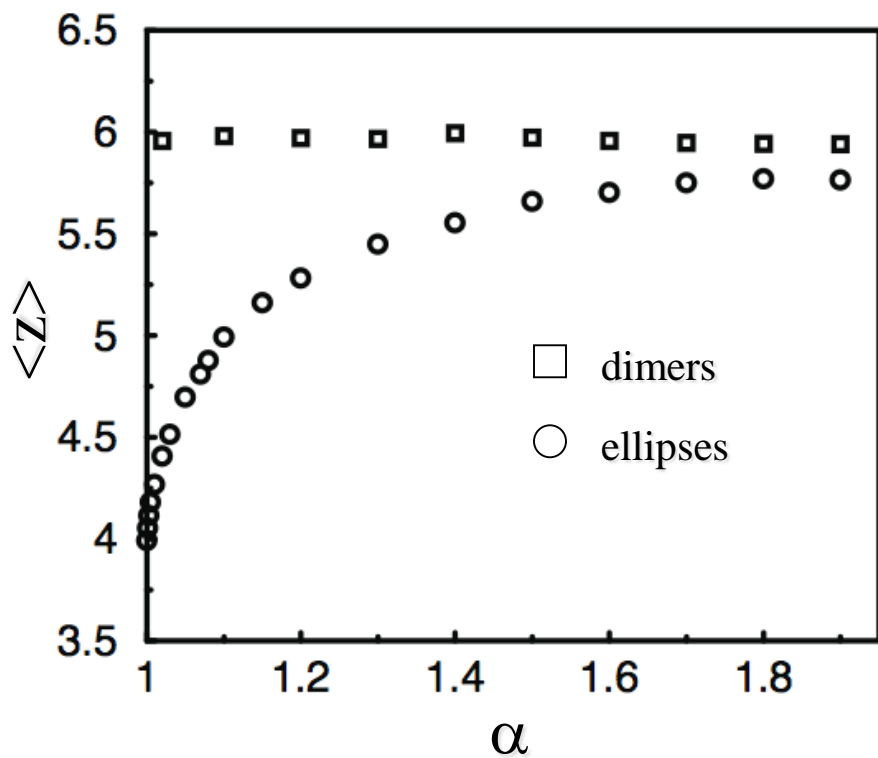
$$\frac{a_1}{b_1} = \frac{a_2}{b_2} = \alpha$$

$$\frac{a_1}{a_2} = 1.4$$

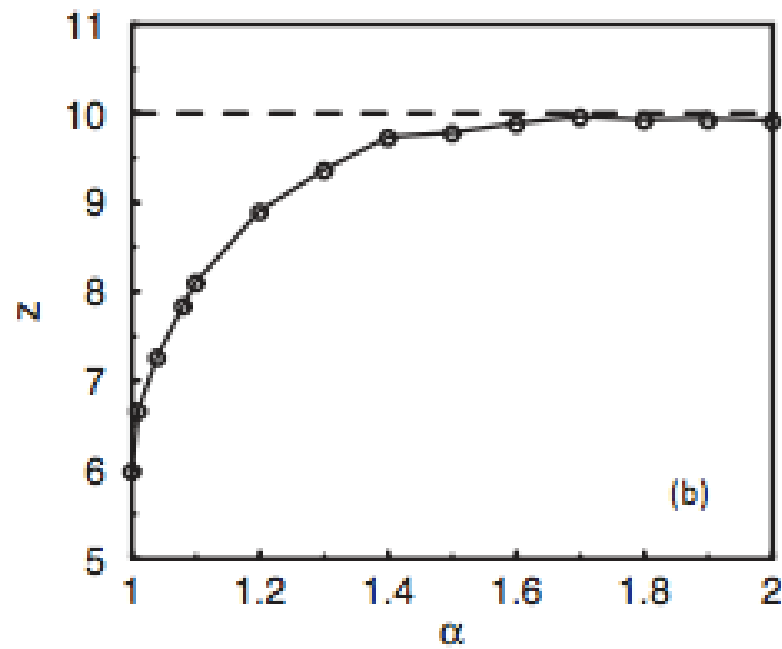
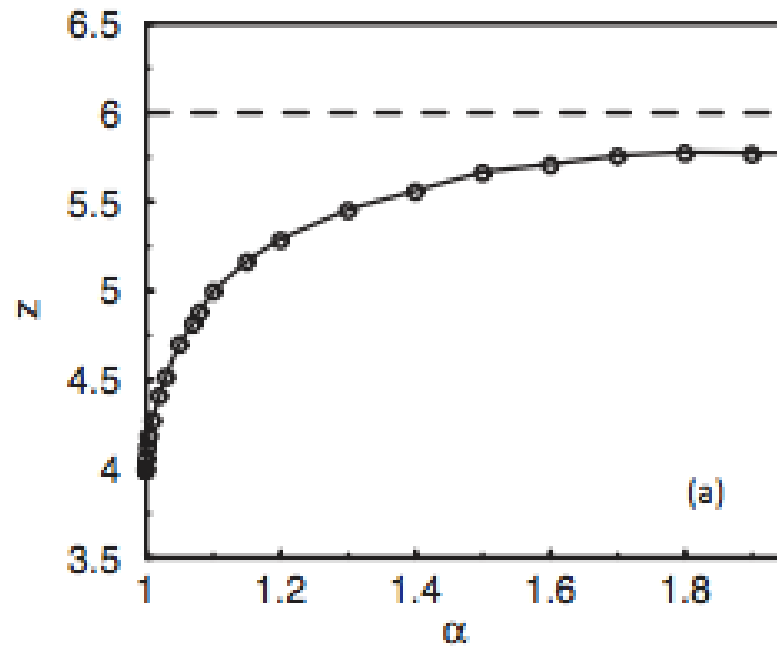


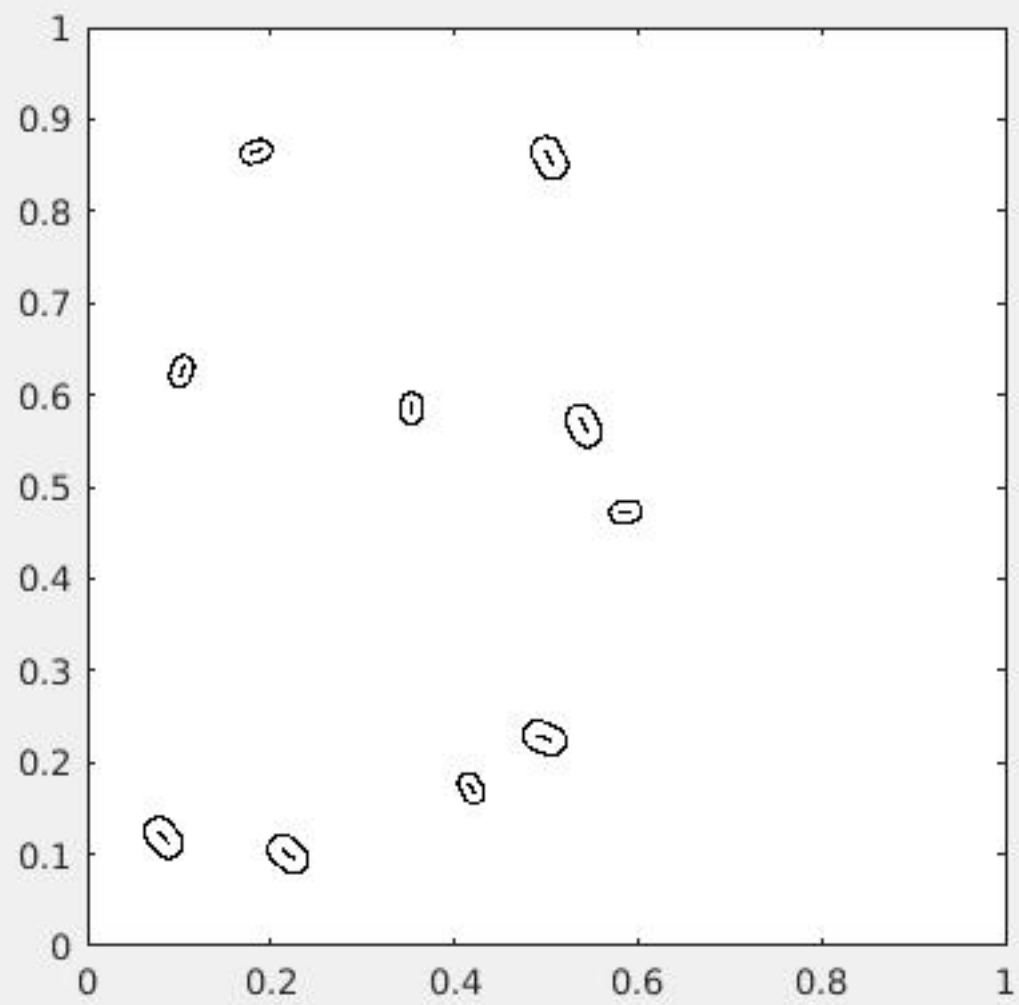
compression method-fixed aspect ratio α

Structural Properties



Prolate ellipsoids





Spherocylinders

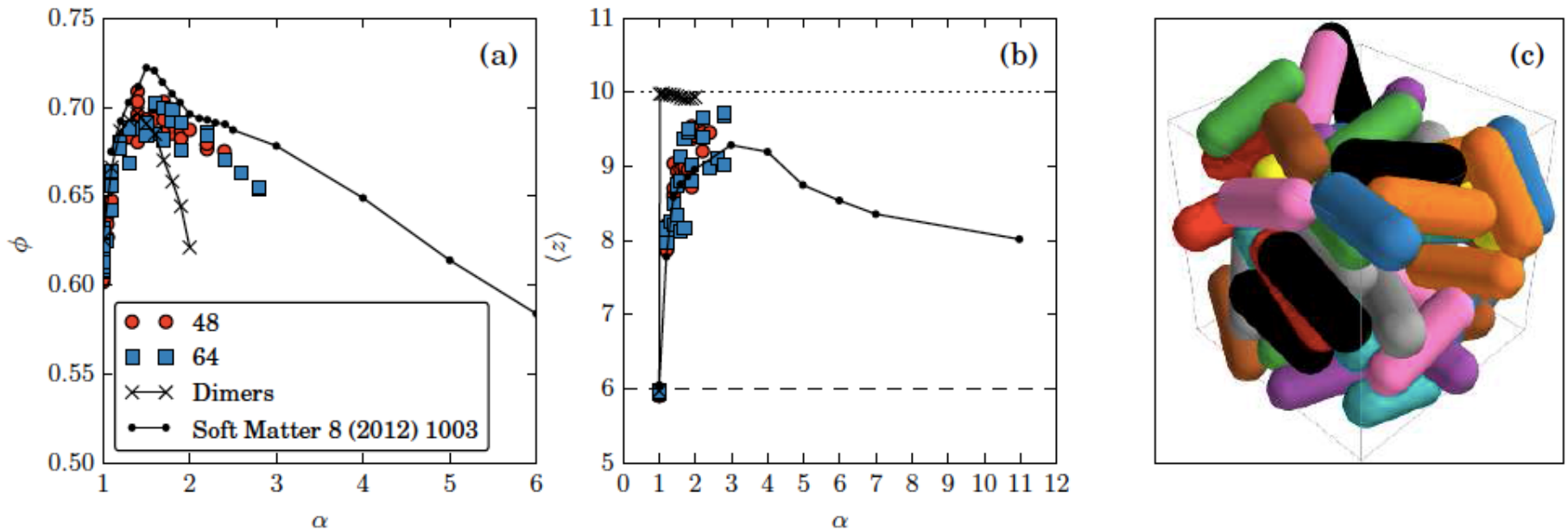
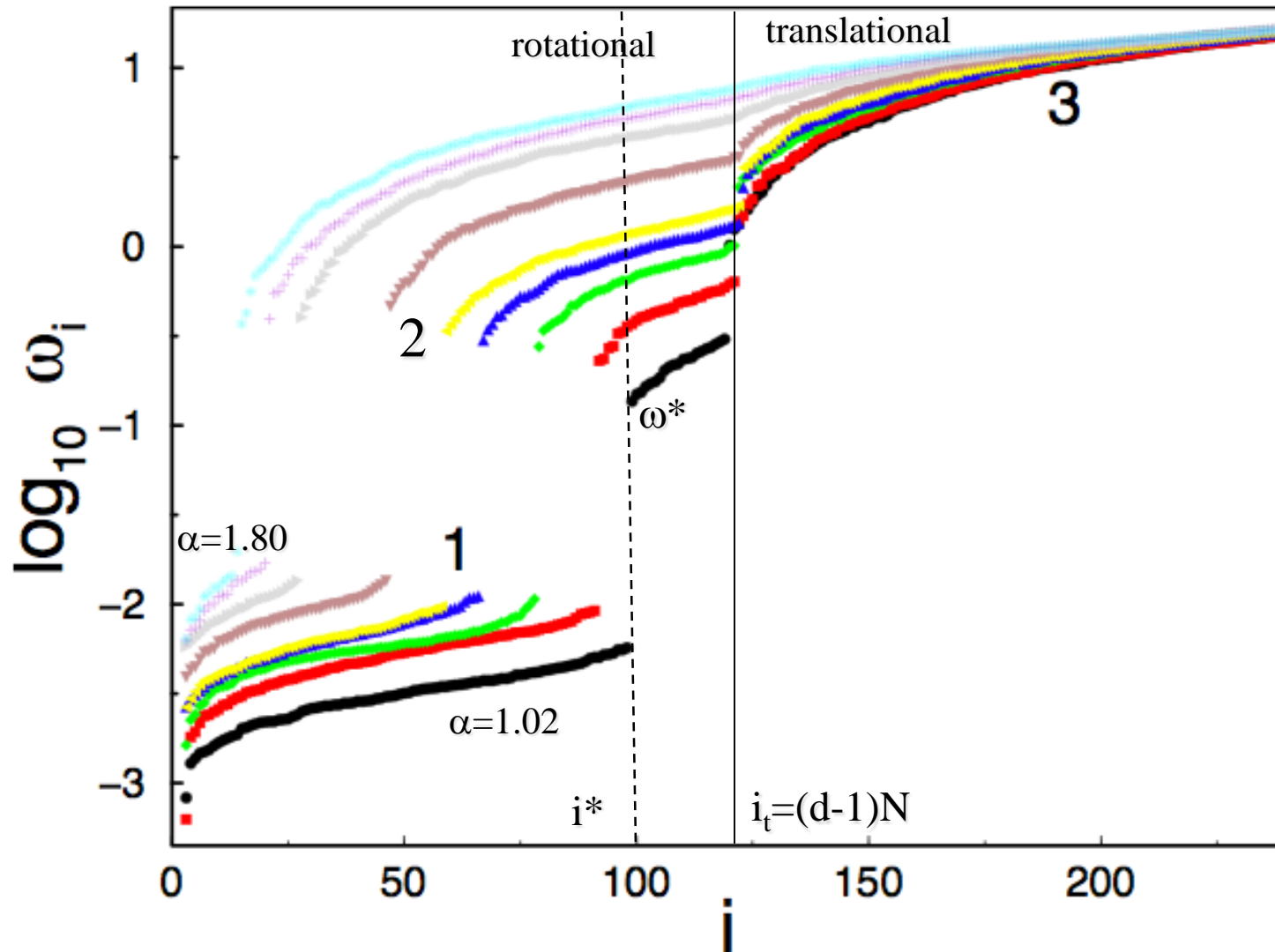


Figure 2: (a) Packing fraction ϕ and (b) coordination number $\langle z \rangle$ for static packings of spherocylinders from our preliminary studies ($N = 48$ and 64 particles) and those of Ref. [51] as well as rigid dimers ($N = 256$) as a function of aspect ratio α . The dotted and dashed horizontal lines in (b) give the values of $\langle z \rangle = 6$ and 10 for isostatic packings of spheres and spherocylinders (or dimers), respectively. (c) Visualization of a static packing of $N = 64$ spherocylinders with $\alpha = 2.8$.

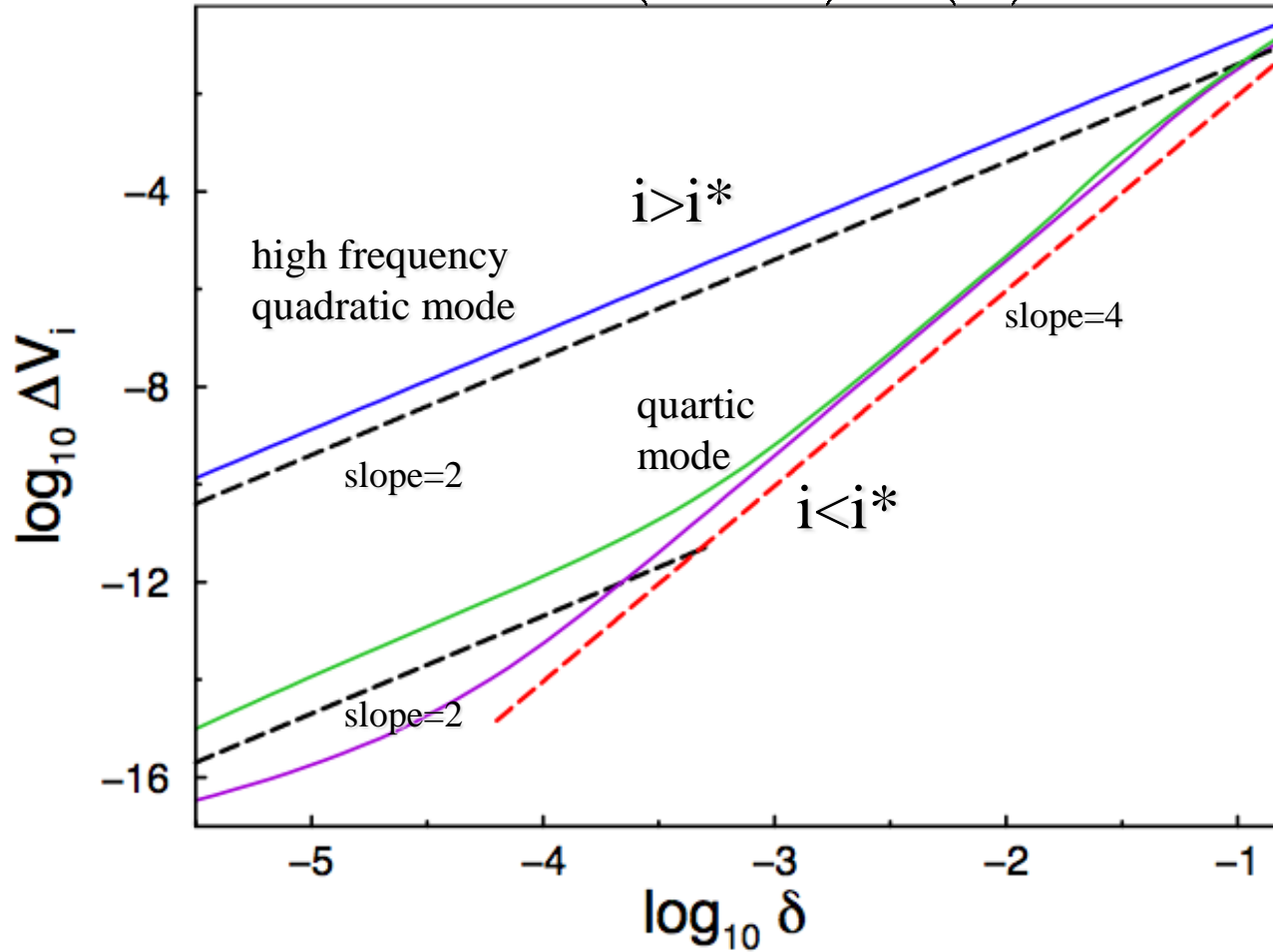
Eigenfrequency Spectra for ellipse packings



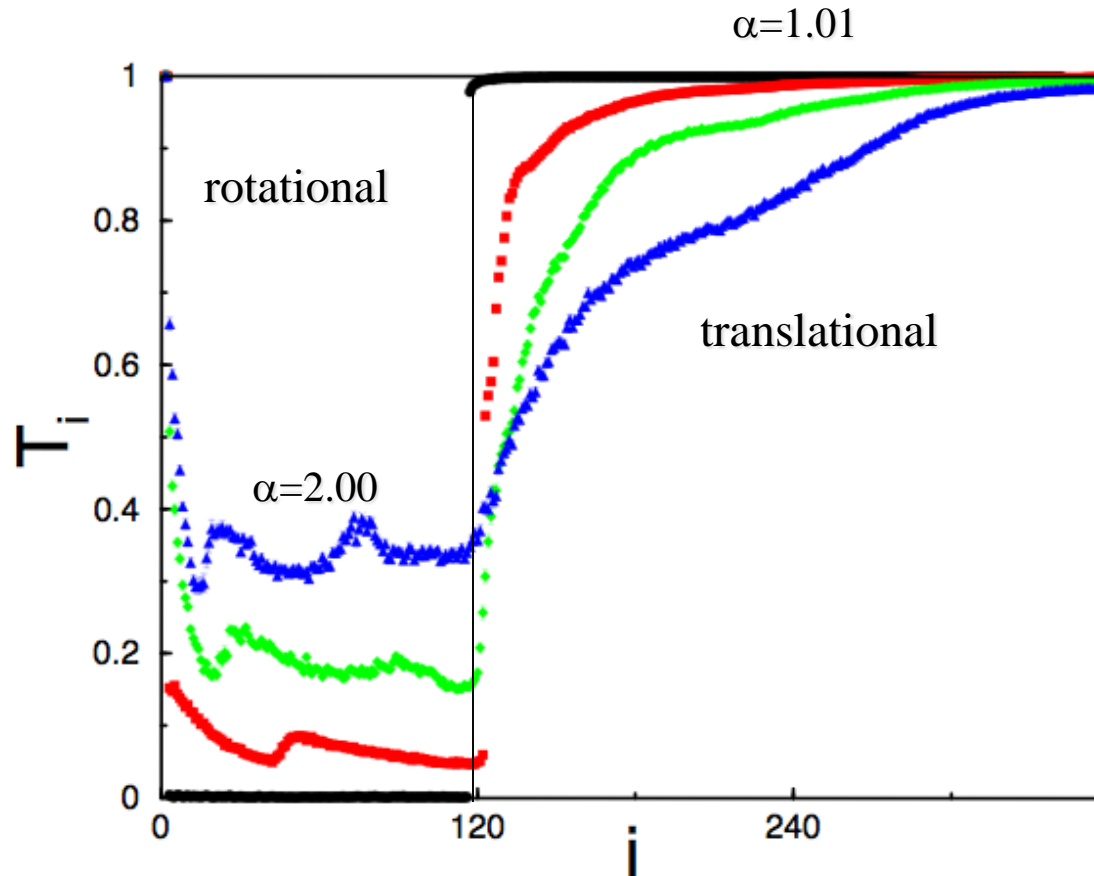
- Two gaps in spectrum over range of aspect ratios
- Onset of first gap depends on aspect ratio
- Second gap closes at large aspect ratios

I. Quartic Modes

$$\Delta V_i = V(\vec{\xi}_0 + \delta \hat{e}_i) - V(\vec{\xi}_0)$$

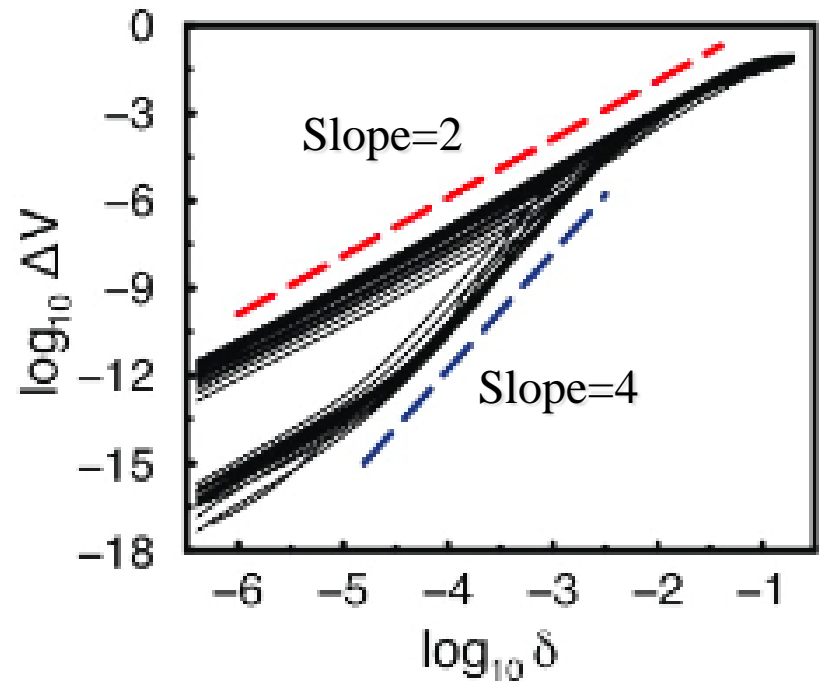
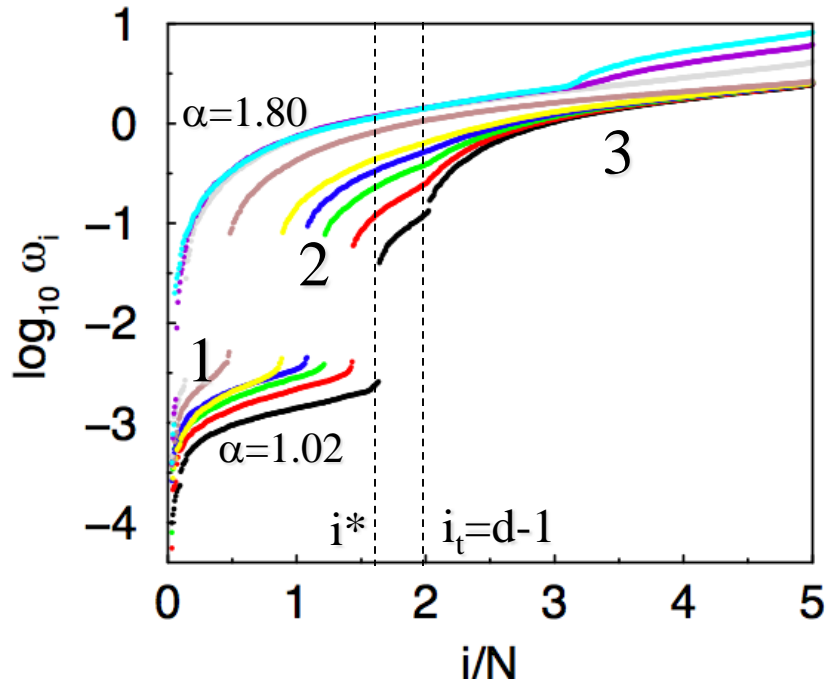


Rotational/Translational Character of Eigenmodes



$$T_i = \sum_{j=1}^N \left[(e_{xi}^j)^2 + (e_{yi}^j)^2 \right] \quad T_i = 1 - R_i$$

2D versus 3D: Same conclusions



- Two gaps in spectrum over range of α
- Onset of first gap depends on aspect ratio
- Second gap closes at large aspect ratios

- Modes $i < i^*$ are quartic in limit overlap $\rightarrow 0$

Summary

How do we develop a theory for z and ϕ as a function of aspect ratio? “Theory” for spherical particles relied on isostaticity.

How do mechanical properties depend on α , friction, and bending stiffness?